

# ABSTRACT

Title of Dissertation: SEPARATIONS OF WATER-IN-OIL EMULSIONS BY ELECTROSTATIC FIELD AT THE ELEVATED TEMPERATURE

**Hak Seung Lee, Doctor of Philosophy, 2019**

Dissertation directed by: Professor Bao Yang, Department of Mechanical

Separation of water from oil has been a significant subject for a crude-oil purification in the petroleum industry and chemical processing. This dissertation reports theoretical and experimental studies on separation of water from water-in-oil emulsions under combined treatment of a radial electric field and elevated temperature. Compared to macroemulsion, there are fundamental differences when considering microemulsion. It is difficult to separate microemulsion by an electric field due to its tiny droplet size. Microemulsion can be transformed to macroemulsion state over the cloud point. Therefore, heating is applied to the microemulsion to change its phase, then an electric field is applied to the system to expedite the separation speed. The enhanced separation performance using the combined method can be mainly attributed to the reduced viscosity and dissociated surfactants at elevated temperature and the accelerated droplet coalescence under the radial electric field. Theoretical analysis shows that temperature and electric strength can strongly affect the movement of the water droplets, and these effects are also experimentally validated by water/oil separation tests. In our experiments, a cylindrical cone-shaped separation tube equipped with coaxial cylindrical electrodes was built to improve

the separation using a non-uniform radial electric field. From the result of the numerical calculations, the precipitation and collision times of water droplets are rapidly reduced as the operating temperature increases. This theoretically expected values accurately predict the experimental results of the water-in-oil emulsion separation tests. It is experimentally observed that increasing the applied voltage and/or temperature can significantly reduce the separation time and the residual water concentration in the emulsion. Lastly, the dynamic water/oil separation system was designed using the combined method of heating and electric field. The effects of operating temperature and flow rate on the quality of the separated oil are investigated by executing several tests at different temperatures and flow rates. From the results of the dynamic separation tests, the residual water concentration in the separated oil reduces as the operating temperature increases under the boiling point. Also, the water concentration of the separated oil increases as the flow rate increases due to the reduced residence time.

# **SEPARATIONS OF WATER-IN-OIL EMULSIONS BY ELECTROSTATIC FIELD AT THE ELEVATED TEMPERATURE**

**By**

**Hak Seung Lee**

Dissertation submitted to the Faculty of the Graduate School of the  
University of Maryland, College Park in partial fulfillment  
of the requirements for the degree of  
Doctor of Philosophy  
2019

**Advisory Committee:**

Dr. Bao Yang (Professor of Mechanical Engineering and Chair of Committee)  
Dr. Amir Riaz (Associate Professor of Mechanical Engineering)  
Dr. Guangming Zhang (Associate Professor of Mechanical Engineering)  
Dr. Xinan Liu (Research Associate Professor of Mechanical Engineering)  
Dr. Kenneth Yu (Professor of Aerospace Engineering and Dean's Representative)

© Copyright by  
Hak Seung Lee  
2019

## **Dedication**

To my wife, daughter, and parents for their continuing love and support in all my efforts and endeavors.

## Acknowledgments

First of all, I would like to sincerely thank my Ph.D. advisor, Dr. Bao Yang, for giving me the opportunity to work on this challenging project when I was struggling with my graduate study. His keen insight and great knowledge of the nature of various mechanical processes has significantly changed my way of looking at both physical theory and experimental processes. My attitude and ability to do research, which will benefit me for the rest of my life, have been significantly improved with his enormous help and patience.

I am also grateful to Dr. Kenneth Yu, who is my former-advisor and one of the committee members. Thanks to his guidance and assistance on my previous M.S. project, I was able to step up carrying out my research. He also provided me with many comments and suggestions for writing and revising this Ph.D. dissertation.

I would like to thank the committee members, Dr. Amir Riaz, Dr. Guangming Zhang, and Dr. Xinan Liu, for their invaluable time reviewing this manuscript and providing me critical feedback. I am also grateful to Dr. Ashwani Gupta, Dr. Marino diMarzo, Dr. Amir Riaz and Dr. Xinan Liu for the experience of working as Teaching Assistants in their classes. This TA experience allowed me to review basic but very important undergraduate course materials. Also, I had chances to teach and communicate with undergraduate students for problem-solving in TA classes.

My colleagues, Zhi Yang, Chaolun Zheng, Jian Zhou, Sevket Yuruker, Beihan Zhao, Yong Pei, Wenshuo Yang, Zhaorui Zhao, and Soohwan Jang in my group have enriched my graduate life in many ways. They helped me a lot for the project in both the lab and office.

Especially, Chaolun Zheng has worked and executed many of the experimental tests with me. While conducting a same arpa-e project, he gave me a lot of advice and suggestions that really helped me to improve the experimental results and data acquisitions. He is also a great friend and time with him is always a learning experience.

I am grateful to Dr. Amardip Ghosh and Dr. Qina Diao for their constant advice and help on my previous NASA CUIP project and paperwork. I would also like to thank my previous colleagues, Sammy Park, Camilo Aguilera, Seungjoon Yang, for helping me out with my previous work and having a great time in the office and campus area.

I would also like to acknowledge the funding that made this research possible. This work was sponsored by a grant from arpa-e. I would like to thank Dr. Ashok Gidwani, a project manager of arpa-e, for his help with various aspects of this project. I am grateful to the faculty members in this project, Dr. Yunho Hwang, and Dr. Amir Shooshtari, for their time and critical evaluation. Also, I would like to thank my colleagues in this project, Stefan Bangerth, Dongyu Chen, and Chaolun Zheng, for their effort and advice in conducting the experiments and lab work.

Most of all, I am grateful to my wife, Seonyoung Choi, my daughter, Chaeah Lee, and my son who will be born next summer for their continuing love and support. Also, I would like to thank my parents, whose supportive role in my education and upbringing is beyond words. Finally, I am grateful to the small town of College Park, for giving me the chance to live learn and grow.

# Table of Contents

<b>Dedication.....</b>	<b>ii</b>
<b>Acknowledgment.....</b>	<b>iii</b>
<b>Table of Contents.....</b>	<b>v</b>
<b>List of Tables.....</b>	<b>viii</b>
<b>List of Figures.....</b>	<b>ix</b>
<b>Nomenclature.....</b>	<b>xv</b>
<b>Chapter 1: Introduction.....</b>	<b>1</b>
1.1 Background and Motivation.....	1
1.2 Objective and Scope.....	3
<b>Chapter 2: Literature Review.....</b>	<b>6</b>
2.1 Introduction.....	6
2.2 Emulsions.....	7
2.2.1 Macroemulsions.....	7
2.2.2 Microemulsions.....	8
2.3 Surfactants Science.....	10
2.4 Crude Oil Purification (Separation).....	11
2.4.1 Crude Oil Properties.....	11
2.4.2 Alternatives to Crude Oil for Scientific Experiments.....	13
2.5 Demulsifications.....	13
2.6 Water/Oil Separation Methods.....	14
2.6.1 Heat Treatment.....	14
2.6.2 Electric Field.....	15
2.6.3 Combined Method (Heating + Electric Field).....	19
2.7 Water Droplets Coalescence by Electric Fields.....	20
2.7.1 Gravitational Force.....	21
2.7.2 Electrophoresis and Dielectrophoresis Forces.....	22
2.7.3 Dipole-dipole Force.....	23
2.7.4 Other Forces.....	24
<b>Chapter 3: Theoretical Considerations.....</b>	<b>25</b>
3.1 Introduction.....	25
3.2 Forces on the Water Droplets in Electric Fields.....	26
3.2.1 Vertical Movement by Gravity.....	28
3.2.2 Horizontal Movement by Electric Fields.....	35
3.3 Dielectrophoresis Force Acting on the Droplets.....	42
3.4 Dimension Effect of the Cylindrical Electrodes.....	45

3.5 Conclusions.....	47
<b>Chapter 4: Experimental Apparatus and Techniques.....</b>	<b>49</b>
4.1 Water-in-Oil Emulsions.....	49
4.2 Water Concentration (%) Measurements.....	49
4.3 Static Separation by Electric Field with the Elevated Temperature.....	51
4.3.1 Overview of Setup.....	51
4.3.2 Separation Tube and Electrodes.....	53
4.3.3 Pressurized Sealed Tube.....	56
4.4 Static Separation by Centrifugal Force with the Elevated Temperature.....	58
4.4.1 Overview of Setup.....	58
4.5 Dynamic Separation by Electric Field with the Elevated Temperature.....	60
4.5.1 Overview of Setup.....	60
4.5.2 Additional Equipment for Dynamic Separation System.....	61
4.5.3 Dynamic Water/Oil Separation System for Lower Flow Rate.....	65
4.5.4 Dynamic Water/Oil Separation System for Higher Flow Rate.....	70
4.5.5 Power Consumption Measurement.....	78
<b>Chapter 5: Design of the Separators.....</b>	<b>80</b>
5.1 Introduction.....	80
5.2 Computational Simulations.....	80
5.3 Experimental Results.....	84
5.3.1 Comparison between Flat Plates and Cylindrical Electrodes.....	84
5.3.2 Thickness of the Center Electrode.....	85
5.3.3 Length of the Center Electrode.....	86
5.3.4 Air-gap between Center Electrode and its Capillary Tube.....	88
5.3.5 Diameter of the Separation Tube.....	90
5.4 Conclusions.....	92
<b>Chapter 6: Water/Oil Separation Results.....</b>	<b>93</b>
6.1 Introduction.....	93
6.2 Phase Change of Microemulsions with Heat Treatment.....	94
6.3 Static Separation of Microemulsions by the Combined Method.....	96
6.3.1 Water/Oil Separations by Heating or Electrostatic Method Alone.....	96
6.3.2 Temperature Dependence.....	99
6.3.3 Voltage Dependence.....	103
6.3.4 Frequency Dependence.....	107
6.3.5 Effect of Duty Cycle.....	110
6.4 Static Separation of Macroemulsions by the Combined Method.....	111
6.4.1 Introduction.....	111
6.4.2 Comparisons of Heating, Electrostatic, and Combined Method Tests.....	111
6.4.3 Temperature Dependence.....	113

6.4.4 Voltage Dependence.....	116
6.4.5 Frequency Dependence.....	118
6.4.6 Extended Test Time.....	121
6.5 Energy Consumptions.....	122
6.6 Comparisons of Miro- and Macroemulsions for Static Separations.....	124
6.6.1 Introduction.....	124
6.6.2 Temperature Dependence.....	126
6.6.3 Voltage Dependence.....	127
6.6.4 Frequency Dependence.....	130
6.7 Static Separations of Microemulsion by Combined Method over the Boiling Point.....	131
6.8 Dynamic Separation of Microemulsions by the Combined Method.....	133
6.8.1 Introduction.....	133
6.8.2 Dynamic Water/Oil Separation at Lower Flow Rate.....	134
6.8.3 Dynamic Water/Oil Separation at Higher Flow Rate.....	135
6.9 Static Separations by Centrifugal Force at the Elevated Temperatures.....	137
6.9.1 Introduction.....	137
6.9.2 Experimental Results.....	138
6.10 Measurement Uncertainty.....	142
6.11 Conclusions.....	142
<b>Chapter 7. Summary and Conclusions.....</b>	<b>145</b>
7.1 Summary of Important Findings.....	145
7.1.1 Theoretical Considerations for the Movement of Droplets in Oil Phase.....	145
7.1.2 Shape of Separation Tube and Electrodes.....	146
7.1.3 Simulations and Experiments for the Design of the Separators.....	146
7.1.4 Static Separation Tests of Water-in-Oil Microemulsions.....	147
7.1.5 Static Separation Tests of Water-in-Oil Macroemulsions.....	148
7.1.6 Dynamic Separation Tests of Water-in-Oil Microemulsions.....	149
7.2 Contributions of this Work.....	150
7.2.1 Academic Contributions.....	150
7.2.2 Practical Contributions in Industries.....	151
7.3 Concluding Remark.....	151
7.4 Recommendations for Future Work.....	152
<b>Bibliography.....</b>	<b>156</b>

## List of Tables

Table 2-1: Viscosities and Densities of three different crude oils.....	12
Table 3-1: Properties of sunflower oil at different temperatures (10 - 140°C).....	29
Table 4-1: Dimensions of Cone-shaped and Pressurized Tubes.....	58
Table 6-1: Water concentration measurements for different temperatures.....	102
Table 6-2: Water concentration measurements for different voltages.....	105
Table 6-3: Water concentration measurements for different frequencies.....	109
Table 6-4: Water concentration measurements for heating, electrostatic, and combined methods.....	112
Table 6-5: Water concentration measurements for different temperatures.....	115
Table 6-6: Water concentration measurements for different voltages.....	118
Table 6-7: Water concentration measurements for different frequencies.....	120
Table 6-8: Water concentration measurements for extended measurement time.....	121
Table 6-9: Residual water concentrations at 90 and 120°C with high pressure tube.....	133
Table 6-10: Water concentrations from the separated oil with different operating temperatures	135
Table 6-11: Water concentrations from the separated oil with different flow rates.....	136

## List of Figures

Figure 2-1: Top view of Flat plates electrodes and cylindrical electrodes: (a) Flat plates electrodes, (b) Cylindrical electrodes.....	18
Figure 2-2: Separated water/crude oil phases in cone-shaped tubes.....	20
Figure 3-1: Balance of the forces acting on a pair of droplets for horizontal electric fields.....	27
Figure 3-2: Densities ( $\text{kg/m}^3$ ) of water and sunflower oil at various temperatures (10 - 140°C)..	31
Figure 3-3: Density differences ( $\text{kg/m}^3$ ) between water and sunflower oil at various temperatures (10 - 140°C) .....	31
Figure 3-4: Sunflower oil dynamic viscosities ( $\mu_o$ ) at various temperatures (10 - 140°C) .....	32
Figure 3-5: Ratios of the sunflower oil viscosity to the density difference at various temperatures (10 - 140°C) .....	33
Figure 3-6: Vertical velocities (falling speed) of the droplet under the influence of temperatures (10 - 140°C) and droplet sizes (10nm - 100 $\mu\text{m}$ ).....	34
Figure 3-7: Precipitation time of the droplet under the influence of temperatures (10 - 140°C) and droplet sizes (10nm - 100 $\mu\text{m}$ ).....	34
Figure 3-8: Dielectric constants of sunflower oil at various temperatures (10 - 140°C).....	37
Figure 3-9: Horizontal velocities of the water droplet under the influence of temperatures (10 - 140°C) and droplet sizes (10nm - 100 $\mu\text{m}$ ) with the constant electric strength ( $E_o = 1\text{kV/cm}$ ) and $l/a$ ratio ( $l/a = 4$ ).....	38

Figure 3-10: Horizontal velocities of the water droplet under the influence of temperatures (10 - 140°C) and electric strength ( $E_o = 1 - 5\text{kV/cm}$ ) with the constant droplet size ( $a = 10\mu\text{m}$ ) and $l/a$ ratio ( $l/a = 4$ ).....	39
Figure 3-11: Horizontal velocities of the water droplet under the influence of temperatures (10 - 140°C) and $l/a$ ratio ( $l/a = 2 - 5$ ) with the constant droplet size ( $a = 10\mu\text{m}$ ) and electric strength ( $E_o = 1\text{kV/cm}$ ).....	39
Figure 3-12: Collision time of the water droplets under the influence of temperatures (10 - 140°C) and electric strength ( $E_o = 1 - 5\text{kV/cm}$ ) with constant $l/a$ ratio ( $l/a = 4$ ) .....	41
Figure 3-13: Collision time of the water droplets under the influence of temperatures (10 - 140°C) and $l/a$ ratio ( $l/a = 2 - 5$ ) with constant electric strength ( $E_o = 1\text{kV/cm}$ ).....	41
Figure 3-14: Schematic diagram of a uniform electric field.....	43
Figure 3-15: Schematic diagram of a non-uniform electric field.....	44
Figure 4-1: Coulometric Karl Fischer Titration.....	50
Figure 4-2: The whole static water-in-oil emulsion separation system.....	52
Figure 4-3: Schematic of water-in-oil emulsion separation setup.....	52
Figure 4-4: Two flat-plate electrodes water-in-oil emulsion separator.....	53
Figure 4-5: Overview of the emulsion separation system using two flat-plate electrodes.....	54
Figure 4-6: Cone-shaped cylindrical water-in-oil emulsion separator.....	55
Figure 4-7: Comparison of chemical reaction effect between uninsulated and insulated electrodes.....	56
Figure 4-8: Pictures of the cone-shaped and pressurized tubes: (a) Cone-shaped tube, (b) Pressurized tube.....	57
Figure 4-9: Centrifuge with heat treatment: Benchmark' 14 from L-K Industries.....	59

Figure 4-10: Cone-shaped separation tube of the heating centrifuge.....	59
Figure 4-11: Overall diagram of the dynamic water-in-oil emulsion separating system.....	60
Figure 4-12: Inline air heater: Omega AHPF series.....	62
Figure 4-13: Variac Voltage Transformers.....	62
Figure 4-14: Flow meter: Omega FPD3002-D.....	63
Figure 4-15: Temperature probe using K-type thermocouple bar.....	64
Figure 4-16: Thermometer: Omega HH74K.....	65
Figure 4-17: Whole setup for the dynamic water/oil separation system for lower flow rate.....	66
Figure 4-18: Peristaltic pump: Masterflex C/L 77122-24 from Cole-Parmer.....	67
Figure 4-19: Dimension of the separation tube for lower flow rate test.....	68
Figure 4-20: Capillary tube with a cap for lower flow rate test.....	69
Figure 4-21: Picture of the customized separation tube for low flow rate.....	69
Figure 4-22: Separation tubes attached to the holder in the heating oven.....	70
Figure 4-23: The whole dynamic water/oil separation system for higher flow rate.....	71
Figure 4-24: Series of the separation tubes in the heating oven.....	72
Figure 4-25: Diagram of the separation tubes fixed on the holder and the flow direction of the emulsion.....	72
Figure 4-26: Peristaltic tubing pump (EW 07522-20 from Cole Parmer).....	73
Figure 4-27: Magnetic gear pump (GJ-N23 from Burt).....	74
Figure 4-28: Dynamic separation tube for higher flow rate.....	75
Figure 4-29: Dimension of the cone-shaped cylindrical separation tube for the continuous water/oil separation system at higher flow rate.....	76
Figure 4-30: Flow controlling needle valve (SS-20VS4 from Swagelok).....	77

Figure 4-31: Power consumption measurement equipment: (a) small resistor, (b) digital multimeter and analogical oscilloscope.....	79
Figure 5-1: Simulation of the magnitude of electric field distribution (by C. Zheng, 2018): (a) top-view, and (b) sectional front view. In the figure shows the configuration (left) and the mapping (right): ① central electrode (5kV applied), ② air gap, ③ insulating glass layer, ④ emulsion, ⑤ glass tube, ⑥ copper foil (ground).....	82
Figure 5-2: Simulation of the $\nabla \vec{E} $ in emulsion (by C. Zheng, 2018): (a) top-view, and (b) sectional front view.....	83
Figure 5-3: Comparison of water/oil separations between flat plates and cylindrical electrodes.	85
Figure 5-4: Comparison of water/oil separation with two different thicknesses of the center electrodes: 7mm (left) vs. 1.65mm (right) .....	86
Figure 5-5: Comparison of water/oil separations with two different lengths of the center electrodes at different temperatures and voltages.....	88
Figure 5-6: Comparison of water/oil separation with the effect of air-gap between the center electrode and its capillary tube.....	90
Figure 5-7: Comparison of water/oil separations with two different lengths of the center electrodes at different temperatures and voltages.....	91
Figure 6-1: Phase change of 5% and 10% water-in-oil microemulsions by increasing temperature.....	95
Figure 6-2: Water-in-sunflower oil macroemulsions by increasing temperature.....	96
Figure 6-3: Separations of water/oil microemulsions by heat treatment.....	97
Figure 6-4: Separations of water/oil microemulsions by applying electric fields.....	98
Figure 6-5: Temperature effect on the separations of 5% water-in-oil microemulsions.....	100

Figure 6-6: Temperature effect on the separations of 10% water-in-oil microemulsions.....	101
Figure 6-7: Decrease of the residual water concentrations in oil phase with increasing temperature.....	103
Figure 6-8: Voltage effect on the separations of 10% water-in-oil microemulsions.....	104
Figure 6-9: Change of water concentrations with increasing voltages.....	106
Figure 6-10: Decreases of water concentration of the separated oil phase with test times (10% water-in-oil microemulsion, 90°C, 1kV, 50Hz) .....	106
Figure 6-11: Frequency effect on the separations of 10% water-in-oil microemulsions.....	108
Figure 6-12: Change of water concentrations with increasing frequencies.....	109
Figure 6-13: Effect of duty cycle for 10% water-in-oil microemulsion.....	110
Figure 6-14: 10% water-in-sunflower oil separations: (a) heating only, (b) electrostatic force only, (c) heating + electrostatic force.....	112
Figure 6-15: 10% water-in-sunflower oil emulsion separations for different temperatures.....	114
Figure 6-16: Decrease of water concentrations with increasing temperature.....	115
Figure 6-17: 10% water-in-sunflower oil emulsion separations for different voltages.....	117
Figure 6-18: Change of water concentrations with increasing voltage.....	118
Figure 6-19: 10% water-in-sunflower oil emulsion separations for different frequencies.....	119
Figure 6-20: Change of water concentrations with increasing frequencies.....	120
Figure 6-21: Power Consumptions of the system with different voltages.....	123
Figure 6-22: Power Consumptions of the system with different frequencies.....	123
Figure 6-23: Precipitation time of the water droplets with various droplet sizes.....	125
Figure 6-24: Collision time of the water droplets with various electric strengths.....	125

Figure 6-25: Comparison of the residual water concentrations between micro- and macroemulsions.....	127
Figure 6-26: Comparison of the residual water concentrations between micro- and macroemulsions with various applying voltages.....	129
Figure 6-27: Comparison of the residual water concentrations between micro- and macroemulsions with different frequencies.....	130
Figure 6-28: Comparison of water/oil separation between high pressure and cone-shaped tubes.....	132
Figure 6-29: Water concentrations of the separated oil with different flow rates.....	137
Figure 6-30: Temperature effect on the W/O separation at 1500 RPM: (a) 5% W/O microemulsion, (b) 10% W/O microemulsion.....	139
Figure 6-31: The effect of revolution speed on the W/O separation at 90°C: (a) 5% W/O microemulsion, (b) 10% W/O microemulsion.....	141

## Nomenclature

nm	= Nanometer
$\Delta G$	= Gibbs free energy
$\Delta A$	= Change of surface area
$\gamma$	= interfacial tension
T	= Temperature
$\Delta S_{\text{conf}}$	= configurational entropy change
$\Delta G_{\text{em}}$	= Required Energy
$V$	= Total volume of the emulsion
$R_f$	= Average radius of the created emulsion
n	= Number of droplets of the dispersed phase
$k_B$	= Boltzmann constant
$\phi$	= Dispersed phase volume fraction
$\mu\text{m}$	= micrometer
cSt	= centistokes
Hz	= Frequency of the electric field
AC	= Alternating current
DC	= Direct current
kV	= Voltage of the electric field
$^{\circ}\text{C}$	= Degree of Celsius

EP = Electrophoretic  
DEP = Dielectrophoretic  
 $a$  = Radius of water droplet  
 $\rho_w$  = Water density  
 $\rho_o$  = Oil density  
 $g$  = Gravity  
 $\mu_o$  = Dynamic viscosity of oil  
 $V_V$  = Vertical velocity  
 $V_H$  = Horizontal velocity  
 $F_{el}$  = Electric force  
 $\epsilon$  = Permittivity of the oil  
 $E_o$  = Electric strength  
 $l$  = Distance between the droplet centers  
 $F_{an}$  = Van der Waals force  
 $F_{V,H}$  = Horizontal flow resistance  
 $F_{V,V}$  = Vertical flow resistance  
 $h$  = Vertical distance of water droplet  
 $t_V$  = Precipitation time  
 $K_e$  = Clausius-Mossotti factor  
 $\epsilon_w^*$  = Complex permittivity of water  
 $\epsilon_o^*$  = Complex permittivity of oil  
 $\omega$  = Angular frequency

$\sigma_w$  = Conductivity of water

$\sigma_o$  = Conductivity of oil

C = Capacity of the capacitor

b/a = Ratio between outer and inner diameter

L = Effective length of the electrode

wt. = Weight

psi = Pounds per square inch

°F = Degree of Fahrenheit

VAC = AC voltage

RPM = Revolutions per minute

W = Electric power

V = Voltage

mA = Current (milliamperes)

$\Omega$  = Ohm (electrical resistance)

# Chapter 1. Introduction

## 1.1 Background and Motivation

The efficient removal of water from oil phase has been an important issue in the petroleum and chemical industry for many decades [1-2]. There are many different aqueous coalescence techniques which are targeted to remove water from the water-in-oil emulsion: gravity, centrifugal, chemical treatment, heating, electrostatic, mechanical, filtration, *etc* [2-4]. These methods can be employed in combination to achieve higher efficiency. In this dissertation, heating and electrostatic methods were combined to achieve higher performance of water/oil separations.

Electrostatic coalescence was first developed in the petroleum-related industries as a solution to promote the coalescence of water droplets in water-in-oil emulsions [2]. This electric field assisted coalescence (electrocoalescence) is regarded as one of the most efficient methods for water/oil separation. When exposed to an electric field, small water droplets move towards or collide with each other due to electrostatic forces, such as dipole-dipole interaction and dielectrophoretic force. As a result, the merging and coalescence of these droplets can increase the droplet size and eventually lead to settling and separation of water from the oil phase.

This water/oil separation by electric field can be further expedited by heat treatment because some properties such as density, viscosity, and dielectric constant of oil phase become more favorable for separation as temperature increases. Viscosity is especially important

because it decreases rapidly as temperature increases, thus accelerating the movement and coalescence of water droplets [2, 5].

In the theoretical study of water droplets movement in oil phase in electric fields, several key forces acting on the water droplets are considered. Dipole-dipole and dielectrophoresis (DEP) forces are two electric forces that mainly affect the movement of water droplets in oil phase. Also, the coalesced droplets can be deposited due to the gravitational force.

In this analysis, dipole-dipole force and gravity are considered to expect the movement of the water droplets in electric field. Droplet movement can be dissected into vertical and horizontal components. Gravity is vertically applied to the droplets, and electric field is applied horizontally due to the vertically located electrodes. The precipitation and collision times of droplets are numerically calculated with the effects of temperature, droplet size, electric strength, and distance between droplets. The results of this calculation will be compared to our experimental data to validate these theoretical calculations.

Emulsions are classified into macroemulsion or microemulsion based on the particle size. The physical characteristics of these two emulsion classes are studied. Microemulsions are more stable compared to macroemulsions due to increased entropy of the surfactant interface. Due to its stability, microemulsions are more difficult to separate into water and oil phases. Therefore, in this paper, the water/oil separations of micro- and macroemulsions will be performed and compared in order to study the effects of phase state on the emulsion.

This study may contribute to both the academic research and industrial application. Firstly, the movement of water droplets in the oil phase under the electric field is investigated for academic purpose. In detail, there are several important factors that affect the water droplet movement such as droplet size, temperature, voltage strength, *etc.* The enhanced mobility of the

droplets by improving these factors may reduce the separation time of the emulsions. The combined water/oil separation system will be used to experimentally validate this study that can work for both microemulsion and macroemulsion.

As an industrial application, we can develop water/oil separation systems using the combined method of heating and electric fields. This combined separating method may reduce the separation time and enhance the quality of the separated oil. The energy consumption of the water/oil separation system is proportional to the operation time. If the operation time is reduced using the combined separation system, we may reduce the energy consumption significantly. This developed water/oil separation system can be also used to develop absorption chillers in industries. Especially, if the microemulsions are used as absorbents, the performance of the absorption chiller may improve significantly compared to the conventional absorbents.

## **1.2 Objective and Scope**

The objective of the present work is to successfully separate water-in-oil emulsions with a high quality of separated oil phase. Both macroemulsion and microemulsion are separated by the combined exposure to radial electric field and elevated temperature. A microemulsion is very difficult to separate through a single separation method due to its tiny water droplet size, which is on the nanometer scale. A combined separating method (*i.e.* heating + electrostatic force) can be used to achieve this goal. This combined method can be used to enhance the separation efficiency of the macroemulsions as a practical application. Overall these results will have broad impact on the crude-oil purification.

Static separation tests for water-in-oil emulsions were executed to investigate the improvement of water/oil separations using this combined method and the effect of temperature,

voltage, and frequency on separation time and quality. The experimental results with these factors are compared to the results of the theoretical calculation. After that, dynamic water/oil separation system was built, and continuous water/oil separation tests were performed with different temperatures and flow rates. Dynamic separation system is more industrially relevant due to its scale-up separation. Therefore, the results of static and dynamic separation will be also compared to validate that dynamic system has comparable separation quality.

In this paper, theoretical calculations are conducted to estimate the movement of the water droplets in oil phase with different temperatures, electric strengths, and droplet sizes. The effects of these factors are also determined by executing experimental tests for water/oil separation, and the results are compared to validate the theoretical considerations. In regard to experimental setup, a separation system was built by using a homemade cylindrical cone-shaped separator equipped with coaxial cylindrical electrodes. Electric fields in combination with heat treatment are utilized to accelerate the water/oil separation from the emulsion. The effects of electric voltage, frequency, and temperature on the separation time and quality of the separated oil will be experimentally investigated. The quality of the separated oil phase is determined by measuring the residual water concentrations in separated oil.

The goal of this work is to obtain high quality of separated oil using this novel water-oil separation system, which combines heating and electric field. Static and dynamic separation systems were used to perform the experiments with different conditions. The technical objectives of this work are as follows:

1. To perform theoretical calculations to determine the movement of the water droplets in the oil phase

2. To study the effect of temperature and electric field (*i.e.* voltage and frequency) on the separations of a water-in-oil emulsion (*i.e.* separation speed and quality)
3. To assess the capabilities of microemulsion separation under a combined treatment of elevated temperature and a radial electric field
4. To conduct crude-oil separation by this novel combined method as a practical, industrial application
5. To establish the improvement of using this new combined system compared to the single methods
6. To measure the power consumption of this combined system to investigate the energy saving of this system in industries
7. To execute separation tests by using a novel designed dynamic water/oil separation system
8. To validate the theoretical calculations compared to the results of the experimental tests under the effects of increasing temperature and electric field

## Chapter 2. Literature Review

### 2.1 Introduction

This chapter will introduce two different types of emulsions based on the particle sizes: macroemulsion and microemulsion. The physics and characteristics of the two emulsions will be studied. Surfactants are added to make water-in-oil emulsions. The types and roles of the surfactants will also be investigated in this chapter. Crude-oil is the most popularly used emulsion in the industry. The types and characteristics of crude-oil will be reviewed. However, crude-oil has limitations for conducting scientific experiments due to its toxicity and different properties based on its origin. Several oils can replace crude-oils, and specifically, sunflower oil substitutes crude-oil in this study. In addition, this chapter will explain the demulsification process of water-in-oil emulsion. There are several methods which initiate or expedite the water-oil separations: heating, centrifugal force, filtration, electric field, *etc.* In this study, heat treatment and electrostatic force will be used, and these two methods will be combined to generate higher efficiency of water/oil separations. Lastly, studies of the forces (*i.e.* gravity, dipole-dipole and dielectrophoresis (DEP) forces) acting on the water droplets in electric fields will be introduced, and numerical calculations will be performed to expect the movement of the water droplets.

## 2.2 Emulsions

Emulsions are formed with mixing of two immiscible phases (*i.e.* water and oil) by adding surfactants. Surfactants can be settled as a monolayer at the interface between the oil and water. Emulsions can be classified into macroemulsions and microemulsions based to their particle sizes. The diameter of the particles in macroemulsions is greater than 100 nm, while it is less than 100 nm in microemulsions [6]. Macroemulsions are kinetically stable and thermodynamically unstable, while microemulsions are the opposite [7].

The thermodynamics of emulsions can be explained by a derivation of the Gibbs free energy equation. The accompanying free energy change can be expressed as a sum of the free energy for generating new area of interface and configurational entropy in the form as shown in Eq. (2-1), where  $\Delta G$  is a free energy of formation,  $\Delta A$  is the change in surface area on emulsification,  $\gamma_{12}$  is the interfacial tension between two phases (e.g., water and oil) at temperature T (K), and  $\Delta S_{conf}$  is a configurational entropy change [8, 9]:

$$\Delta G_{form} = \Delta A \gamma_{12} - T \Delta S_{conf} \quad (2-1)$$

### 2.2.1 Macroemulsions

Macroemulsions, generally called emulsions, have droplets with a diameter larger than 0.1 $\mu$ m. Macroemulsions are opaque (or white) because the bulk of the droplet is larger than wavelength of light, and most of the oils have higher refractive indices than water [10]. They are kinetically stable and thermodynamically unstable [11]. Therefore, if they remain stable for long period of time, they will finally reach phase separation to achieve a minimum in free energy.

Macroemulsions can be formed by stirring or shaking of the immiscible water and oil phases [12-13]. The particle sizes of the macroemulsions depend upon the amount of energy used to mix the phases. Higher mixing energy can create smaller size of the particle. The energy required to generate a certain size of the particles can be roughly estimated in the Eq. (2-2), where  $\Delta G_{em}$  is the required energy,  $\gamma$  is the interfacial tension between two phases,  $V$  is the total volume of the emulsion, and  $R_f$  is the average radius of the created emulsions [14]:

$$\Delta G_{em} = \frac{3\gamma V}{R_f} \quad (2-2)$$

### 2.2.2 Microemulsions

Microemulsions are isotropic mixtures of immiscible water and oil phases. The average diameter of the particles is approximately 10 – 50 nm. They are clear and thermodynamically stable. Microemulsions may become unstable and change their phase at especially low or high temperatures.

The formation of microemulsion is described as a subdivision of the dispersed phase into very small droplets. Then, the configurational entropy change,  $\Delta S_{conf}$ , can be roughly demonstrated as indicated in Eq. (2-3), where  $n$  is the number of droplets of the dispersed phase,  $k_B$  is the Boltzmann constant, and  $\phi$  is the dispersed phase volume fraction [8, 15]:

$$\Delta S_{conf} = -nk_B [\ln \phi + \{(1 - \phi) / \phi\} \ln(1 - \phi)] \quad (2-3)$$

Substituting Eq. (2-3) into Eq. (2-1) gives an expression for obtaining the maximum interfacial tension between two phases. The droplet number increases and  $\Delta S_{\text{conf}}$  is positive in dispersed condition. If the surfactant can reduce the interfacial tension to a sufficiently low value, the energy term ( $\Delta A\gamma_{12}$ ) in Eq. (2-1) becomes relatively small and positive, thus allowing a negative free energy change, that is, spontaneous microemulsification. Thermodynamic theory considers the entropy of droplets and thermal fluctuations at the interface as significant parameters leading to interfacial bending instability. In order for a microemulsion to be formed, a negative value of  $\gamma$  is required.

Microemulsions are typically more stable than the macroemulsions due to the increased entropy of the surfactant interface. Talmon and Prager [16-17] considered the entropy of mixing of the water and oil regions, and they first estimated the entropy. Recently, a thermodynamic model for microemulsion has been considered not only the entropy of the interface but also the bending energy. The relatively large entropy of mixing droplets and continuous medium explains the spontaneous formation of microemulsion. Schulman et al. [18] drew attention to the importance of the interfacial film. They considered that the formation of a complex film at the water-oil interface induces the spontaneous formation of microemulsion droplets.

The large dispersion of entropy arises from the mixing of one phase in the other in the form of large numbers of small droplets. There are also other favorable entropic contributions arising from other dynamic processes such as surfactant diffusion in the interfacial. Thus, a negative free energy of formation is achieved when large reductions in surface tension are accompanied by significant favorable entropic change. In such cases, microemulsification is unconstrained and the resulting dispersion becomes thermodynamically stable. The aggregation of the surfactant and co-surfactant at the interface induces a decrease of chemical potential which

creates an additional negative free energy change called a dilution effect [19]. This phenomenon describes the role of co-surfactant and salt in a microemulsion formed with ionic surfactants. The co-surfactant decreases surface tension and produces an additional dilution effect.

When the interfacial tension is low but positive, the interface may become unstable due to a sufficiently large increase in entropy by dispersion. The entropy change decreases the free energy and overpowers the increase caused by the formation of interfacial area. Therefore, net free energy change is negative [20].

## **2.3 Surfactants Science**

Surfactants are added into the water and oil phases to make a stable emulsion. Surfactants (SURface ACTive AgeNTs) are amphiphilic molecules which contain water-loving head (hydrophilic) and oil-loving hydrocarbon tail (hydrophobic) groups. The surface of the dispersed phase is covered with a single layer of the surfactant with their hydrophobic group. Surfactants can reduce the surface tension and stabilize emulsion from flocculation and coalescence [21].

Surfactants have the hydrophilic head attached to the aqueous phase and the hydrophobic tails dissolved in the oil phase. Co-surfactants may be added and these can reduce the surface tension and fluidize the surfactant film. The addition of surfactants and co-surfactants can increase the entropy of the system and lead the system to reach a thermodynamically stable condition [21].

There are two types of surfactants: ionic and non-ionic surfactants. Ionic surfactants consist of molecules that have either negatively or positively charged heads. Anionic has negative charge (–), cationic has positive charge (+), and Zwitterionic has both positive and negative charges (+) and (–) [22]. On the other hand, non-ionic surfactants have polar head group.

They do not have any electrical charge. Their heads are polymeric chains dissolved in water. These polymeric chains can push off other droplets for stopping them from coalescing. Non-ionic surfactants reduce surface tension of water. This non-electric charged surfactant is not ionized in aqueous solutions because its hydrophilic group is non-dissociable [23].

The addition of non-ionic surfactants to the water-oil emulsion was found to stabilize the adsorption state in an electrostatic field. The addition of surfactants into water-oil solution is very effective for eliminating electric charge. If electric charge accumulates in the vessel, the adsorption of water droplets becomes out of control. The negative charge on the aqueous droplets is reduced by adding surfactants, and as a result the droplets retain stable. Non-ionic surfactants have several advantages compared to ionic surfactants. They can cover a wide range of HLB values. They are environmentally friendly because they are easily biodegradable [24-26].

The dissociation of surfactants during demulsification process has been studied. When the emulsion is broken, water phase can be coalesced and settled. The head of the surfactant is in contact with the released water phase at the bottom of the test vessel. If there is enough surface area to observe all of the surfactants, surfactants can be destabilized. Finally, the surfactants reach a new balanced state and leave the interface between water and oil phases. This allows water droplets to coalesce [2, 27].

## **2.4 Crude Oil Purification (Separation)**

### **2.4.1 Crude oil Properties**

Crude oil is a mixture of hydrocarbons and can be considered as a macroemulsion due to its water droplet sizes, which are measured in micrometer ( $\mu\text{m}$ ) scale, in the oil phase. Crude oil initially contains 5-20% of water when it is pumped from the ground. The water particles in

crude oil emulsion are surrounded by the natural surfactants such as asphaltenes and resins [28-30]. This water must be removed before it enters refinery system. Therefore, the extracted crude oils must be purified by removing the water particles inside the oil phase. Many technologies have been invented and developed in last several decades to enhance the efficiency of the crude oil purification.

Crude oils consist of a mixture of various components. Its chemical compositions are varied depending on its geographic origin. Crude oils can be classified into three different types based on the viscosity and density: light, medium and heavy crude oils [31]. The American Petroleum Institute (API) gravity is a unit for the inverse measurement of petroleum’s density. API indicates how light or heavy a petroleum is compared to water which has 10 API. If the API gravity is greater than 10, it is lighter and can float on water; otherwise, it is heavier and will sink. Heavier crude oil shows higher density and viscosity compared to lighter crude oil as indicated in Table 2-1. Due to the difference of density and viscosity, heavier crude oil is much difficult to be purified than lighter crude oil [32-33].

**Table 2-1: Viscosities and Densities of three different crude oils**

<b>Types of Crude Oil</b>	<b>Kin. Viscosity (cSt)</b>	<b>Density (API)</b>	<b>Density (kg/m<sup>3</sup>)</b>
Light crude oil	5.96 – 4.01 (40 – 60°C)	> 31.1°	< 870
Medium crude oil	34.63 – 17.76 (40 – 60°C)	31.1° - 22.3°	870 – 920
Heavy crude oil	223.5 – 78.71 (40 – 60°C)	22.3° - 10°	920 – 1000

### **2.4.2 Alternatives to Crude oil for Scientific Experiments**

Crude oils are the most popularly used and focused oils in industries and academic areas for last century. However, crude oils are toxic and contain different components from one reservoir to another. These characteristics of crude oils limit the ability to obtain accurate and reliable experimental results. Therefore, crude oils can be substituted for several oils for academic tests. For example, silicone oil, sunflower oil, and castor oil are popularly used as replacements for light, medium, and heavy crude oils respectively for the scientific water-oil separation tests. This is due to their similar properties such as density, viscosity, and dielectric constant with crude oils. In this study, water-in-sunflower oil emulsion is used as a substitute for medium-crude oil emulsion.

## **2.5 Demulsifications**

Demulsification, also called water-oil separation, is the action of breaking water-oil emulsion into water and oil phases. There are two steps of this process: Flocculation (also called aggregation, agglomeration, coagulation) and coalescence. In flocculation process, droplets can cluster together and they still have their identity. The speed of flocculation depends on the temperature, viscosity, density, and electric fields. In the coalescence process, water droplets move toward each other and coalesce to form larger droplets. Coalescence can be expedited by higher rate of flocculation, higher interfacial tension and temperature, lower oil and interfacial viscosities, and chemical demulsifiers.

External forces may be applied to expedite the demulsification process. For example, electric fields can break emulsion by attracting the water droplets which are oppositely charged. This electrostatic coalescence is suitable because the oil phase has a remarkably lower dielectric

constant than that of the water phase. The emulsion breaking processes by applying electric fields have been described by many authors [6, 12, 34]:

1. Emulsions pass through the electric fields between insulated electrodes
2. Emulsions start breaking in the electric fields
3. The emulsions existing in the coalescer can be almost completely broken

## **2.6 Water/Oil Separation Methods**

### **2.6.1 Heat Treatment**

Heat treatment can expedite the water droplet coalescence and separation in water-in-oil emulsions. Generally, the viscosity of the oil and solubility of surfactant decreases with increasing temperature, which allows the water droplets to move more rapidly and enhances the coalescence rate [2, 5, 35].

In addition, the phase transition of microemulsions may be induced by elevated temperature. Microemulsions become unstable and change to a macroemulsion state when the temperature is over the cloud point. Therefore, heating may speed up the separation of microemulsions by changing the microemulsion phase into the macroemulsion state over the cloud point.

Temperature is also a critical parameter for surfactants due to the strong dependence of their solubility on temperature in emulsion. The solubility of surfactants decreases with increasing of temperature because they tend to curl into hydrophilic coils at a lower temperature and to be randomized by heating while a presenting more hydrophobic nature. As a result, the dissociation of surfactants is induced by increased temperature [36]. As the temperature increases

above cloud point, surfactants become insoluble and emulsion starts separating into two phases [37-38]. The denser (lower) phase contains most of the surfactants [24].

Sellman et al. [39] executed viscosity and density measurements of water-in-oil emulsion with various temperatures (40 - 140 °C). They used API 18 and API 30 crude oils and the frequency range was 50 - 60 Hz. Atta et al. [40] used cone-shaped separation tube for water-in-crude oil separation tests at the high temperature. The water concentration range was 10 – 50%. The water-in-crude oil emulsions were stored at 85°C and then applied electric field for 20 minutes. This separated emulsions were settled for another 10 minutes. The emulsions were clearly separated and the separated water became almost transparent at the bottom.

Hajivand et al. [41] investigated the effects of various temperatures for water-in-crude oil separation. They used six different temperatures (10, 20, 50, 60, 70, 80°C), and measured the amounts (%) of the separated water. They concluded that higher temperatures can promote destabilization of emulsions due to increased Brownian motion and mass transfer across the interface. The interfacial viscosity of the continuous oil phase decreases as the temperature increases. This reduced viscosity drives the momentum of the particles increased.

### **2.6.2 Electric Field**

Electrostatic coalescence was invented for the petroleum-related industries, and this method uses electric fields to promote the coalescence of small water droplets in water-in-oil emulsions [2]. The small water droplets move towards each other or collide with each other due to the electrostatic forces, such as dipole-dipole interaction and dielectrophoretic force, acting on them. The merging and coalescence of those droplets enhanced by the electric field can increase the droplet size and eventually lead to settling and separation of water from oil phase.

There are several factors affecting electrocoalescence, such as type of current flow, voltage, frequency, electrode configuration, *etc.* Different types of current flow have been used for the electrocoalescence method: AC, DC, and pulsed DC [42-46]. DC is efficient in promoting droplet coalescence, but usually causes electrolytic corrosion. Therefore, it is rarely used in water-oil separation. AC was the most common method used in crude oil emulsion due to its tolerance to high water concentrations before the pulsed DC was introduced. Pulsed DC was proposed with insulated electrodes for high water content emulsions and has been extensively used since 1980s [2, 47]. AC field or pulsed DC is preferred to avoid chain formation. Pulsed DC provides a marked performance advantage over AC or DC power [2, 48-49]. Bailes and Larkari [50] showed that for pulsed DC electric field, 8 Hz of frequency delivered optimum coalescence rate. While pulsed DC has different types of wave shapes (*e.g.* sine, square, ramp, pulse, noise waves), square wave shape shows higher efficiency than other wave shapes [51]. Lesaint et al. [52] found that square waves show higher efficiency than sinusoidal and triangular waves. Therefore, in this paper, the square wave of pulsed DC is used for all of the tests.

High voltages (*e.g.* over 1kV) are normally required for electrostatic separation of water-in-oil emulsions. Increased voltage and frequency can increase water/oil separation speed and quality. However, electrical malfunctions such as short-circuit may occur if the amount of applied voltage or frequency is too high. Therefore, establishing optimum voltage and frequency is significant for enhancing the efficiency of water/oil separation. Zhang et al. [53] explained that establishing an optimum frequency is important for AC electric fields. Optimum frequency is affected by many factors such as physical and electrical properties, concentrations (%) of dispersed phase, droplet size, *etc.* Lundgaard et al. [54] used electro-coalescence in stagnant emulsions. Plane electrodes without insulation were used with 20 mm gap. The ranges of voltage

and frequency are 1.3 - 7.5 kV and 1 – 10,000 Hz. They executed many different tests to find the optimum voltage and frequency.

Coalescers are devices that are primarily used for emulsion separations. For an electric coalescer, the design for electrodes is one of the key factors. Electrodes are electrical conductors used to make contact with a nonmetallic part of circuit. There are two types of electrodes: uninsulated and insulated electrodes. Uninsulated electrode may cause short-circuit problem. The chance of the electric short-circuits significantly increases when the water concentration is above 20%. Since the crude oil may contain water concentration above 20%, it may not be a wise choice to use the uninsulated electrode. On the other hand, insulated electrodes have electrical breakdown strength to withstand the voltage. This can reduce electrical potential at the electrode emulsion interface [55-59]. In addition, the insulated electrodes can also enhance separation efficiency [60]. Fjeldy et al. [61] showed coated electrodes help preventing short-circuit and enhancing water separation and quality. Therefore, in this study, insulated electrodes are used for all of the separation tests.

The configuration (*e.g.* plate or cylinder) of electrodes can also affect separation performance due to their effect on electric fields [62]. As shown in Fig. 2-1, flat plate electrodes would create uniform electric fields, while cylindrical electrodes can generate non-uniform electric fields inside the separation tube. Non-uniform electric fields can enhance the water-oil separations compared to uniform fields [52, 60, 63-64]. In addition to generating non-uniform electric fields, cylindrical electrodes can create electric fields that cover most of the space in the tube. Therefore, in this experiment, instead of using two flat copper plate electrodes, cone-shaped cylindrical electrodes were used.

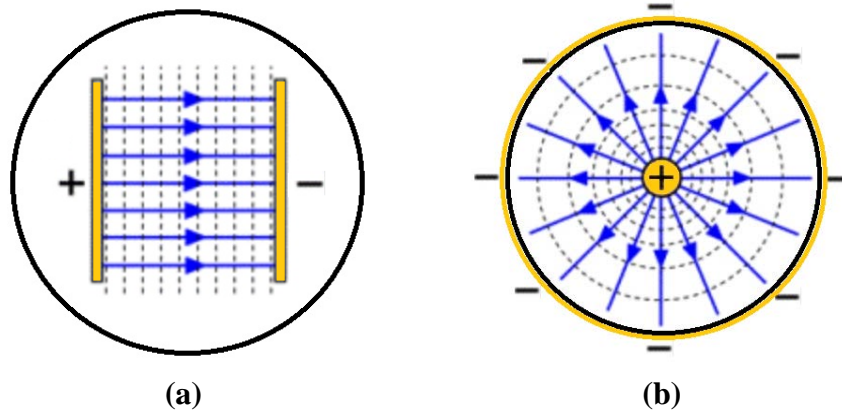


**Figure 2-1: Top view of Flat plates electrodes and cylindrical electrodes:  
 (a) Flat plates electrodes, (b) Cylindrical electrodes**

Hsu et al. [65] explained that electrodes are normally arranged as either widely-spaced short or closely separated long electrodes. Hosseini et al. [45] used cylindrical electrodes and generated non-uniform electric fields. One electrode was placed inside the emulsion and the other is submerged in acid vessel (electrolyte solution). The droplet sizes are the range of 20 – 200 nm for the experiments. Kim et al. [66] used water-in-crude oil emulsions which contain 20% of water phase. The ranges of AC voltage and frequency were 2 - 20 kV and 60 – 2,000 Hz. The electrodes were made of two flat copper plates which were located horizontally to the ground. The bottom electrode has many holes on the surface and this helps the separated water move down to the bottom of the separation chamber.

### **2.6.3 Combined Methods (Heating + Electric Field)**

A further enhancement can be achieved when two or more water/oil separating methods are combined or when applying multi-stage separators. For instance, heating, centrifugal force, filtration, and chemical addition have been utilized coupling with electric treatment. These combined methods enhanced the separation efficiency in various ways [2]. Lesaint et al. [52] used AC electric fields for executing dehydration of water-in-oil emulsion. The experiments were operated at three different temperatures: 20, 40, 60°C. The voltage range is 2 – 10 kV, and frequency range is 50 – 50,000 Hz. Several waveforms were used such as sine, triangular and square waves. Atta et al. [40] used cone shape separation tube for water-in-crude oil separation. The water concentration range was 10 – 50%. The water-in-crude oil emulsions were stored at 85°C and then applied electric field for 20 minutes. This separated emulsions were settled for another 10 minutes. The separated water and crude oil are shown in Fig. 2-2. The emulsions were clearly separated and the separated water became almost transparent at the bottom. In addition, the separated water phase is clearly observed by using the cone-shaped separation tube with reducing the volume in the bottom.

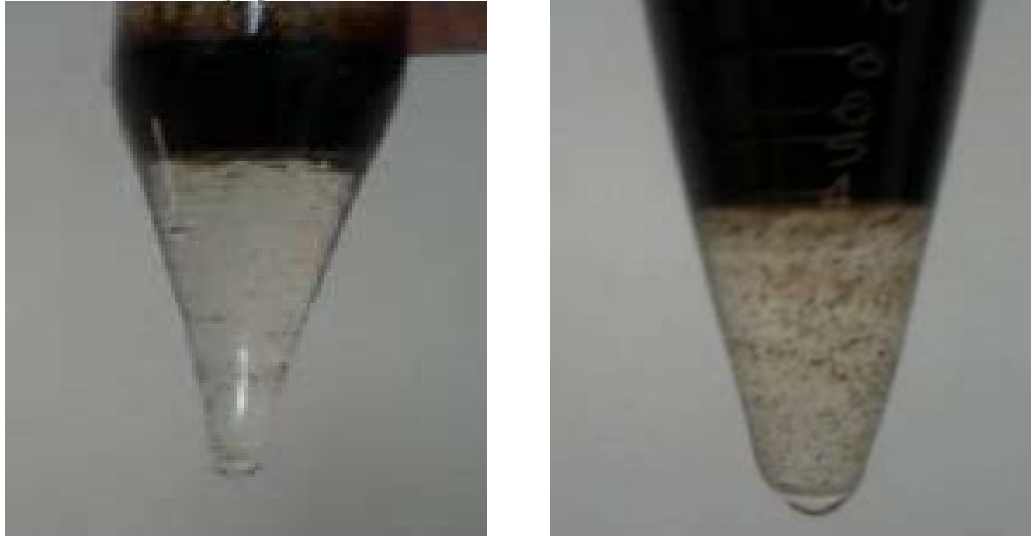


**Figure 2-2: Separated water/crude oil phases in cone-shaped tubes**

## **2.7 Water Droplets Coalescence by Electric Fields**

The separated water droplets coalescence process depends on two factors: breakdown of the continuous (oil) phase film and attractive force between water droplets. The film, which is located between water and oil phase, may be broken by any other external forces including electrostatic breakdown [67].

Electrostatic coalescences happen following these processes. First, droplets become polarized and move towards each other. Then, thin film is formed between the droplets. As long as this film exists, there is no droplets contact due to hydrodynamic resistance induced by the presence of the thin film. Coalescence can occur when the thin film separating two droplets is ruptured. The rupture of the film requires a certain level of energy. When the rupture happens, smaller water droplets coalesce into large droplets, and this promotes settling and separation of water from oil phase. The electrostatic force depends on the strength of electric field, droplet sizes, and distances. In lower electric fields, the water droplets have a tendency to return to a

random distribution when the electric field is switched off. Therefore, an electric field over the critical electric field, which is the value causing irreversible breakdown, is often applied to the system. In this paper, the voltage and frequency will be considered as factors affecting the water/oil separation along with the heating effect.

### 2.7.1 Gravitational Force

Water droplets between electrodes are under the influence of five forces: gravitational, hydraulic, electrophoretic (EP), dielectrophoretic (DEP), and dipole-dipole forces. Gravitational force, which is toward the ground, is equal to the droplet weight, while hydraulic force is a drag force to the opposite direction [68]. The movement of water particles by gravity is mainly affected by the size of the particles and temperature. The velocity of the water particle has been defined by the following Eq. (2-4), where  $a$  is a radius of water droplet,  $\rho_w$  is a water density,  $\rho_o$  is a density of oil phase,  $g$  is gravity and  $\mu_o$  represents a viscosity of oil phase:

$$V_V = \frac{a^2(\rho_w - \rho_o)g}{4.5\mu_o} \quad (2-4)$$

As indicated in Eq. (2-4), an oil phase viscosity and densities of water and oil phase can be influenced by the temperature. The density difference between water and oil phase increases and an oil viscosity decreases as temperature increases. This result brings that the sedimentation speed of the water droplets can be accelerated by the heat treatment.

Souza et al. [28] studied water droplets' sedimentation velocity in water-in-crude oil emulsions by the effects of water content (%), temperature and average droplet size. Mean water

droplet size is increased by increasing of water concentration (%) due to the condensed water droplets in oil phase. Sedimentation velocity of water particles increases as temperature increases and water concentration decreases.

### **2.7.2 Electrophoresis and Dielectrophoresis Forces**

There are two kinds of droplet movement under the influence of electrical fields: electrophoretic (EP) and dielectrophoretic (DEP) forces [69]. Electrophoresis is the motion of separated particles under the effect of a uniform electrostatic fields. Electrophoretic force relies on the electric field strength, droplet size, oil conductivity and viscosity, while it is independent on droplet spacing. In uniform electric field, a water particle, which is charged either positive (+) or negative (-), can move to the oppositely charged direction by the EP force. It can be maintained by replenishing the droplet charge [70].

On the other hand, dielectrophoretic force is applied on dielectric particles in non-uniform electric fields. It is dependent upon the droplet size and electric field strength, and is independent on the distance of the droplets. This force acts to gather water droplets in areas where the strongest electrostatic fields exist. If a water particle is equally polarized on both ends in a non-uniform electric field, the water particle can move to the direction of the stronger electric field [71]. This DEP force is negligible in a uniform electric field. Therefore, the water droplet coalescence can be enhanced in non-uniform electric field due to the simultaneous effect of DEP force with other forces [72].

Mhatre et al. [73] executed the water-oil separation efficiency tests with five different electrodes including parallel plate, quadruple, pin-plate, four-pin, and annular electrodes. They showed that pin-plate electrodes, which create asymmetric non-uniform fields, showed the

highest efficiency for the separation of water-in-oil emulsions. They also found the flow recirculation of the emulsion occurred under the non-uniform field generated by the pin-plate electrodes. This flow current may expedite the droplet coalescence by pushing finer droplets to higher electric field area.

Molla et al. [74] utilized DEP force to push droplets to the electric field maxima in their membrane filtration process. However, the sharp electric charges of the droplets exist only close to the electrodes. Hence, the DEP force affects strongly in the small distance and decays rapidly in the far field (54\_Molla 2005). Alinezhad et al. [75] measured the demulsification rates of water-in-crude oil emulsion and observed the electrocoalescence behavior under the non-uniform fields. The increase of the demulsification rate is due to the higher voltage gradient and greater accumulation of electric flux near the center electrode.

### **2.7.3 Dipole-dipole Force**

Dipole-dipole force represents the attractive force between one positive end and one negative end molecules. Dipole coalescence may occur when droplets are accumulated by several interactions such as Brownian motion, flocculation, electrophoresis, and sedimentation. Ion-dipole force represents the interaction between a charged ion and a polar molecule, while dipole-dipole force is created between two polarized droplets. The dipole-dipole interaction is dominant under a uniform electric field. This attraction is only effective at close distances between polarized droplets because the dipole-dipole force decreases rapidly as the inter-droplet distance increases. If the droplets are located far away, this effect alone is not enough to encourage droplet coalescence in a uniform field [76]. This dipole-dipole force between two droplets can be simply expressed in the Eq. (2-5), where  $\epsilon$  is a permittivity of the oil phase,  $E_o$  is

an electric strength,  $\alpha$  is a radius of water droplet, and  $l$  is the distance between the droplet centers [48]:

$$F_{el} = \frac{24\pi\epsilon E_0^2 \alpha^6}{l^4} \quad (2-5)$$

#### 2.7.4 Other Forces

There are several other forces acting on the droplets in water-oil emulsions: Van der Waals force, electrostatic repulsion, steric repulsion, Ostwald ripening, and Capillary forces. Van der Waal force represents electric attraction force between opposite charges. Electrostatic repulsion can be generated by the adsorption of ionic surfactants. Steric repulsion can be created by nonionic surfactants or polymers. Ostwald ripening is the phenomenon when smaller droplets in solution dissolve and deposit on larger droplet in order to reach a thermodynamically stable state. The ratio of the surface to area can be minimized in this state. Lastly, capillary force represents the force that a liquid can flow in narrow spaces without assisting any other external forces [77-78].

The droplets located near an electrode can be also polarized when contacting the electrode. This charges of droplets can be transfer to another neighboring droplets through contact. However, this droplet-contact effect is only applicable to the droplets next to the electrode and can be negligible to the general analysis on the study of the droplet in the bulk emulsion.

## Chapter 3. Theoretical Considerations

### 3.1 Introduction

One of the most efficient methods for water-oil separation is electric field assisted coalescence (electrocoalescence). Dipole-dipole force and dielectrophoresis (DEP) force are two major electric forces that affect to the droplet movement in oil phase. Dipole-dipole force represents the attractive force between two polarized droplets, while DEP force is exerted on the polarized particles in non-uniform electric field. The particles can be collided or coalesced with the interactions of these electric forces. The coalesced droplets can be moved down due to the gravitational force. Therefore, dipole-dipole force, DEP force, and gravity can be considered as main factors in deciding the movement of water particles in the oil phase.

This chapter will introduce the balance of the forces acting on the droplets in electric fields. Dipole-dipole force and gravity will be mainly considered in this analysis. The movement of the water droplets will be divided into two directions vertically and horizontally. The precipitation and collision time of the droplets will be calculated with different temperatures, droplet sizes, electric strengths, and distances between two droplets. Moreover, the effect of DEP force will be also studied separately. Especially, DEP force is considered as a significant factor in non-uniform electric fields [79].

### 3.2 Forces on the water droplets in electric fields

This chapter primarily considers the kinetic study of the droplet-droplet coalescence under the electric field. The balance of the forces acting on a pair of droplets is indicated in Fig. 3.1. In this model, dipole-dipole force between two droplets and gravity are considered as main forces. Dielectrophoresis (DEP) force is also one of the major forces especially in non-uniform electric field. However, DEP force can only strongly affect to the droplets near the center electrode and its electric strength decreases rapidly in the far field [74]. Also, DEP force is negligible especially in the uniform electric field. Therefore, DEP force cannot be considered in the general analysis of the water droplet movement, this force will be considered separately.

As shown in Fig. 3-1, horizontal electric fields can be created from the vertically located electrodes in this system, while the gravity ( $F_g$ ) acts vertically to the ground. Two attraction forces, electric dipole-dipole force ( $F_{el}$ ) and Van der Waals force ( $F_{an}$ ), are horizontally generated between two droplets. The flow speeds of the droplets, which are  $V_H$  horizontally and  $V_V$  vertically, can generate the forces of flow resistance ( $F_v$ ). The forces of flow resistance are divided into horizontal ( $F_{v,H}$ ) and vertical ( $F_{v,V}$ ) forces [34, 47, 79].

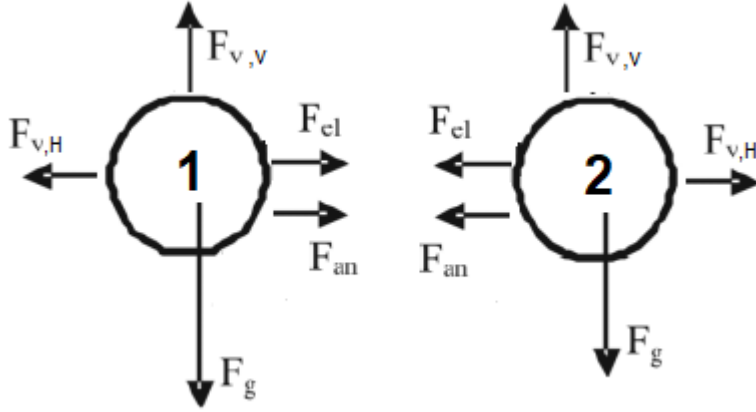


**Figure 3-1: Balance of the forces acting on a pair of droplets for horizontal electric fields**

The force of gravity ( $F_g$ ) on the water droplets with radius  $\alpha$  and water density  $\rho_w$ , dispersed into a continuous oil phase of density  $\rho_o$  is expressed in Eq. (3-1). The forces of flow resistance, which are the Stokes forces, through the continuous viscosity phase  $\mu_o$  along with the velocities  $V_H$  and  $V_V$  are indicated in Eq. (3-2) and (3-3).

$$F_g = \frac{4}{3}\pi\alpha^3(\rho_w - \rho_o)g \quad (3-1)$$

$$F_{V,V} = 6\pi\mu_o\alpha V_V \quad (3-2)$$

$$F_{V,H} = 6\pi\mu_o\alpha V_H \quad (3-3)$$

The electric force ( $F_{el}$ ) is the result of an external electrical field. This attractive dipole-dipole force ( $F_{el}$ ) between two water droplets can be simplified in the Eq. (3-4), where  $\epsilon$  is a permittivity of the medium surrounding oil,  $E_o$  is the strength of the electric field, and  $l$  is the distance between the droplet centers [35, 48]:

$$F_{el} = \frac{24\pi\epsilon E_0^2 \alpha^6}{l^4} = \frac{24\pi\epsilon E_0^2 \alpha^2}{(l/\alpha)^4} \quad (3-4)$$

The radii  $\alpha$  of the two droplets are assumed identical in Eq. (3-4). Therefore, the ratio of  $l/\alpha$  must be larger than two ( $l > 2\alpha$ ). Another attracting force applied between two droplets is Van der Waals force ( $F_{an}$ ). In this calculation, the Van der Waals force ( $F_{an}$ ) is ignored because this force is negligible in relation to the electrical force ( $F_{el}$ ) unless the distance between the droplets is around 1-10 nm [34].

### 3.2.1 Vertical Movement by Gravity

First, the vertical movement of the water droplets is investigated. In this movement, the force of gravity ( $F_g$ ) along with the force of vertical flow resistance ( $F_{v,v}$ ) is considered. For a droplet, applying the balance of forces in the vertical position can deliver the Eq. (3-5), where  $m$  represents the mass of the droplet, by using the equations of (3-1) and (3-2). The equation (3-7) for  $dV_V/dt$  is obtained from the Eq. (3-5) and (3-6) [79].

$$m \frac{dV_V}{dt} = \frac{4}{3}\pi\alpha^3(\rho_w - \rho_o)g - 6\pi\mu_o\alpha V_V \quad (3-5)$$

$$m = \frac{4}{3}\pi\alpha^3\rho_w \quad (3-6)$$

$$\frac{dV_V}{dt} = \frac{(\rho_w - \rho_o)g}{\rho_w} - \frac{4.5\mu_o V_V}{\alpha^2\rho_w} \quad (3-7)$$

Considering that this is a pseudo-steady state ( $dV_V/dt \approx 0$ ) [34], the vertical velocity ( $V_V$ ) can be calculated in Eq. (3-8). The sedimentation time ( $t_V$ ) of the droplet is also obtained in the Eq. (3-10) with the vertical distance  $h$  from the Eq. (3-9) [79].

$$V_V = \frac{\alpha^2(\rho_W - \rho_O)g}{4.5\mu_O} \quad (3-8)$$

$$\frac{dh}{dt} = V_V = \frac{\alpha^2(\rho_W - \rho_O)g}{4.5\mu_O} \quad (3-9)$$

$$t_V = \frac{4.5\mu_O h}{\alpha^2(\rho_W - \rho_O)g} \quad (3-10)$$

**Table 3-1: Properties of sunflower oil at different temperatures (10 - 140°C)**

Temp. (°C)	Water density (kg/m <sup>3</sup> )	Sunflower oil density (kg/m <sup>3</sup> )	Density diff. (kg/m <sup>3</sup> )	Sunflower oil kin. Vis. (mm <sup>2</sup> /s)	Sunflower oil dyn. Vis. (kg/m-s)	Sunf. oil dielectric constant
10	999.7	925.1	74.6	118.72	0.1098	3.21
20	998.2	916.9	81.3	73.45	0.0673	3.17
30	995.7	911.4	84.3	48.46	0.0442	3.12
40	992.3	904.3	88.0	33.78	0.0305	3.08
50	988.1	899.4	88.7	24.48	0.0220	3.04
60	983.2	892.6	90.6	18.52	0.0165	3.00
70	977.7	887.7	90.0	14.44	0.0128	2.96
80	971.8	879.8	92.0	11.53	0.0101	2.93
90	965.3	874.3	91.0	9.44	0.0083	2.89
100	958.4	867.0	91.4	7.78	0.0067	2.85
110	951.0	860.2	90.8	6.50	0.0056	2.81
120	943.1	853.6	89.5	5.62	0.0048	2.77
130	934.8	847.2	87.6	4.91	0.0042	2.73
140	925.9	840.8	85.1	4.37	0.0037	2.69

The vertical velocity ( $V_v$ ) is a function of the density difference between water and oil ( $\rho_w - \rho_o$ ), oil viscosity ( $\mu_o$ ), and the radius ( $\alpha$ ) of the water droplets as indicated in Eq. (3-8). The density and viscosity can be affected by the temperature. In this numerical calculation, we use sunflower oil as a continuous oil phase. Table 3-1 shows the values of water density and the density, viscosity and dielectric constant of sunflower oil with the increment of temperature (10 – 140 °C) [51, 55-56, 80]. The densities of water and sunflower oil decrease with increasing temperature as shown in Fig. 3-2. Density difference ( $\rho_w - \rho_o$ ) between water droplet and continuous oil phase is important to decide the droplet velocity as shown in Eq. (3-8). The density difference is indicated in Fig. 3-3 with various temperatures. The density difference increases up to around 100°C, then it starts decreasing if the temperature is over 100°C because the density of water decreases faster over the boiling point (100°C) as shown in Fig. 3-3 [79].

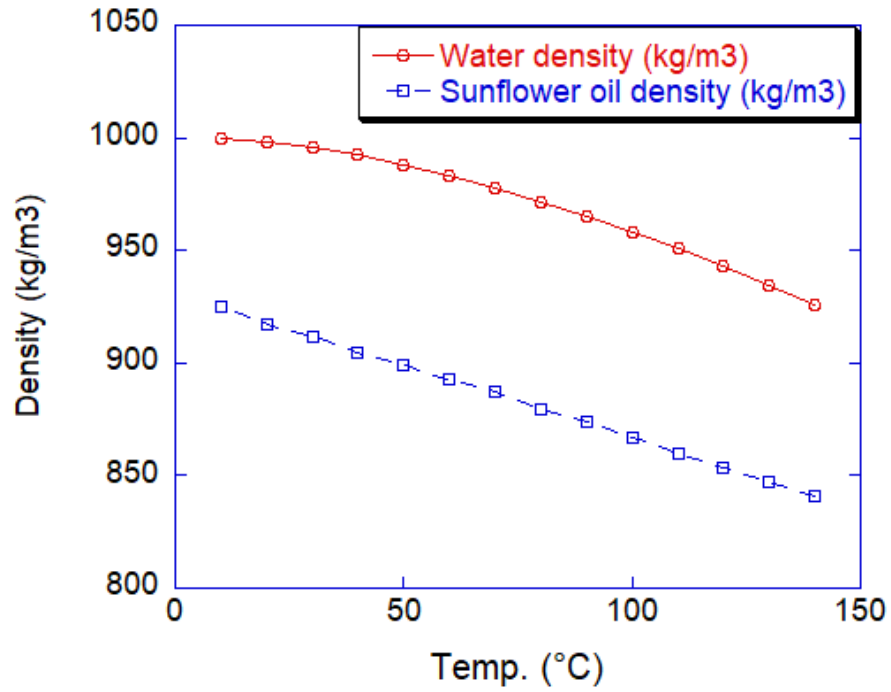


Figure 3-2: Densities (kg/m<sup>3</sup>) of water and sunflower oil at various temperatures (10 - 140°C)

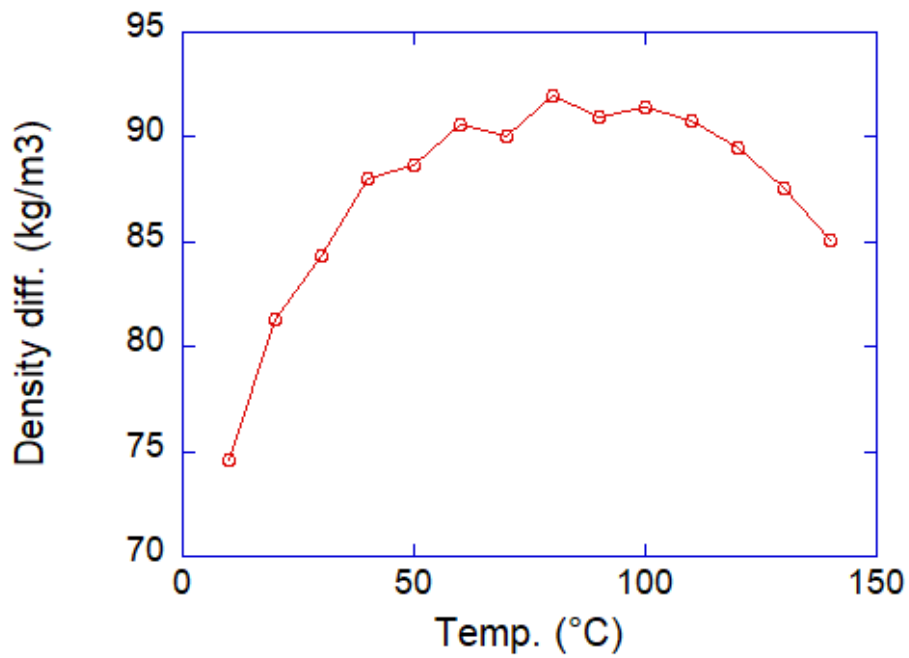
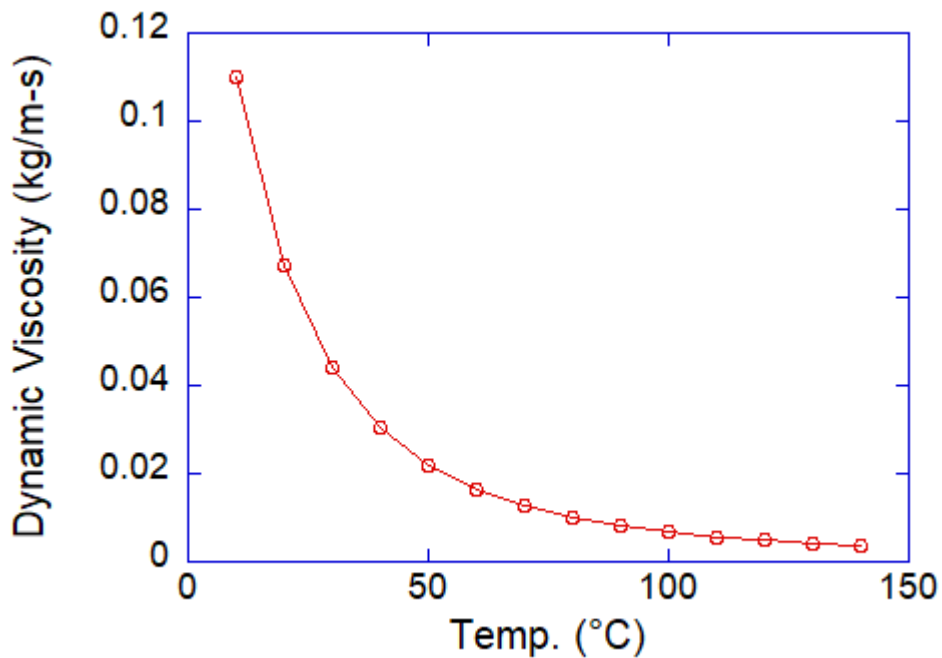
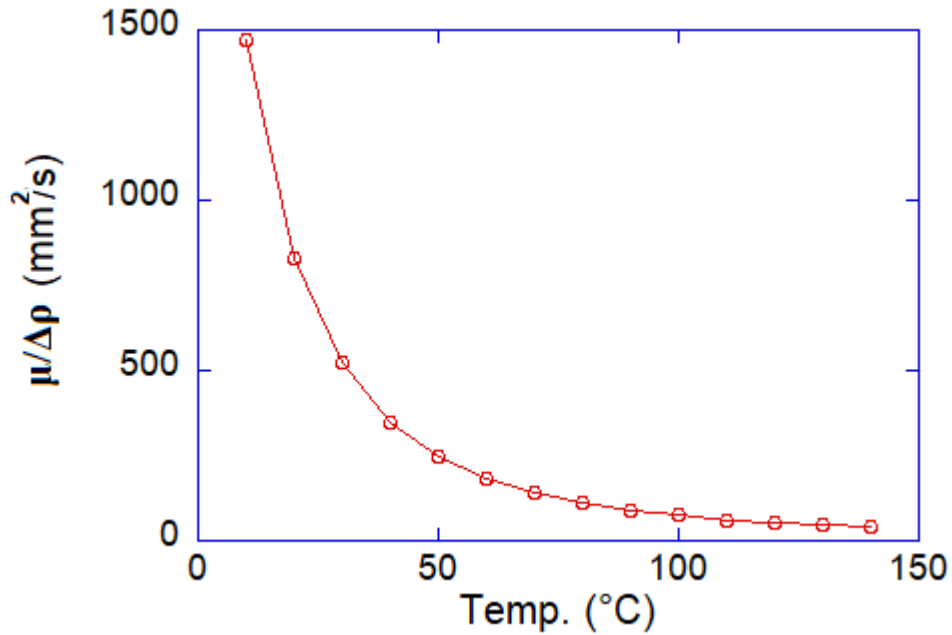


Figure 3-3: Density differences (kg/m<sup>3</sup>) between water and sunflower oil at various temperatures (10 - 140°C)

The dynamic viscosity of sunflower oil ( $\mu_o$ ) decreases as temperature increases. The viscosity decreases rapidly at the lower temperatures such as 10 - 50°C, then it decreases slowly at the higher temperature (over 80°C) as shown in Fig. 3-4. From the results of Figs. 3-3 and 3-4, oil viscosity is more sensitive than density difference with the increase of operating temperature. The density difference increases about 10% at the higher temperature (100°C) compared to the room temperature (25°C), while the oil viscosity decreases more than 10 times at the elevated temperature (100°C). The vertical velocity ( $V_v$ ) of the water droplet is proportional to the square of the droplet size ( $a^2$ ) and inversely proportional to the ratio of  $\mu_o/\Delta\rho$  as indicated in Eq. (3-8). Fig. 3-5 shows that the ratios of  $\mu_o/\Delta\rho$  keep decreasing as the temperature increases. Therefore, the vertical velocity is a function of the operating temperature and droplet size, and this must be increased by the increment of the temperature as well as its droplet size [79].



**Figure 3-4: Sunflower oil dynamic viscosities ( $\mu_o$ ) at various temperatures (10 - 140°C)**



**Figure 3-5: Ratios of the sunflower oil viscosity to the density difference at various temperatures (10 - 140°C)**

The calculations of the vertical velocity as effects of the droplet size and operating temperature are indicated in Fig. 3-6. This figure explains that increasing both droplet size and temperature can enhance the vertical velocity (precipitation speed) of the water droplet. Therefore, the precipitation of the water droplets can be expedited as the size of droplets and the operating temperature increase. The corresponding sedimentation times of the water droplets are also calculated. The vertical distance ( $h$ ) is assumed to be 10cm in this system. The precipitation time of the droplets decreases as droplet size and temperature increase as indicated in Fig. 3-7. This reduced precipitation time of the droplets can expedite the separation speed of the water-in-oil emulsions [79].

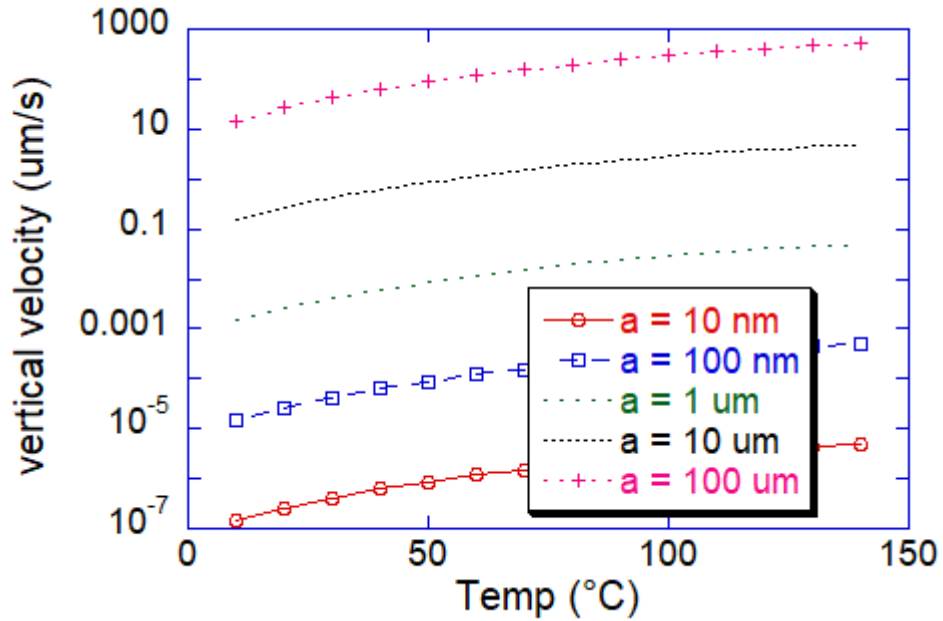


Figure 3-6: Vertical velocities (falling speed) of the droplet under the influence of temperatures (10 - 140°C) and droplet sizes (10nm - 100µm)

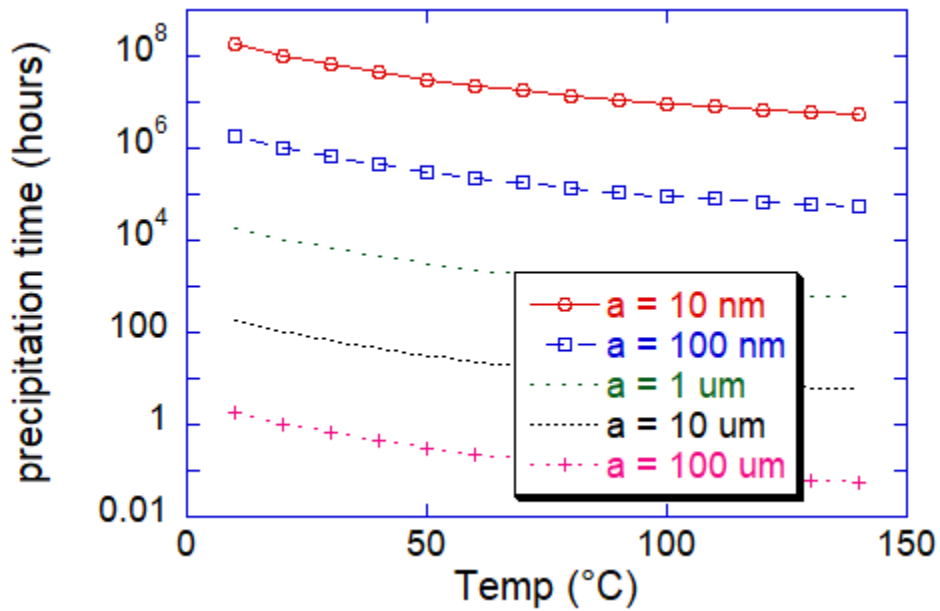


Figure 3-7: Precipitation time of the droplet under the influence of temperatures (10 - 140°C) and droplet sizes (10nm - 100µm)

For further investigation of the emulsion states, the equations and figures obtained above will be applicable in the macroemulsion state (*e.g.*  $d \approx 1 - 100 \mu\text{m}$ ). However, when the size of droplet diminishes to extremely small levels such as a microemulsion scale (*e.g.*  $d \approx 10 - 50 \text{ nm}$ ), this mechanism may fail. From the results above, the velocity of the droplet in macroemulsion state is the range of  $0.1 - 1000 \mu\text{m}/\text{sec}$ , while it is rapidly decreased in the microemulsion state to the range of  $10^{-7} - 10^{-5} \mu\text{m}/\text{sec}$  as shown in Fig. 3-6. In Fig. 3-7, the droplets in macroemulsion can be deposited within several hours to several days. However, water droplets in microemulsion state cannot be deposited by gravity without any external force [79, 81].

### 3.2.3 Horizontal Movement by Electric Field

Next, horizontal movement ( $V_H$ ) of the water droplets by the electric field is studied. In this movement, the electric force of the droplet ( $F_{el}$ ) along with the force of horizontal flow resistance ( $F_{v,H}$ ) is considered as shown in Fig. 3-1. The balance of the forces on the droplet in the horizontal direction can lead the Eq. (3-11). The equation (3-12) of  $dV_H/dt$  is obtained from the Eq. (3-11) and (3-6) [34, 35, 79].

$$m \frac{dV_H}{dt} = 24\pi\epsilon E_0^2 \alpha^6 l^{-4} - 6\pi\mu_0 \alpha V_H \quad (3-11)$$

$$m = \frac{4}{3} \pi \alpha^3 \rho_w \quad (3-6)$$

$$\frac{dV_H}{dt} = \frac{18\epsilon E_0^2 \alpha^3}{\rho_w l^4} - \frac{4.5\mu_0 V_H}{\alpha^2 \rho_w} \quad (3-12)$$

The horizontal velocity ( $V_H$ ) can be also calculated by considering a pseudo-steady state ( $dV_H/dt \approx 0$ ) assumption as seen in Eq. (3-13) [34]. The horizontal velocity is a function of  $\epsilon$ ,  $E_o$ ,  $\alpha$ ,  $\mu_o$ , and  $l/a$ , and this velocity can be numerically calculated by these values. Also, the droplet velocity immediately before the collision can be calculated by assuming  $l/a = 2$ . The collision time ( $t_c$ ) calculated by integrating Eq. (3-14) is expressed in Eq. (3-15). The collision time is essentially influenced by the  $l/a$  ratio, which is 5<sup>th</sup> power of this ratio. This indicates the droplet size and the distance between droplets are the most important factors to decide the collision time. However, the collision time is not affected by the droplet size if the  $l/a$  ratio is constant as shown in Eq. (3-15). In addition, dielectric constant ( $\epsilon$ ), electric strength ( $E_o$ ) and viscosity ( $\mu_o$ ) are also significant factors for the droplet velocity and collision time as shown in Eq. (3-13) and (3-15). The horizontal velocity of the droplet is proportional to the dielectric constant and the square of the electric strength, and it is inversely proportional to the viscosity, while the collision time is vice versa. In Eq. (3-13), dielectric constant ( $\epsilon$ ) and viscosity ( $\mu_o$ ) are deeply influenced by the operating temperature. Both dielectric constant ( $\epsilon$ ) and viscosity ( $\mu_o$ ) of sunflower oil decrease as the operating temperature increases as shown in Figs. 3-4 and 3-8. Viscosity decreases rapidly at the lower temperature (*i.e.* 10 - 50°C), then it decreases slowly at the higher temperature (over 80°C), while dielectric constant decreases almost linearly as temperature increases [47, 82].

$$V_H = \frac{4\varepsilon E_0^2 \alpha^5}{\mu_0 l^4} = \frac{4\varepsilon E_0^2 \alpha}{\mu_0 (l/\alpha)^4} \quad (3-13)$$

$$\frac{dl}{dt} = V_{H,1} + V_{H,2} = 2V_H = \frac{8\varepsilon E_0^2 \alpha^5}{\mu_0 l^4} \quad (3-14)$$

$$t_c = \frac{\mu_0 l^5}{40\varepsilon E_0^2 \alpha^5} = \frac{\mu_0}{40\varepsilon E_0^2} \cdot \left(\frac{l}{\alpha}\right)^5 \quad (3-15)$$

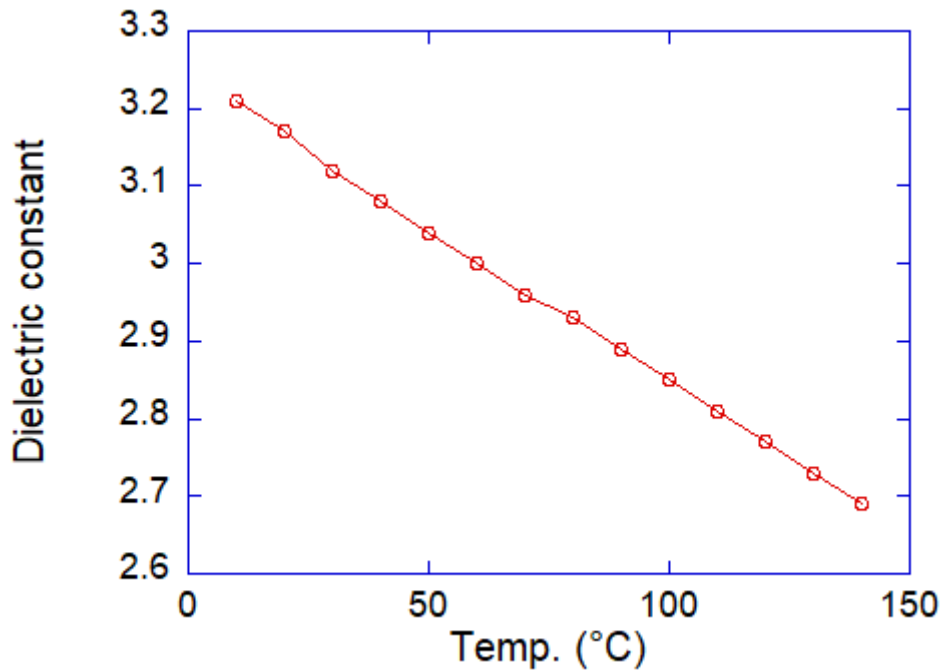


**Figure 3-8: Dielectric constants of sunflower oil at various temperatures (10 - 140°C)**

The horizontal velocities created by its electric field under the influences of the droplet size, electric strength, and  $l/a$  ratio along with the increment of the temperature is shown in Figs. 3-9 – 3-11. As indicated in these figures, these four factors are very significant in deciding the velocity of the water droplets in the electric fields. Especially, as indicated in Fig. 3-9, the velocity of the droplet in the microemulsion induced by electric fields is very small ( $10^{-5} - 10^{-2}$

$\mu\text{m}/\text{sec}$ ), and the mechanism of the droplet movement may not be applicable in the range of nano-scale. Therefore, this result indicates that it is very difficult to predict the separation speed of the microemulsion by electrostatic force alone due to its tiny droplet size and stability [79].

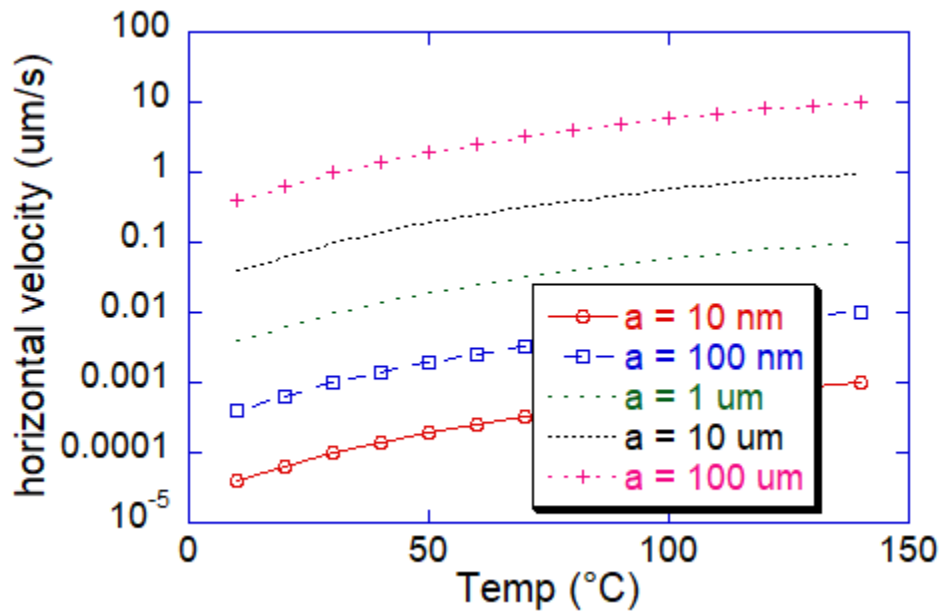


**Figure 3-9: Horizontal velocities of the water droplet under the influence of temperatures (10 - 140°C) and droplet sizes (10nm - 100 $\mu\text{m}$ ) with the constant electric strength ( $E_0 = 1\text{kV}/\text{cm}$ ) and  $l/a$  ratio ( $l/a = 4$ )**

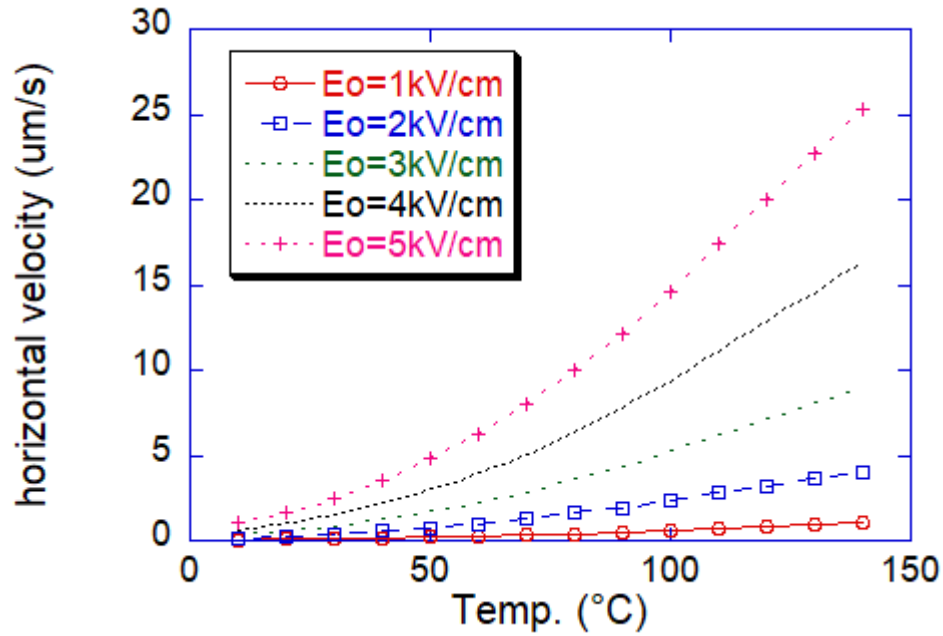


Figure 3-10: Horizontal velocities of the water droplet under the influence of temperatures (10 - 140°C) and electric strength ( $E_o = 1 - 5\text{kV/cm}$ ) with the constant droplet size ( $a = 10\mu\text{m}$ ) and  $l/a$  ratio ( $l/a = 4$ )

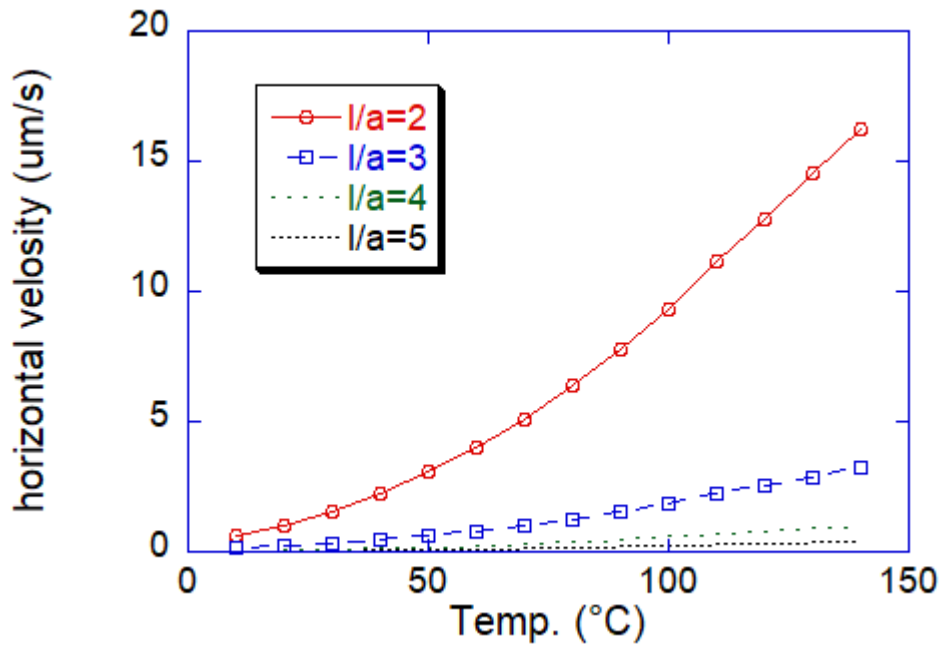


Figure 3-11: Horizontal velocities of the water droplet under the influence of temperatures (10 - 140°C) and  $l/a$  ratio ( $l/a = 2 - 5$ ) with the constant droplet size ( $a = 10\mu\text{m}$ ) and electric strength ( $E_o = 1\text{kV/cm}$ )

The collision time ( $t_c$ ) of the droplets is influenced by the viscosity, dielectric constant, electric strength, and  $l/a$  ratio as shown in Eq. (3-15). In this equation, viscosity and dielectric constant are a function of the temperature. Therefore, temperature, electric strength, and  $l/a$  ratio are the significant factors in deciding the collision time of the droplets. The effects of electric strength and  $l/a$  ratio as increase of the operating temperature on the collision time are numerically calculated as shown in Figs. 3-12 and 3-13. The  $l/a$  ratio is the most significant factor to decide its collision time. In addition, if the  $l/a$  ratio is 2, the collision time should be physically zero because two droplets are barely touched each other. Based on this numerical calculation, the collision time reaches close to zero when the  $l/a$  ratio is 2 as shown in Fig. 3-13 [79].

Electric strength and temperature are also important factors. The collision time reduces as temperature and/or electric strength increase as shown in Fig. 3-12. This indicates that the electrostatic coalescence of the water droplets can be accelerated by elevating temperature such as 90°C. For instance, the collision time of the water droplets is reduced by 5-10 times at high temperature (90°C) when compared to the result at room temperature (25°C) [79].

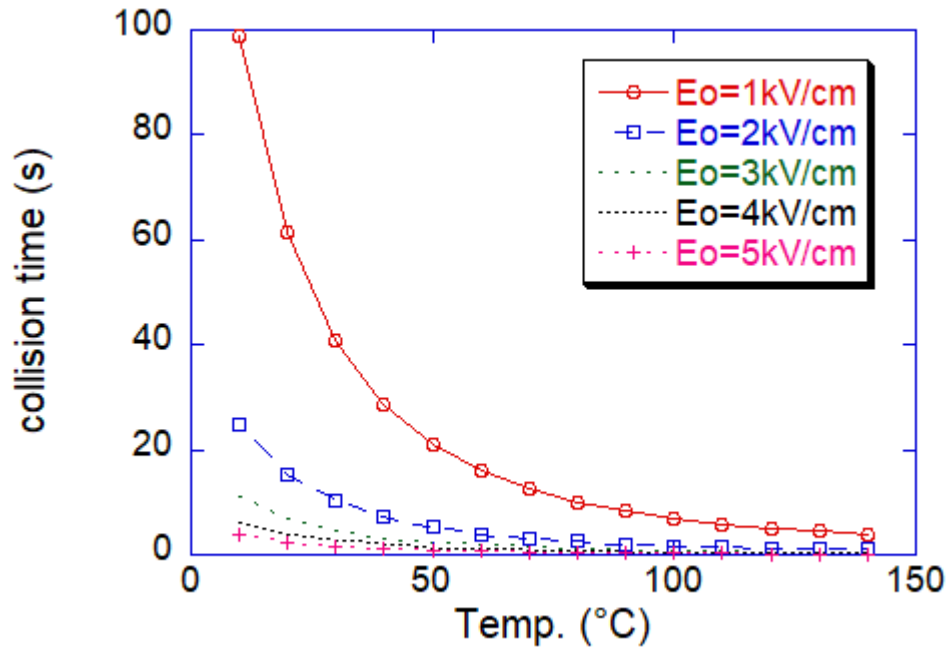


Figure 3-12: Collision time of the water droplets under the influence of temperatures (10 - 140°C) and electric strength ( $E_o = 1 - 5\text{kV/cm}$ ) with constant  $l/a$  ratio ( $l/a = 4$ )

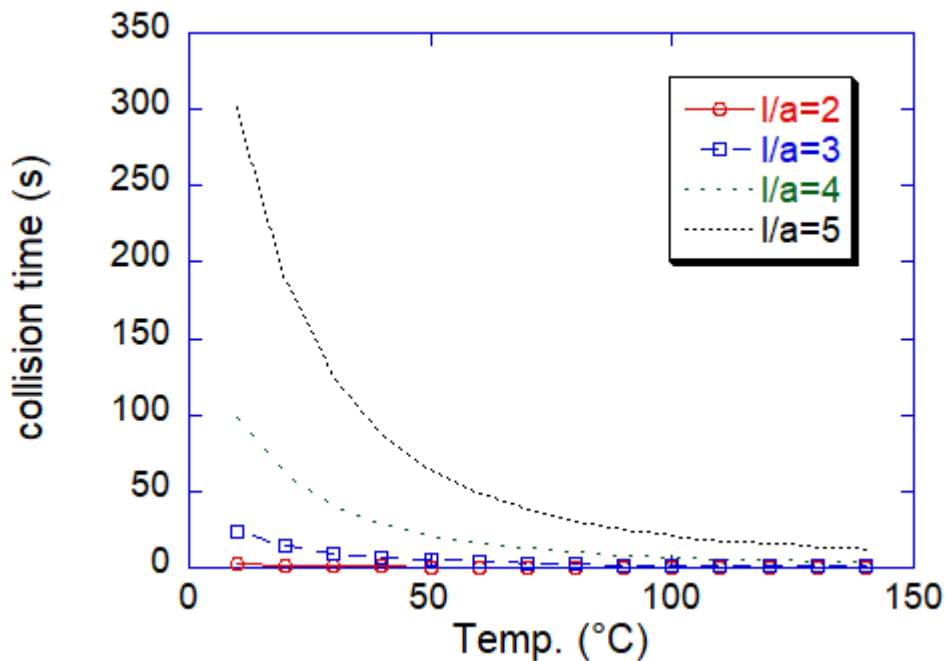
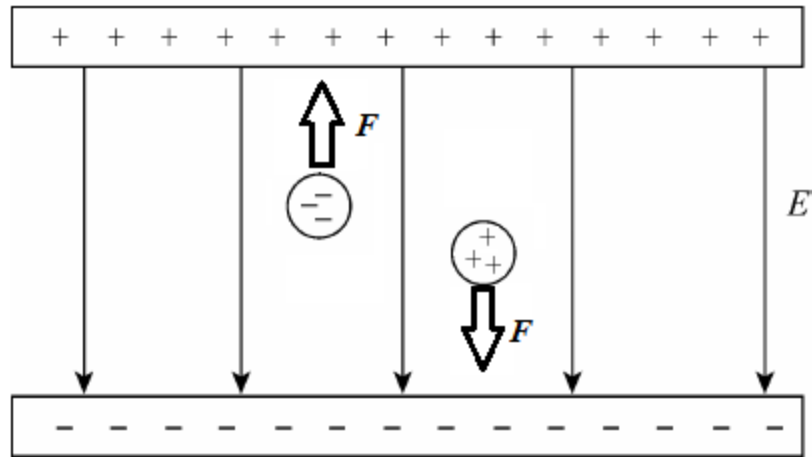


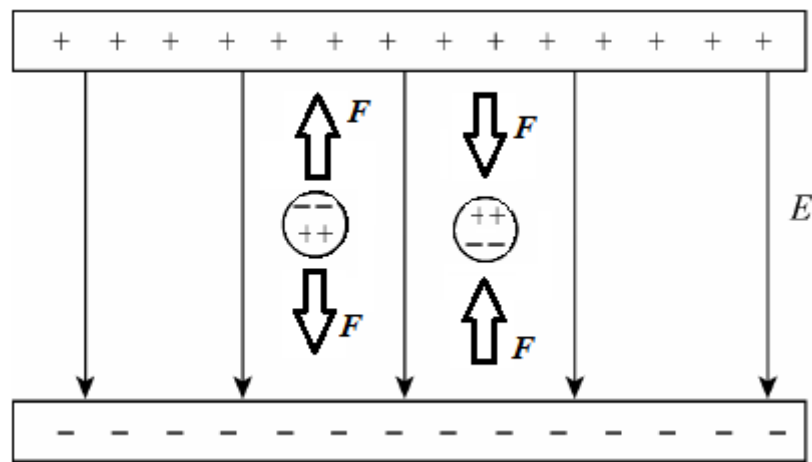
Figure 3-13: Collision time of the water droplets under the influence of temperatures (10 - 140°C) and  $l/a$  ratio ( $l/a = 2 - 5$ ) with constant electric strength ( $E_o = 1\text{kV/cm}$ )

### **3.3 Dielectrophoresis (DEP) force acting on the droplets**

Dielectrophoresis (DEP) force can be created in non-uniform electric field, and this force can drive droplets either merging toward the central electrode or pulling to the surrounded area. This action may expedite the speed of the water droplet coalescence. Non-uniform electric field can enhance the coalescence of water droplets compared to uniform field because the combined dipole-dipole and dielectrophoresis (DEP) forces act on the particles simultaneously. Fig. 3-14 indicates the droplet movements in uniform electric fields. If a water particle is charged either positive (+) or negative (-), the particle can move to the direction of the oppositely-charged electrode as shown in Fig. 3-14 (a). However, if the particle is equally polarized on both ends, the forces on the dipole ends are equal and opposite as seen in Fig. 3-14 (b). In this case, the net forces exerted on the droplet can be cancelled [33]. However, in non-uniform electric fields, the electric field near the center electrode is much stronger than the far-field region. Therefore, the polarized droplets can be pushed or pulled by this electric field as illustrated in Fig. 3-15. This increased mobility of the droplets can drive the dipole-dipole interaction when they approach to other neighboring droplets, and this process can expedite the droplet coalescence [33, 76].



(a) For charged particles (positive or negative)



(b) For polarized particles

**Figure 3-14: Schematic diagram of a uniform electric field**

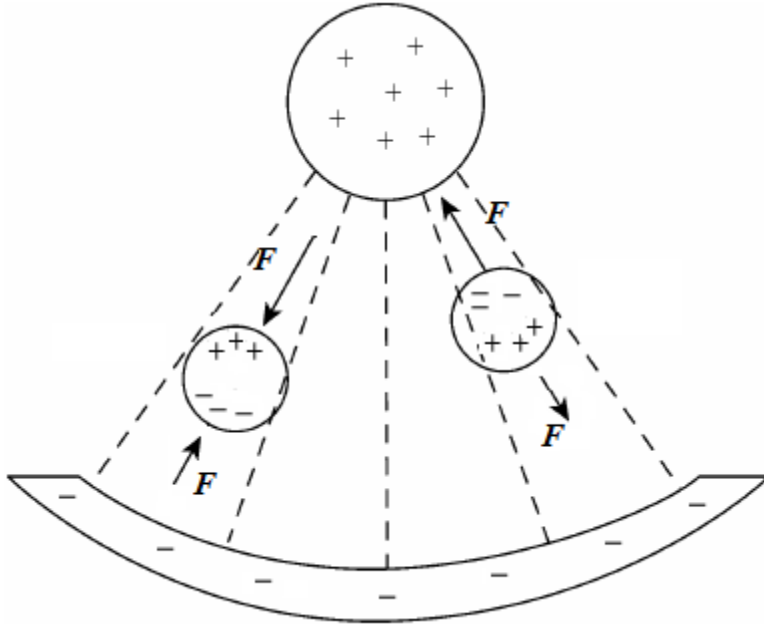


**Figure 3-15: Schematic diagram of a non-uniform electric field**

The DEP force in non-uniform fields can be expressed in the Eq. (3-16), where  $a$  is a droplet radius,  $\epsilon$  is a permittivity of the medium surrounding oil,  $\nabla|\vec{E}|^2$  is the gradient of the root-mean-square of the applied electric field squared:

$$F_{DEP} = 2\pi a^3 \epsilon K_c \nabla|\vec{E}|^2 \quad (3-16)$$

In the Eq. (3-16), the frequency dependence of the Clausius-Mossotti factor ( $K_c$ ) is defined in the following Eq. (3-17), where  $\epsilon_w^*$  and  $\epsilon_o^*$  are the complex permittivities of the water droplet and oil phase:

$$K_e = Re \left( \frac{\varepsilon_w^* - \varepsilon_o^*}{\varepsilon_w^* + 2\varepsilon_o^*} \right) \quad (3-17)$$

If we separate the complex Clausius-Mossotti equation into the real and imaginary parts, we can obtain the Eq. (3-18), where  $\varepsilon_w$  and  $\varepsilon_o$  are the permittivities of the water droplet and medium oil,  $\omega$  is an angular frequency, and  $\sigma_w$  and  $\sigma_o$  are the conductivities of the water particle and oil phase [83]:

$$K_e = \frac{\omega^2(\varepsilon_w - \varepsilon_o)(\varepsilon_w + 2\varepsilon_o) + (\sigma_w - \sigma_o)(\sigma_w + 2\sigma_o)}{\omega^2(\varepsilon_w + 2\varepsilon_o)^2 + (\sigma_w + 2\sigma_o)^2} \quad (3-18)$$

As indicated in the Eq. (3-16), the DEP force is highly influenced by the particle size ( $a$ ) and the electric strength ( $E$ ). DEP force is promotional to the cube of the droplet radius and square of the electric strength. The electric strength in the uniform electric field is constant, and this delivers the zero DEP force in the uniform electric field. In the non-uniform electric field, however, the electric strength near the center electrode is much stronger than the surrounding region. Hence, the water particles next to the center electrode can be strongly influenced by the DEP force, while the particles in the surrounding area have minimal effect. In addition, DEP force is also affected by the frequency ( $\omega$ ) as seen in Eq. (3-16) and (3-18) [71, 72].

### 3.4 Dimension Effect of the Cylindrical Electrodes

The magnitudes of electric forces acting on the water droplets depend significantly on the electric field's properties inside the separator. Therefore, the strength of the electric fields inside the cylindrical separator changes inversely proportional to the radius as indicated in Eq. (3-19)

using Gauss' law, where  $\delta$  is the charge per unit length on the central electrode, and  $\epsilon$  is the permittivity of the medium [84-85]. As a result, reducing the thickness of central electrode can also enhance the electric fields in the emulsion, resulting in a superior separation performance.

$$E(r) = \frac{\delta}{2\pi\epsilon r} \quad (3-19)$$

The energy of cylindrical electrodes can be calculated by Eq. (3-20), where C is the capacity, and V is the applied voltage [84].

$$\text{Energy} = \frac{1}{2} CV^2 \quad (3-20)$$

This energy can also be calculated by integrating the energy in the electric field using Eq. (3-21), where E is the magnitude of electric field.

$$\text{Energy} = \frac{1}{2} \epsilon \int_V |E|^2 dV \quad (3-21)$$

Eq. (3-22) is obtained by combining Eq. (5) and (6),

$$\frac{1}{2} CV^2 = \frac{1}{2} \epsilon \int_V |E|^2 dV \quad (3-22)$$

Therefore, if the applied voltage is constant, the magnitude of the electric field can be enhanced by increasing the capacity. The capacity (C) of the cylindrical capacitor can be

calculated by using Eq. (3-23), where L is the effective length of electrode, and b/a is the ratio between outer and inner diameter [86].

$$C = \frac{2\pi\epsilon L}{\ln(b/a)} \quad (3-23)$$

In Eq. (3-23), the capacity of the system increases as the effective length (L) of the center electrode extends and the b/a ratio reduces. The b/a ratio decreases as the diameter of the separation tube increases. Therefore, a higher electric field magnitude can be created in emulsion by reducing the diameter of the separator and/or extending the length of the electrode.

### 3.5 Conclusions

In this chapter, the balance of the forces and the movement of water droplets under the electric fields were investigated. Gravity, dipole-dipole and DEP forces significantly affect this movement. The analytical considerations show that temperature, droplet size, and electric strength play important roles to determine the precipitation and collision time of the droplets. The velocity of the water droplets increases as temperature, droplet size, and electric strength increase as proven in theoretical calculations. The velocity and collision time of the water droplets are deeply related to the separation speed and quality of the water-in-oil emulsions.

From the results of the theoretical calculation, the precipitation and collision times of water droplets in the oil phase is significantly related to the increment of the temperature and electric field. The precipitation and collision times are reduced by 5-10 times by increasing the process temperature to 90°C when compared to the process under the same electric field at 25°C.

This reduced coalescence time of water droplets can accelerate the separation speed of water-in-oil emulsion. Water-in-oil emulsion contains aggregations of the water droplets in the oil phase. Therefore, if the movement of the single droplet accelerates, water/oil separation time is reduced. The effect of temperature and electric field will be also determined by water/oil separation tests to validate the results of analytical considerations.

In addition, the DEP force, which is generated in non-uniform electric fields, is highly influenced by the droplet size  $a$  and the gradient of electric field  $\nabla|\vec{E}|$ , and becomes zero in the uniform electric field. Non-uniform electric fields can be created by a cylindrical separator. The magnitude of the electric field can be enhanced by changing the dimensions of the cylindrical separator. Specifically, the strength of the electric field enhanced by increasing the length of the electrode or reducing the diameter of the separator. Therefore, the optimum design of the cylindrical separator will be determined by performing computational and experimental tests with different dimensions of the separator.

Based on the theoretical calculations, the effects of temperature, droplet size, and electric strength will be experimentally studied to validate the results of the analytical considerations. In this experimental setup, we can apply various temperatures (*i.e.* 25 – 120 °C) and voltages (*i.e.* 0 – 1kV) with different frequencies (*i.e.* 10 – 5,000Hz). Also, two types of water-in-oil emulsions, macro- and micro-emulsions, are used to study the effect of the droplet sizes.

## Chapter 4. Experimental Apparatus and Techniques

### 4.1 Water-in-Oil Emulsions

Two types of water-in-oil emulsions, macro- and micro-emulsion, were used for the water-oil separation tests to study the effect of water droplet size. Water-in-sunflower oil emulsion was used as a replacement of medium-crude oil due to its similar properties such as viscosity, density, and dielectric constant. This emulsion is regarded as a macroemulsion due to its water particle size. Also, home-made microemulsions were fabricated with hydrocarbon oils and utilized for the microemulsion tests. Surfactant addition into water droplet solution is very effective for the elimination of electric charge. The water-in-oil emulsions include 5% or 10% water phase which contains 0.1% (wt./wt.) surfactant. The water and oil phase were mixed by an ultrasonic processor with 250W power for 12 minutes to make water-in-oil emulsions. The residual water concentrations (%) in oil phase were measured after the test to compare the qualities of the separated oils.

### 4.2 Water Concentration (%) Measurements

Measuring residual water concentrations (%) of the separated oil is important because this value indicates the quality of the water/oil separations. The Water concentrations of the separated oil can be measured either manually or mechanically. The manual measurement and calculation of the water concentrations from the separated oil is expressed in the Eq. (4-1):

$$\text{water concentration}(\%) = \frac{(\text{initial mass of water} - \text{mass of separated water})}{(\text{initial mass of water} - \text{mass of separated water}) + \text{mass of initial oil}} \quad (4-1)$$

For more accurate measurement of the water concentrations, the water content measurement equipment, Coulometric Karl Fischer Titration, was used as shown in Fig. 4-1. Karl Fischer Titration is the specific standard method for the determination of water content and gives accurate and precise results within minutes.



**Figure 4-1: Coulometric Karl Fischer Titration**

## 4.3 Static Separation by Electric Field with the Elevated Temperature

### 4.3.1 Overview of Setup

Separation of water-in-oil emulsions was carried out using a combined method of heating and electrostatic as shown in Fig. 4-2. This system consists of a function generator, a voltage amplifier, a temperature-controlled oven, and a homemade separator. A schematic of the overall experimental arrangement is displayed in Fig. 4-3 [68, 73, 87-89]. The function generator (*i.e.* Agilent 33511) can generate DC/AC/pulsed DC electric fields with different wave shapes such as square, sine, and arbitrary. The voltage amplifier (*i.e.* TREK 20/20c) can amplify the input voltage by 2000 times. The maximum voltage and frequency created from these equipment are 10 kV and 7.5 kHz. A temperature-controlled oven (*i.e.* YAMATO DKN402C) was used to elevate operating temperature [90-92]. This heating oven is spacious enough to place the separation tubes and can reach the operating temperature up to around 260 °C. In this static test, the ranges of the operating temperature, voltage and frequency were 25 - 90°C, 0 - 1kV and 10 - 5,000Hz.

In this test, the emulsion is first heated in the oven until it reaches the targeted temperature. After that, voltage is applied to the emulsion while the emulsion temperature is maintained in the oven during the test. The electric field in combination with heat treatment is utilized to accelerate the separation of water from the emulsion. The effects of electric voltage, frequency, and temperature on the separation time and concentration of residual water in the emulsion were investigated. The influences of separation time on residual water concentration and the power consumption of different separation methods were also studied [42, 46, 66, 68, 73, 93-100].



**Figure 4-2: The whole static water-in-oil emulsion separation system**

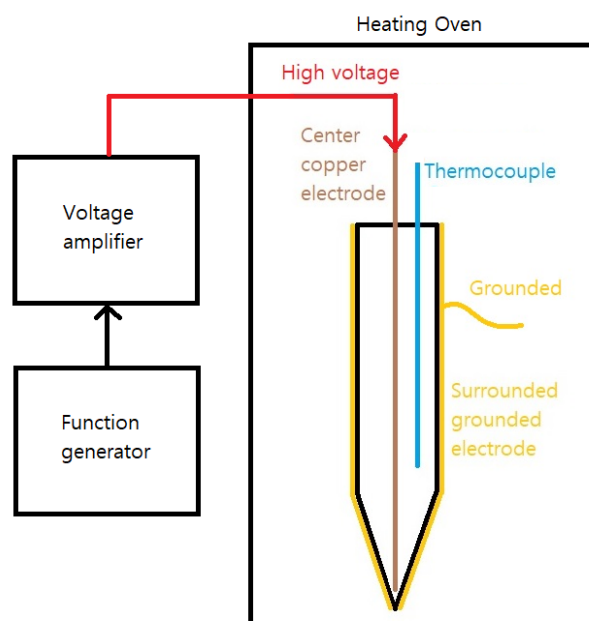


**Figure 4-3: Schematic of water-in-oil emulsion separation setup**

### 4.3.2 Separation Tube and Electrodes

In the beginning, separation tests of water-in-oil emulsion were executed by using two flat plate electrodes as shown in Fig. 4-4. The schematic diagram of this initial separation system is indicated in Fig. 4-5. This flat-plate copper electrodes were covered by PFA Teflon bags for electrical insulation. However, the separation of water phase cannot be easily observed due to its flat bottom of the bottle. Also, this flat plate electrodes may create uniform electric field, which is regarded less efficient than non-uniform electric field. The separation speed of the water-in-oil emulsion was not fast enough as expected. Therefore, we decided to design a cylindrical type of separation tube which can generate non-uniform electric fields.



**Figure 4-4: Two flat-plate electrodes water-in-oil emulsion separator**

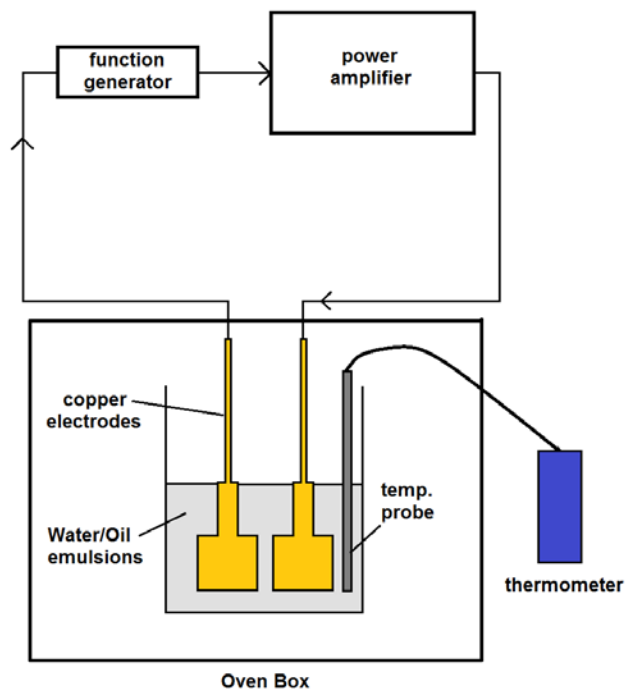


**Figure 4-5: Overview of the emulsion separation system using two flat-plate electrodes**

To improve the separation speed and observation, a homemade cylindrical cone-shaped separator equipped with coaxial cylindrical electrodes was fabricated for the static water/oil separation tests. The conical separation tube and electrodes are shown in Fig. 4-6. A cylindrical conical glass tube, copper foils and wires were used to design the cone-shaped separator. The dimensions of the conical separation tube are 128 mm height, 17 mm of outer diameter, and 13 mm of inner diameter. The volume of the separation tube is around 15mL. A cap is used to seal the top and hold the center electrode and temperature probe. The separation tube is surrounded by a copper foil, which plays a role as a ground electrode.

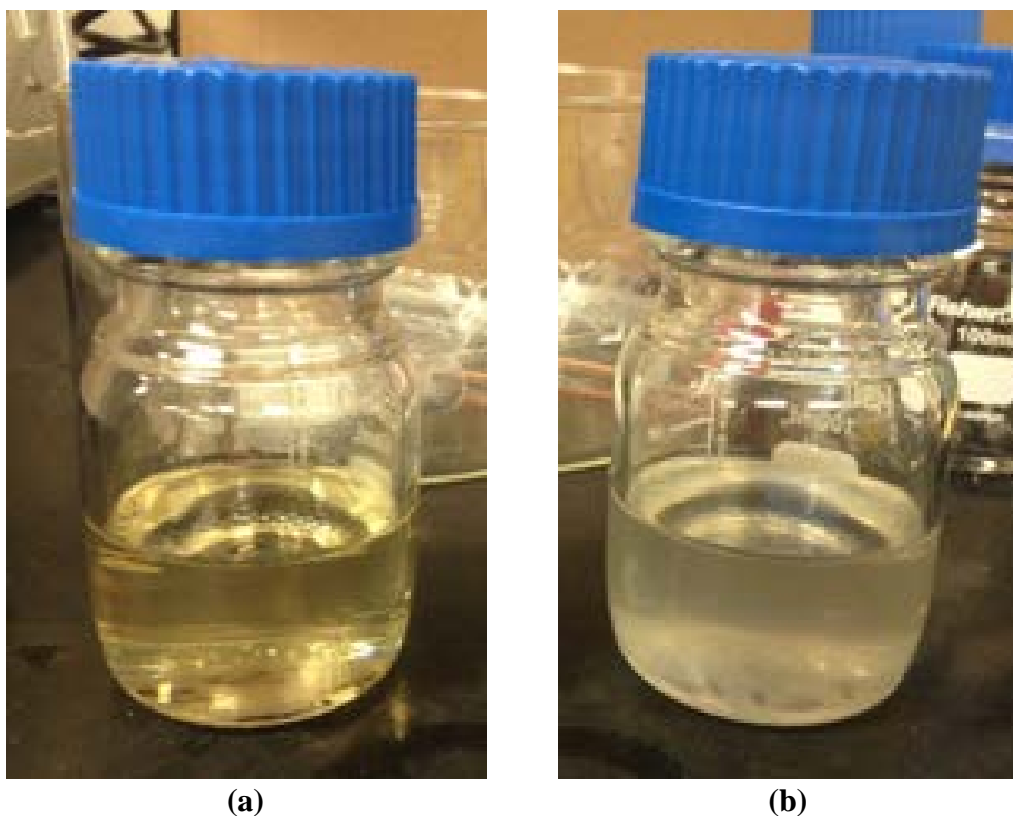
A central electrode and thermocouples are insulated by glass capillary tubes to prevent short-circuits and chemical reactions between the metal electrodes (*e.g.* copper) and emulsion.

Fig. 4.7 shows the effect of the electrode insulation from chemical reactions. The color of emulsion, which used uninsulated electrodes, turns yellow after the separation test due to its chemical reactions as shown in Fig. 4-7 (a). However, the color of the emulsion, which used insulated electrodes, is not changed as shown in Fig. 4-7 (b). This insulated electrodes can also enhance the separation speed and the quality of the separated oil [101].

The thickness of the center copper electrode is 1mm, and this center electrode only has minimized gap with the capillary tube, which has 1.15mm of inner diameter. This small gap between the center electrode and capillary tube can reduce the loss of electrical strength in the gap. The thicknesses of the center electrode and its capillary tube were optimized by executing many tests with different sizes. A separation tube is supported by a cone-shaped tube holder as shown in Fig. 4-6.



**Figure 4-6: Cone-shaped cylindrical water-in-oil emulsion separator**



**Figure 4-7: Comparison of chemical reaction effect between uninsulated and insulated electrodes**

### 4.3.3 Pressurized Sealed Tube

A special pressurized tube was designed for extremely high temperature tests because the previous cone-shaped tube has water evaporation problems at the high temperatures over the boiling point ( $100^{\circ}\text{C}$ ). This pressurized tube can be only used for extremely high temperature tests (*e.g.* over  $100^{\circ}\text{C}$ ) because the electrical strength of this pressure tube is reduced compared to the previous cone-shaped tube due to its enlarged dimensions. If the operating temperature is less than  $100^{\circ}\text{C}$ , previous cone-shaped separation tube is used.

The overall design of this tube is similar to the cone-shaped separation tube. This tube has larger diameters of its body (25.5mm) and center electrode (5mm), and larger wall thickness (0.8mm) of the center capillary tube compared to the cone-shaped tube. This increased thicknesses of the center electrode and the glass capillary tube decrease the strength of the electric field. Fig. 4-8 shows the pictures of the cone-shaped and pressurized sealing tubes. Table 4-1 indicates the dimensions of the previous and new pressurized tubes.

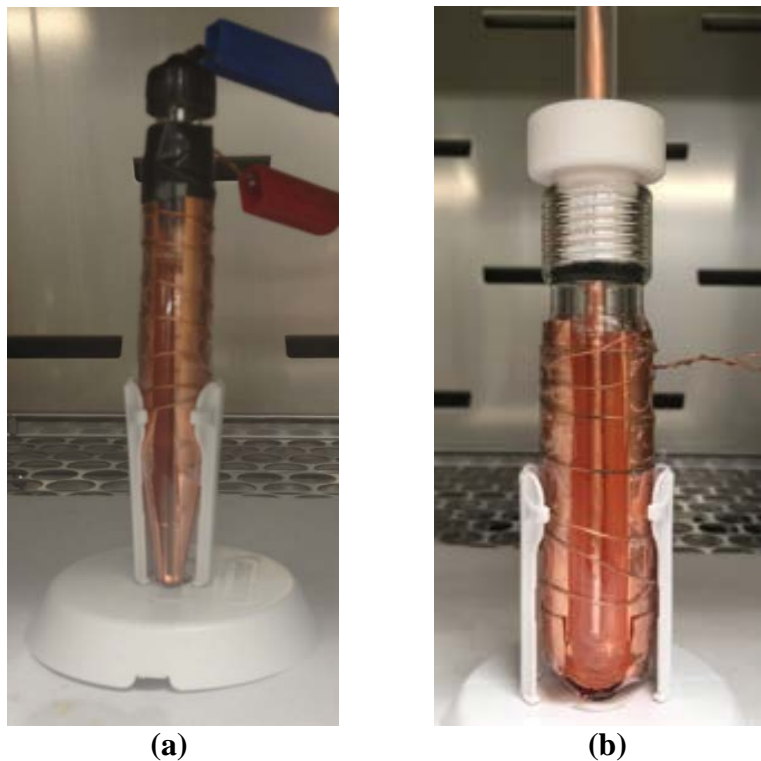


**Figure 4-8: Pictures of the cone-shaped and pressurized tubes: (a) Cone-shaped tube, (b) Pressurized tube**

**Table 4-1: Dimensions of Cone-shaped and Pressurized Tubes**

<b>Dimensions</b>	<b>Cone-shaped Tube</b>	<b>Pressurized Tube</b>
Tube Outer Diameter (mm)	17	25.5
Tube Wall Thickness (mm)	2	4
Tube Height	126	120
Center Electrode Thickness (mm)	1	5
Capillary Tube Wall Thickness (mm)	0.2	0.8
Sealing Property	Vapor leaking	Very Good (150 psi)

## **4.4 Static Separation by Centrifugal Force with the Elevated Temperature**

### **4.4.1 Overview of Setup**

Centrifugal force and heat treatment also can be combined to enhance the efficiency of the water/oil separation. To execute this static test, a centrifuge which has a heating system is used. Fig. 4-9 shows the picture of the centrifuge, which is Benchmark 14 from L-K industries. This centrifuge is designed to apply two combined separating methods: heating and centrifugal force. First, the emulsion tubes in this machine are heated to the targeted temperature, then the tubes start rotating. The temperature limit of this centrifuge is 270 °F (132°C), and the rotating speed is up to 2300 RPM. The separation tube of this system is also cone-shaped as displayed in Fig. 4-10, and its sealing property is excellent to prevent water evaporation at high temperatures over 100°C. The separation tubes have the dimensions of 200 mm height and 32 mm outer diameter. Four separation tubes can be used at the same time, and the maximum volume of the separation tube is 100mL.



**Figure 4-9: Centrifuge with heat treatment: Benchmark' 14 from L-K Industries**



**Figure 4-10: Cone-shaped separation tube of the heating centrifuge**

## 4.5 Dynamic Separation by Electric Field with the Elevated Temperature

### 4.5.1 Overview of Setup

In order to build the dynamic water/oil separation system, additional lab equipment were installed such as pump, flow meter, inline air heaters, *etc.* The overall diagram of the continuous water/oil emulsion separation system is shown in Fig. 4-11. The water-in-oil emulsion stored in the reservoir is enforced to move to the separation system by pump. The water-in-oil emulsion can be heated by passing through the inline air heaters. The elevated temperature can be maintained at the operating temperature in the high temperature oven. Several electrostatic separation tubes are located in the heating oven. The heated water-in-oil emulsion can be separated by the electric fields with three separation tubes. The separated water phase can be moved down to the water outlets located on the bottom of the tubes. The separated oil phase can move up to next separation tube, and finally moves to the oil outlet. High voltages are applied to all of the separation tubes by the function generator and voltage amplifier.

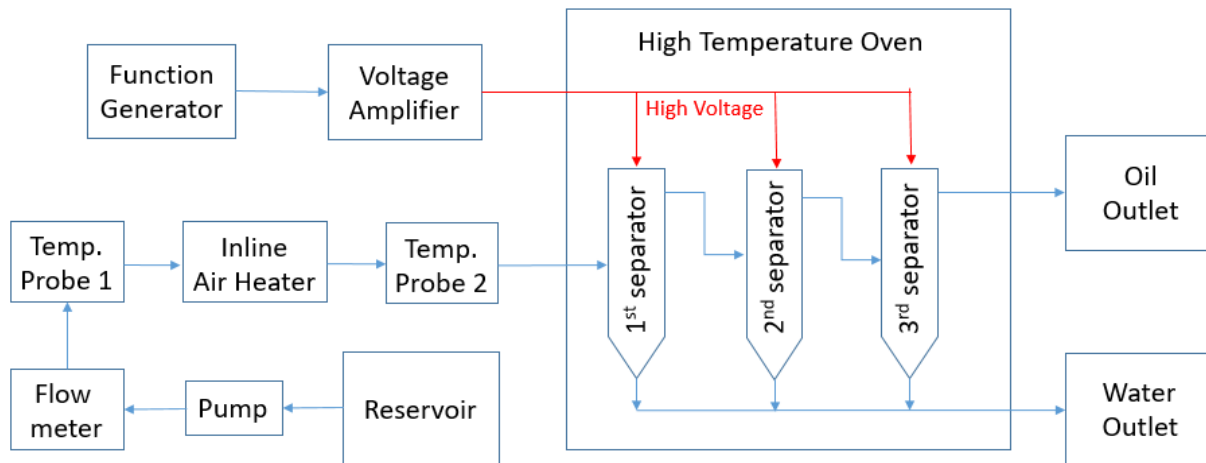


**Figure 4-11: Overall diagram of the dynamic water-in-oil emulsion separating system**

#### **4.5.2 Additional Equipment for Dynamic Separation System**

Continuous water/oil separation system requires several additional experimental equipment such as pumps, inline air heaters, voltage transformers, flow meters, temperature probes, cooling system, and many tube fittings.

Either a peristaltic tubing or a gear pump can be used for the dynamic water/oil separation tests with different flow rates. A peristaltic tubing pump can cover a wide range of flow rates and is more suitable for the lower flow rate test, while a gear pump has a narrow range of flow rates but is more stable for the higher flow rate test. Two different kinds of peristaltic pumps were used for this dynamic separation tests depending upon the flow rates.

Inline air heaters were used to apply heating to the emulsions. It is a very simple and effective method to increase the temperature of the emulsion. Omega AHPF series of inline air heaters, as shown in Fig. 4-12, were installed to the system. One inline air heater can generate the power of 400 – 1200 W based on the length of the heater. One or multiple inline air heaters were used depending on the emulsion's flow rates.



**Figure 4-12: Inline air heater: Omega AHPF series**

Variac voltage transformers, as shown in Fig. 4-13, were used to control the power of inline air heaters. The power codes of the inline heaters are connected to the variac voltage transformer, and the temperature of the flowing emulsion in the system can be controlled by changing the voltage of this voltage transformer. The range of the applied AC voltages is 0 – 130 VAC.



**Figure 4-13: Variac Voltage Transformers**

A Flow meter was added to the system to measure accurate flow rate of the emulsion. FPD3002-D from Omega, as shown in Fig. 4-14, was used for this test. This flow meter can be used for the high viscous water-in-oil emulsions and withstand the high temperature up to 80°C. The range of the flow rate from this flow meter is 33.3 – 1,666 mL/min for lower viscosity (less than 5cPs) and 8.33 – 1,666 mL/min for higher viscosity (over 5cPs). Therefore, this flow meter may cover most of the flow rates except very low flow rates.



**Figure 4-14: Flow meter: Omega FPD3002-D**

Two temperature probes were attached to the system for measuring the temperature of the flow. The K-type of thermocouples and thermometers were used for the temperature sensors as

shown in Figs. 4-15 and 4-16. The first temperature probe is located in between the flow meter and inline air heater, and this probe measures the temperature of the emulsion before heating. The second temperature probe is connected between the inline air heater and heating oven, and this temperature probe can monitor the temperature of the heated emulsion.



**Figure 4-15: Temperature probe using K-type thermocouple bar**



**Figure 4-16: Thermometer: Omega HH74K**

#### **4.5.3 Dynamic Water/Oil Separation System for Lower Flow Rate**

Dynamic water/oil separation system for lower flow rate was designed by using three separation tubes, low flow pump, inline air heaters, variac transformers, and other supplements. The whole experimental setup for this test is shown in Fig. 4-17. The flow rate of the emulsion is restricted less than 10 mL/min (or 0.15 g/sec) in this system.

The procedure of this water/oil dynamic separation is followed. Water-in-oil emulsion is initially stored in a bottle, and the emulsion moves through the system by pump. This emulsion is heated when it passes through an inline air heater, and the heated emulsion moves to the heating oven. In the heating oven, the emulsion can be separated by the applied electric field in the separation tubes. Multiple separation tubes are used to obtain higher quality of the separated oil phase, and this customized separation tubes are fabricated in “Ace glass Inc.”.

High voltage can be applied to the central copper electrode at the center of each separation vessel. The vessels were covered by a copper roll, and the surrounding copper roll acts as a grounded electrode. Stopcocks, which are attached to the separation tube, can control the emulsion flows of the inlets and outlets. Teflon tubes were used to connect the flow between each vessel. All of the separation vessels were made of glass with the thickness of 4mm. All of the materials can resist high temperature such as over 120°C.



**Figure 4-17: Whole setup for the dynamic water/oil separation system for lower flow rate**

Masterflex C/L 77122-24 from Cole-Parmer, which is shown in Fig. 4-18, was used for this lower flow rate test. The flow rate can be determined based on the size of the tube and its revolution speed (RPM). The maximum flow rate of this peristaltic pump for water flow is 43

mL/min. However, the flow rate of the water-in-oil emulsions is reduced due to the increased viscosity, and the maximum flow rate with the emulsion is around 8.4 mL/min.



**Figure 4-18: Peristaltic pump: Masterflex C/L 77122-24 from Cole-Parmer**

Three customized separation tubes were fabricated by Ace Glass and added to the system. The dimension of the separation tubes is shown in Fig. 4-19. The inner diameter of this tube is 17mm, and the outer diameter is 25mm (1 inch). This tube has an emulsion inlet, water and oil outlets, and the flow rate can be controlled by the three controlling valves. The picture of the capillary tube and cap is indicated in Fig. 4-20. The center electrode is made of a copper wire, and the electrode is insulated by this capillary tube. Fig. 4-21 shows the whole picture of the customized separation tube. These separation tubes are connected to one another and located in the heating oven as indicated in Fig. 4-22.

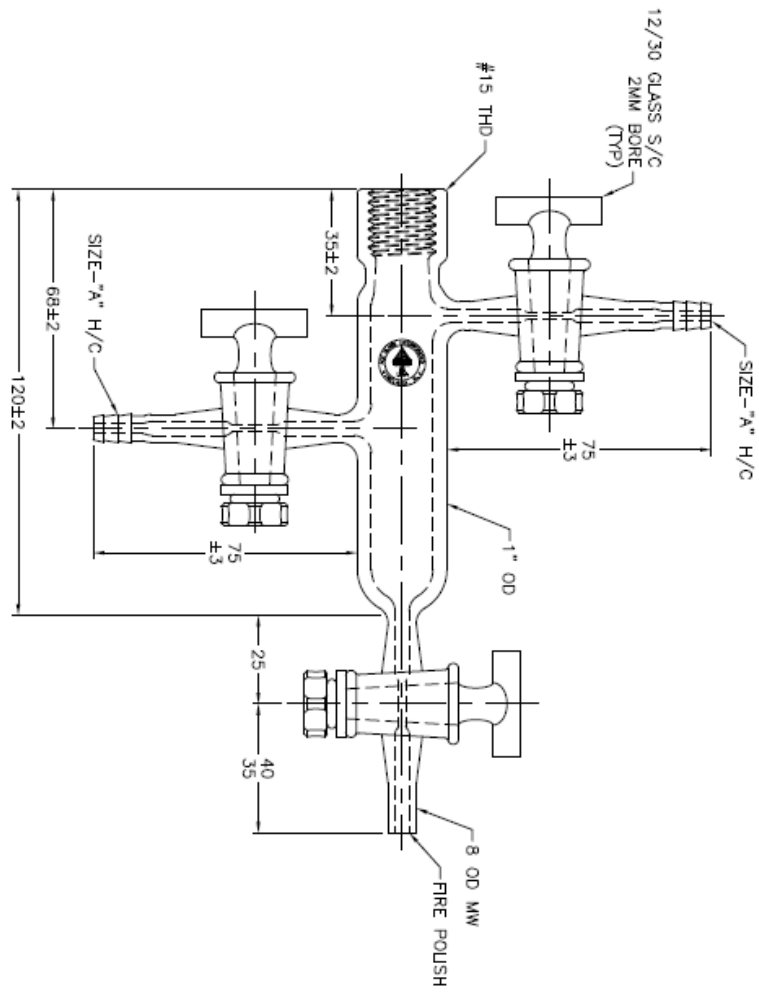


**Figure 4-19: Dimension of the separation tube for lower flow rate test**



**Figure 4-20: Capillary tube with a cap for lower flow rate test**



**Figure 4-21: Picture of the customized separation tube for low flow rate**



**Figure 4-22: Separation tubes attached to the holder in the heating oven**

#### **4.5.4 Dynamic Water/Oil Separation System for Higher Flow Rate**

Dynamic water/oil separation system for higher flow rate was also designed by using several separation tubes, peristaltic or magnetic gear pump, two inline air heaters, variac transformers, flow meter, and other supplemental components. The whole experimental setup of this high flow rate test is shown in Fig. 4-23. The range of the flow rate for this setup is approximately 10 – 500 mL/min. The process of this water/oil separation test with higher flow rate is similar to the lower flow rate tests. There are several separation tubes coupled together in the oven to enhance the quality of the separated oil phase as shown in Fig. 4-24. The maximum quantity of the separation tubes in this system is six, and these tubes are attached to the tube holder as shown in Figs. 4-24 and 4-25. Water-in-oil emulsion can be separated by passing through these separation tubes in sequence.

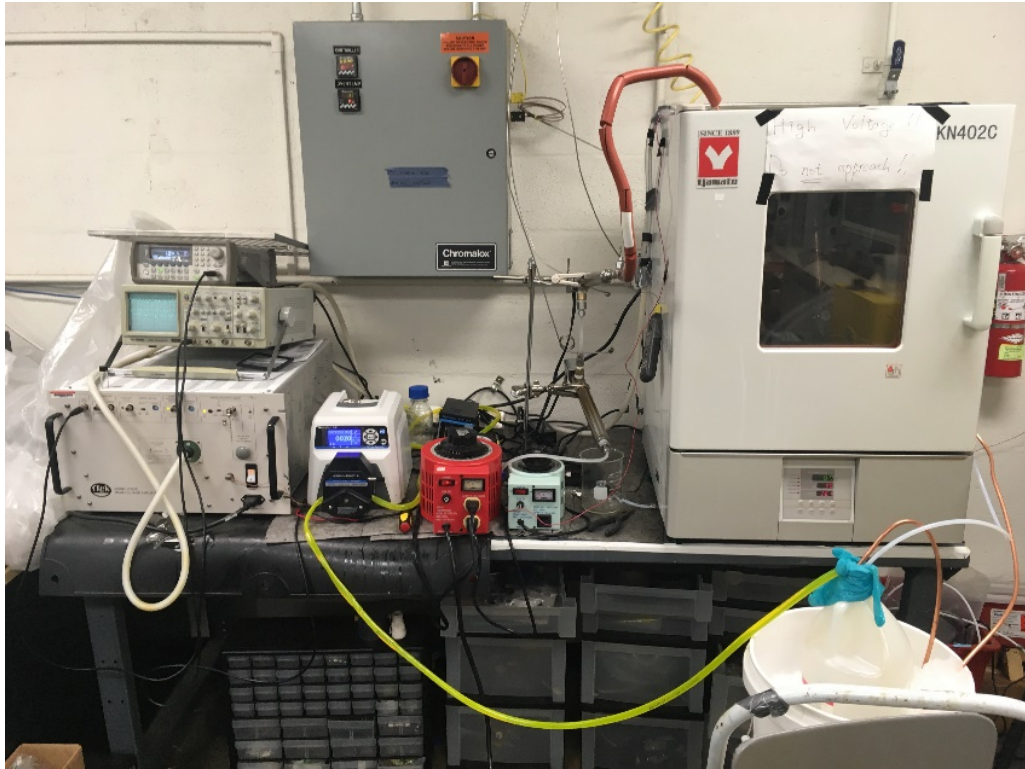


**Figure 4-23: The whole dynamic water/oil separation system for higher flow rate**



**Figure 4-24: Series of the separation tubes in the heating oven**

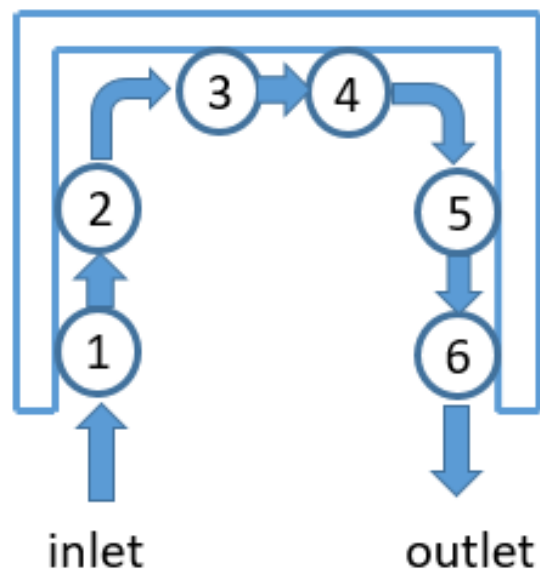


**Figure 4-25: Diagram of the separation tubes fixed on the holder and the flow direction of the emulsion**

Either a peristaltic tube pump, EW 07522-20 from Cole Parmer, or a magnetic gear pump, GJ-N23 from Burt, was used for the higher flow rate tests as shown in Figs. 4-26 and 4-27. The range of the flow rate with the peristaltic pump is 0.001 - 3400 mL/min with L/S tubing. This pump may cover a wide range of flow rates for experiments. However, magnetic gear pumps are only applicable for higher flow rate tests. The maximum flow rate of this gear pump is 3520 mL/min.



**Figure 4-26: Peristaltic tubing pump (EW 07522-20 from Cole Parmer)**



**Figure 4-27: Magnetic gear pump (GJ-N23 from Burt)**

The larger capacity of the separation tubes is required for this higher flow rate test. The efficiency of water/oil separation may decrease if the size of the tube is enlarged. Therefore, it is important to find the optimum size (*e.g.* diameter and height) of the separation tubes. For example, if the diameter of the tube is too large, such as 8cm, the strength of the voltage in the tube is reduced. This may decrease the efficiency of the water/oil separation by electric fields. On the other hand, if the inner diameter of the tube is too small such as 17mm of the lower flow rate tube, the emulsion cannot stay in the tube sufficiently to be separated. This reduced residence time may also decrease the quality of the separated oil phase.

The optimum dimension of the separation tube for higher flow rate was decided by executing many static separation tests with several different diameter of the tubes. The inner and outer diameters of the tube were decided 30mm and 34mm, respectively. Figs. 4-28 and 4-29 indicate the picture and dimensions of the separation tube for this higher flow separation system. The shape of the new separation tube is also cylindrical cone-shaped, and this enlarged separation tube can contain around 100 mL of volume. The increased residence time can improve

the quality of the separated oil. Several separation tubes are located in series in the system, and water-in-oil emulsion can pass through these tubes one by one. Each separation tube can produce the separated water phase. This separated water phase can move to the water outlet, located on the bottom of the tube. The flow speed of this separated water phase can be controlled by the bonnet needle valve, which is SS-20VS4 from Swagelok, as shown in Fig. 4-30.



**Figure 4-28: Dynamic separation tube for higher flow rate**

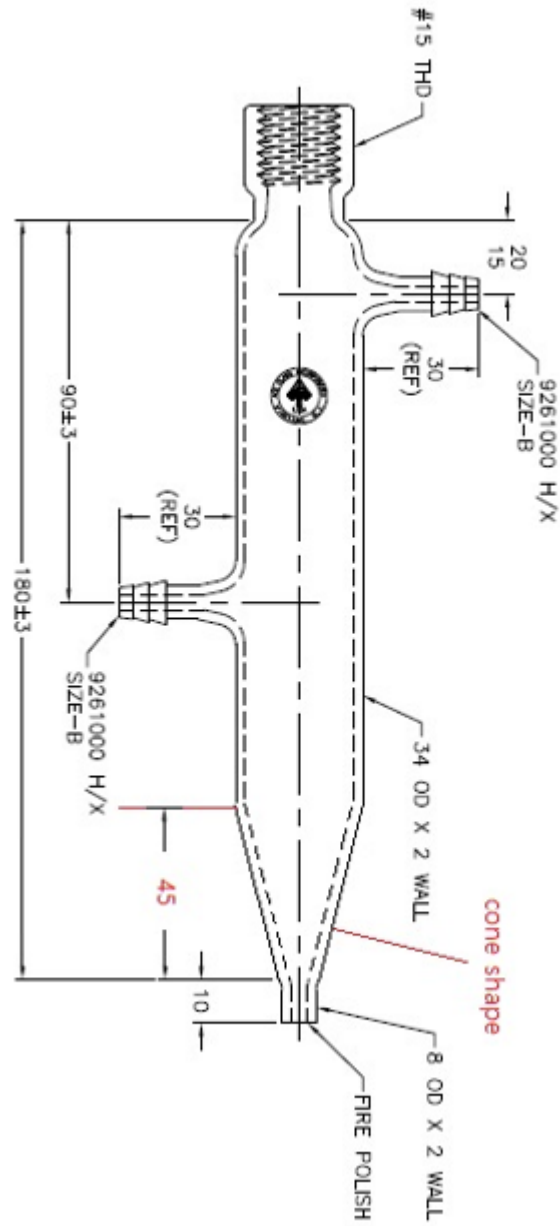


**Figure 4-29: Dimension of the cone-shaped cylindrical separation tube for the continuous water/oil separation system at higher flow rate**



**Figure 4-30: Flow controlling needle valve: SS-20VS4 from Swagelok**

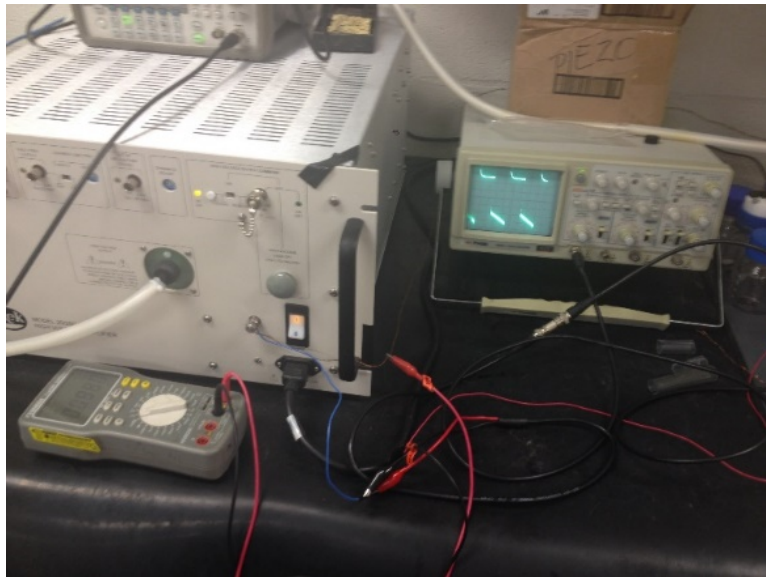
Two different copper electrodes were designed and used for this high flow rate test. The central copper electrode is covered by the thin capillary glass tube for the purpose of electrical and chemical insulations. The gap between center electrode and capillary tube may affect the efficiency because the air inside the capillary tube can decrease the electrical strength in the separation tube. Several tests were performed to find the optimum thicknesses of the central electrode and capillary glass tube. A copper wire with 1mm thickness was chosen for the use of center electrode, and the capillary tube has 1.15mm of inner diameter and 1.65mm of outer diameter. This thickness (1mm) of copper electrode is also robust enough to prevent breaking from the high speed flow rate. The separation tube is covered by thin copper roll, and this surrounding copper roll plays a role as a grounded electrode.

#### 4.5.5 Power Consumption Measurement

The electric power (W) of the separation system can be calculated by measuring its voltage (V) and current (mA). It is important to estimate the power consumptions of the separation system because it is directly related to energy consumptions. This measurement can help to obtain the optimal voltage and frequency. We can minimize the unnecessary usage of the power consumption by using the optimum voltage and frequency. It is impossible to measure the currents of the system directly because the resistance of the whole system cannot be obtained. Therefore, the small resistors were used to measure the currents. Initially, three different resistors were used for the measurements: 323  $\Omega$ , 1.476 k $\Omega$ , 147.8 k $\Omega$ . Choosing a proper resistor is important because if the resistance is too small, the measurement error can be increased, while if the resistance is too large the resistor can affect the total resistance of the system. After executing several tests, the resistor which has 147.8 k $\Omega$  was selected, and this resistor was used for most of the tests. Digital multimeter and analogical oscilloscope were used to measure the corresponding voltages. The small resistor and whole measurement system are shown in Fig. 4-31. The result of this power consumption measurement will be displayed in the next chapter.



(a)



(b)

**Figure 4-31: Power consumption measurement equipment: (a) small resistor, (b) digital multimeter and analogical oscilloscope**

## Chapter 5. Design of the Separators

### 5.1 Introduction

In this chapter, the design of the water/oil separator will be investigated by computationally and experimentally. Different shapes (*i.e.* flat plates and cylindrical) of separators were designed to compare the influence of the configuration. In addition, the effects of the thickness and length of the center electrode, and the air-gap between the center electrode and its insulated capillary tube will be investigated. Lastly, the influence of the separator's diameter will be also studied.

### 5.2 Computational Simulations

The influence of the separation tube design on the separation efficiency was investigated by computational simulation. The ANSYS Maxwell, which is a high-end interactive tool using Finite Element Analysis (FEA) for electric and magnetic modeling, simulates variables such as the separation tube diameter, length of the central electrode, and the air-gap between the center electrode and its insulated capillary tube. The electrostatic force acting on the water droplets in the emulsion is considered to be the main factor to improve the separation, as it promotes the movement and coalescence of water droplets [102]. When an object (*e.g.* a water droplet) is placed in electric fields, the electrostatic force acting on that can be calculated by integrating the dipole-dipole and DEP forces over their close surfaces [103-105]. The dipole-dipole force is in proportion to the square of the electric field strength.

Fig. 5.1 shows the magnitude map of electric fields over the separator with a 5kV voltage applied to the central electrode and the grounded copper foil. The left figures show the models before simulation, while the right ones show the results of mapping. As can be seen in Fig. 5-1 (a)-(b), a very strong electric field is observed within the 0.075mm air-gap between the copper wire and the insulated capillary tube. This strong electric field would result in a great loss of electric field energy, thus reducing the electric field in the emulsion section significantly. Therefore, reducing or even eliminating the air-gap would be an effective way to increase the magnitude of electric fields in an emulsion. This assumption is also verified in Fig. 5-2, which shows that the average electric field magnitude within emulsion will increase with decreasing of air-gap. In contrast to the air-gap, the electric field within the insulated capillary tube is relatively weak, which may result from its large relative permittivity (*i.e.* ~5.5 for glass). Another notable observation in Fig. 5-1 is that the magnitude of the electric field decreases significantly with an increase of radius [102]. It is consistent with our theoretical consideration in the previous section.

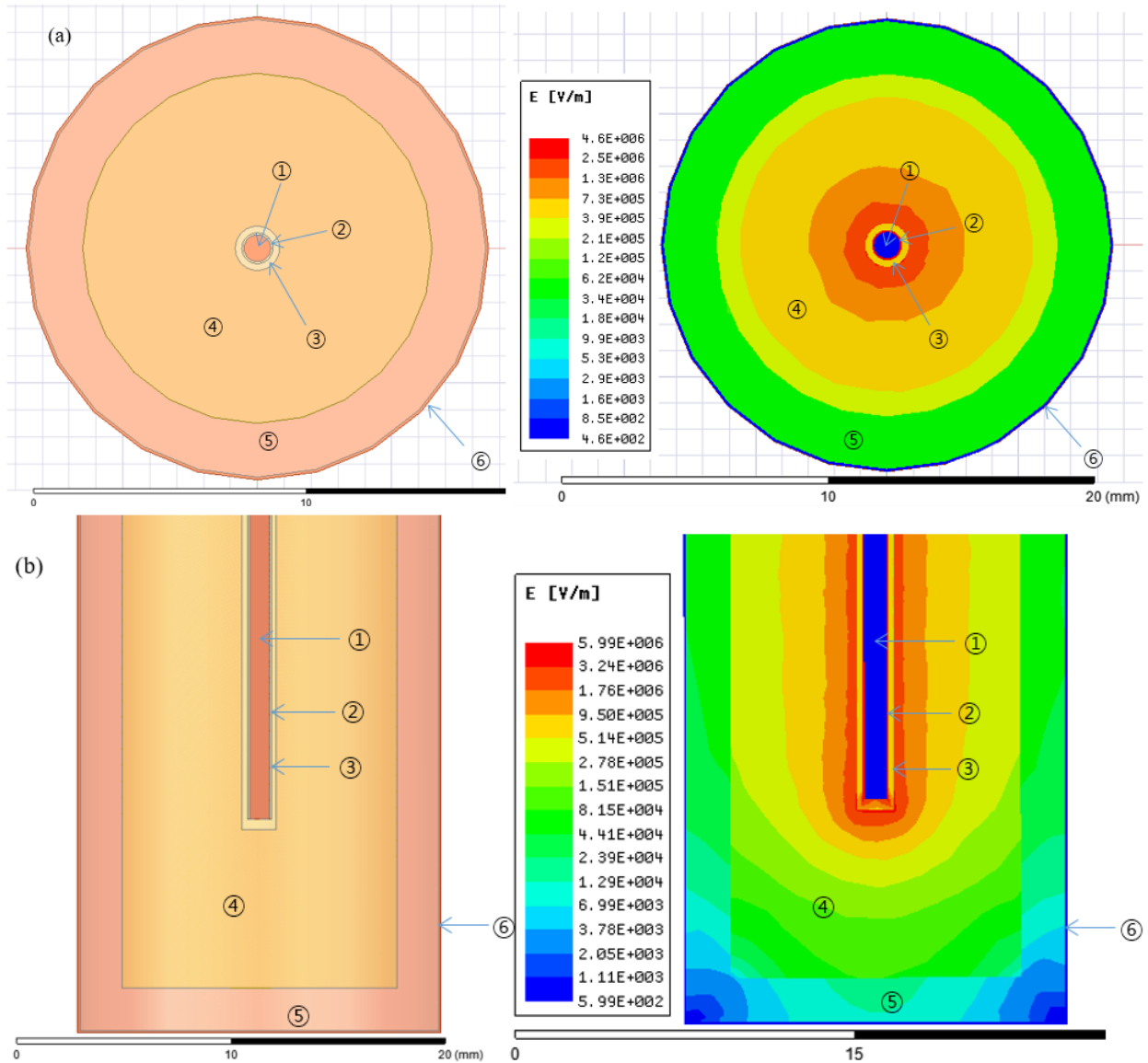


**Figure 5-1: Simulation of the magnitude of electric field distribution (by C. Zheng, 2018): (a) top-view, and (b) sectional front view. In the figure shows the configuration (left) and the mapping (right): ① central electrode (5kV applied), ② air gap, ③ insulating glass layer, ④ emulsion, ⑤ glass tube, ⑥ copper foil (ground)**

Besides the dipole-dipole force, DEP force is also introduced in the separator by the non-uniform electric fields. DEP force is proportional to the square of the magnitude of the electric

field. Fig. 5-2 plots the magnitude of  $\nabla|\vec{E}|$  over the emulsion. As shown in Fig. 5-2, the value of  $\nabla|\vec{E}|$  increases dramatically with decreasing of the radius. Therefore, the gradient of the electric fields inside the cylindrical separator changes inversely proportional to the square of the radius and can be calculated by Eq. (5-1).

$$\left| \frac{dE(r)}{dr} \right| = \frac{\delta}{2\pi\epsilon r^2} = \frac{E}{r} \quad (5-1)$$

As indicated in Eq. (5-1), the magnitude of the gradient is only related to the electric field strength and the radius. Therefore, the factors that we discussed above (*i.e.* separator size, the center electrode length, and the width of air-gap) have a similar influence on the electric field gradient in the emulsion [102].

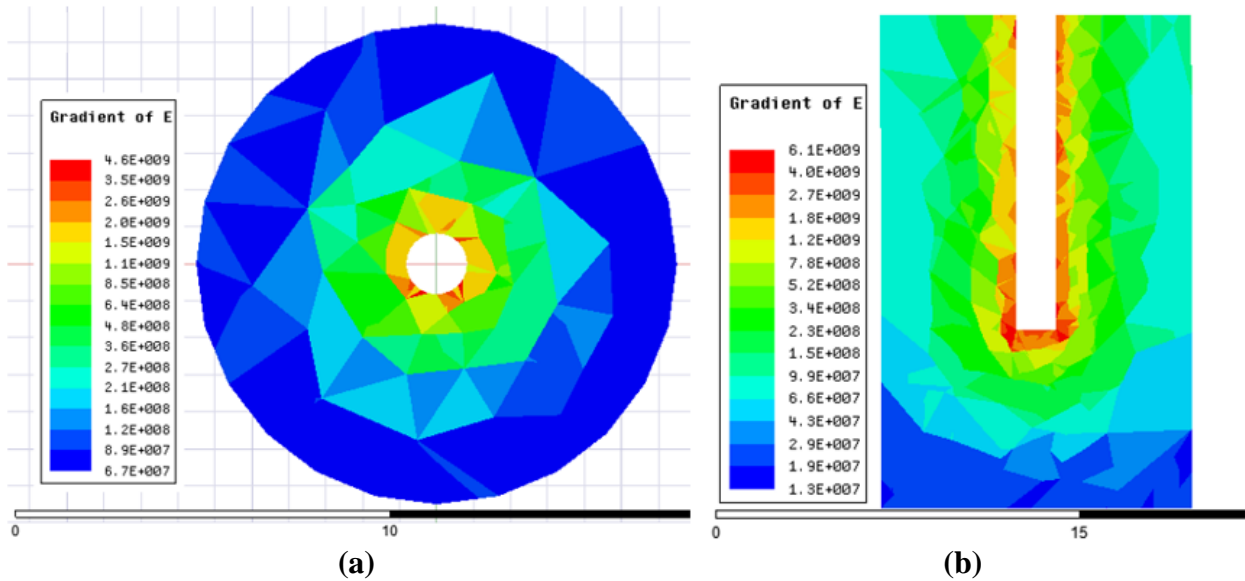


**Figure 5-2: Simulation of the  $\nabla|\vec{E}|$  in emulsion (by C. Zheng, 2018): (a) top-view, and (b) sectional front view**

## **5.3 Experimental Results**

In this experimental process, 10% water-in-oil microemulsion is heated to the targeted temperature. Once the emulsion reaches the temperature, a voltage is applied to the system for 10 minutes. The water/oil separation can be observed after the emulsion is exposed to the high electric fields.

### **5.3.1 Comparison between Flat Plates and Cylindrical Electrodes**

In this test, two different separators, which use flat plates and cylindrical electrodes respectively, were designed to perform water/oil separation tests. The flat plate separator is used to create uniform electric fields, while the cylindrical separator is used to provide the non-uniform electric fields. Water/oil separation tests were performed and compared the efficiency of the separation. In this test, 1kV of voltage was applied with 50Hz of frequency, and an operating temperature is 80°C.

The progress of the water/oil separation for these two separating systems is shown in Fig. 5-3. The separation speed of water-in-oil emulsion using cylindrical tube can be much expedited when compared to the results using flat plate electrodes as shown in Fig. 5-3. After the 10-minutes test, the white deposit of the water droplets still remained in the flat plate separator, while the emulsion was completely separated in the cylindrical separator. This result indicates that the cylindrical water/oil separation system, which generates non-uniform electric fields, is more efficient for water/oil separation compared to the flat plates' separation system.

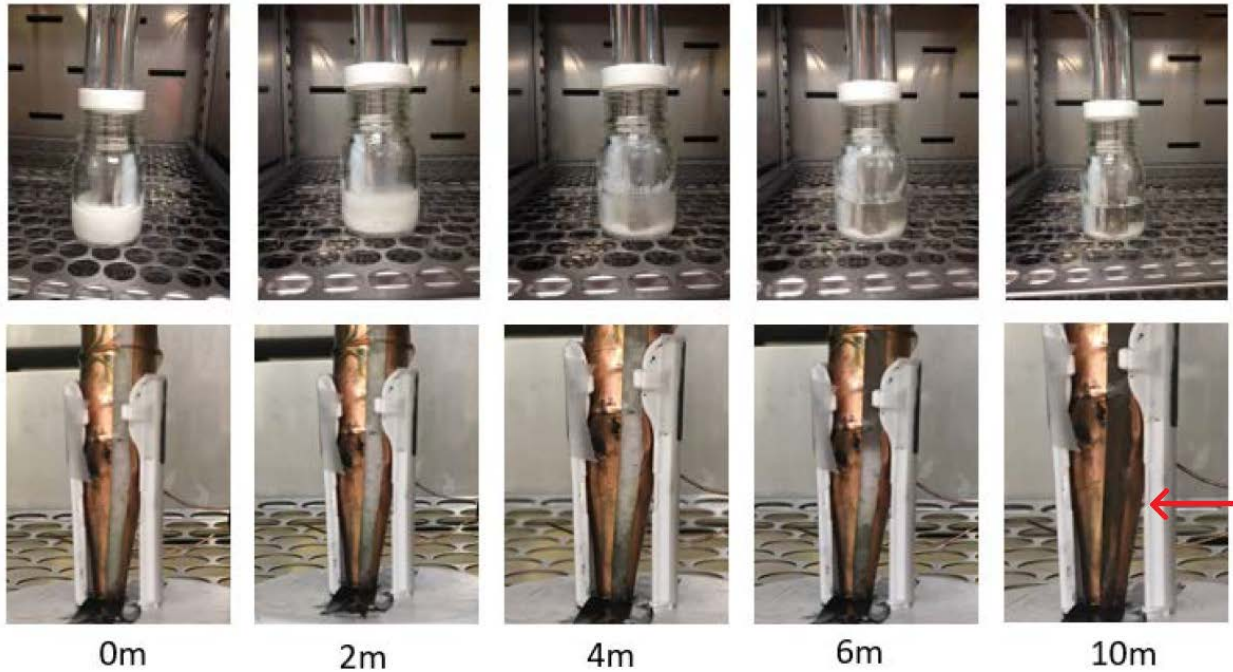


**Figure 5-3: Comparison of water/oil separations between flat plates and cylindrical electrodes**

Based on this result, a further investigation regarding the design of the cylindrical electrodes was performed by changing the thickness of the center electrode and the capillary tube. Also, the effect of the length of the center electrode and gap between the electrode and insulated lass layer was determined.

### 5.3.2 Thickness of the Center Electrode

The thickness of the center electrode may influence the efficiency of the water/oil separation due to its effects on the strength and gradient of electric fields. As validated in the simulation, the strength and gradient of the electric field inside the separator increase as the thickness of the center electrode decreases. The thickness effect of the center electrode on the

water/oil separation was investigated by performing water/oil separation tests using two center electrodes with different thicknesses. As shown in Fig. 5-4, two separators were used in the test. Both separators have an inner diameter of 17mm and an outer diameter of 25mm. The separator on the left has a thicker (7 mm) central electrode, while the one on the right has a thinner (1.65 mm) center electrode. There is a 15mm gap between the edge of the center electrode and the bottom of the separators. High voltage was applied to the two separation tubes at the same time. The applied voltage and frequency were 5kV and 5 kHz with a square wave and the operating temperature was maintained at 90°C.

As indicated in Fig. 5-4, the reduced thickness of the center electrode can expedite the separation speed of the emulsion. The residual water concentrations of the separated oil phase were also measured after the 10-minutes test. The water concentration of the thinner electrode (5.02%) showed smaller value compared to the result of the thicker electrode (5.90 %). Therefore, the quality of the separated oil can also be improved by reducing the thickness of the center electrode.

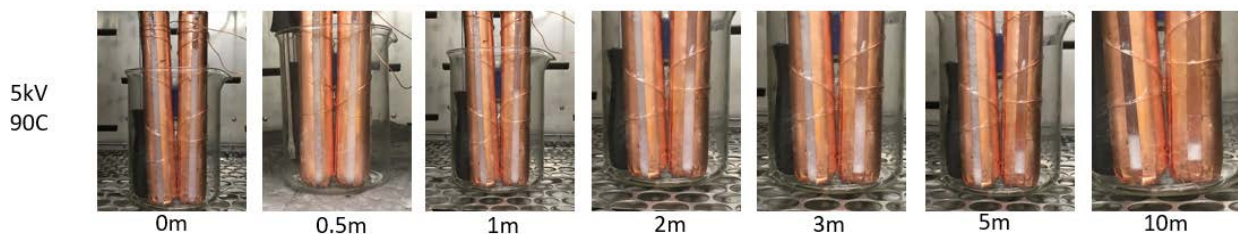


**Figure 5-4: Comparison of water/oil separation with two different thicknesses of the center electrodes: 7mm (left) vs. 1.65mm (right)**

### 5.3.3 Length of the Center Electrode

The length of the central electrode can affect the separation time of the water-in-oil emulsion. Several tests for water/oil separation are executed to determine the length effect of the center electrode. Two identical cylindrical separation tubes are used in this test. The separation tube on the left-hand side has a shorter central electrode (105mm), which results in a 15mm gap to the bottom of the tube. The separation tube on the right-hand side has an extended length (120mm) of the center electrode, which results in a minimal gap to the bottom of the tube. The use of this elongated center electrode may enhance the electric fields in the separator, especially around the bottom area. The thickness of the center electrode is 0.65 mm for both separation tubes. Two different voltages and temperatures are used in this test. The applied voltage is 5kV or 10kV with 5 kHz of frequency, and the operating temperature is 90°C or 100°C.

The simulation shows that the extended length of the center electrode should enhance separation. It is verified by our experimental tests. As can be seen in Fig. 5-5, the extended length of the center electrode can promote the separation speed. Especially, huge differences are observed around the lower part of the separators. The white layer, which indicates incompletely separated emulsion, remains on the left side tube after the 10-minutes test, while the emulsion is completely separated after several minutes on the separator which has an extended center electrode. That phenomenon may result from the enhanced electric field around the bottom area of the separator by using the elongated central electrode.

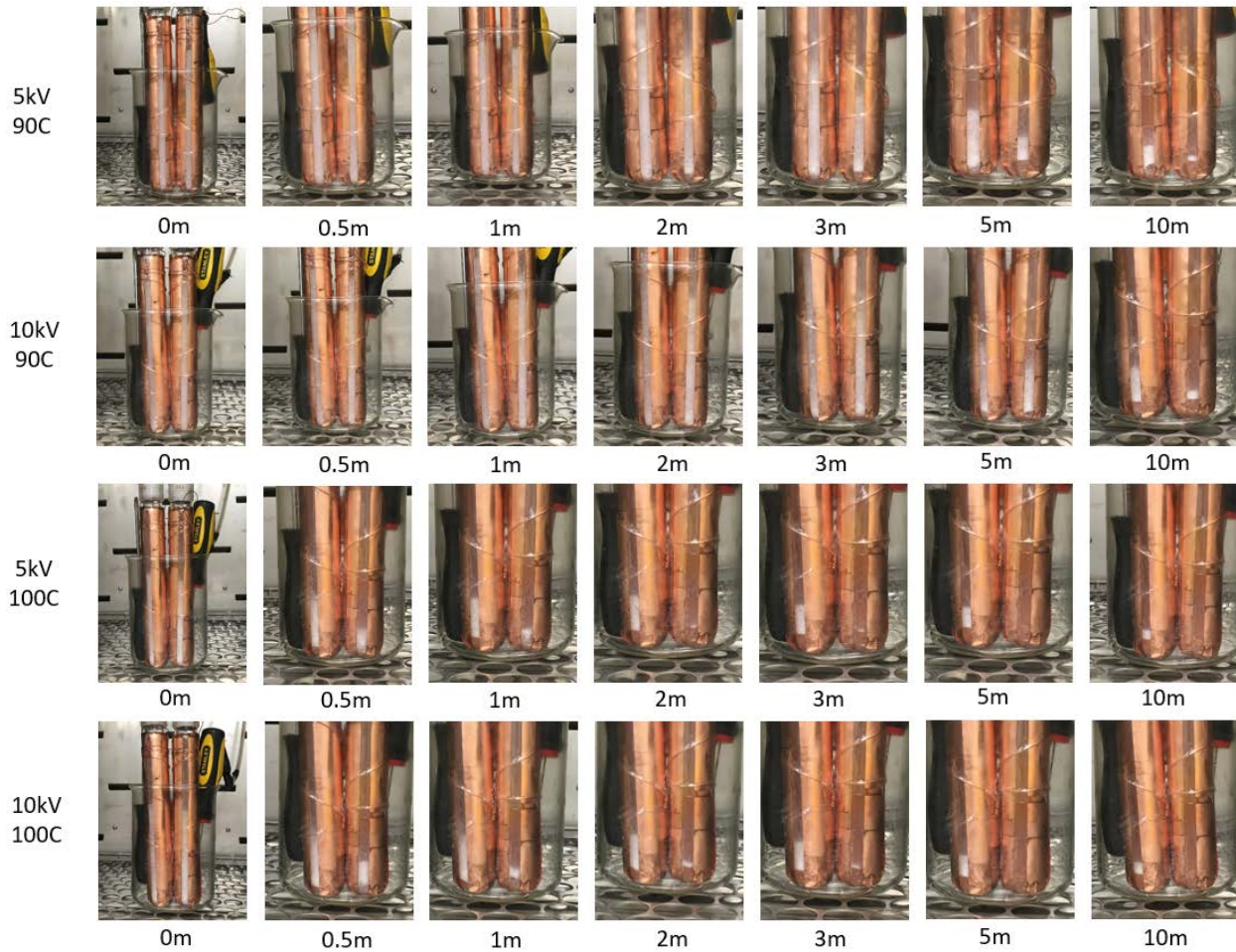


**Figure 5-5: Comparison of water/oil separations with two different lengths of the center electrodes at different temperatures and voltages**

### 5.3.4 Air-gap between Center Electrode and its Capillary Tube

In the separator, insulated electrodes are used to prevent electric short-circuits. This design is achieved by inserting the copper wire into a thin capillary glass tube. As a result, there would always be a thin air-gap between the copper wire and the insulated capillary tube. From previous tests, it has been determined that the thickness and length of the center electrode can

affect the separation speed. However, it still remains unclear whether the air-gap has an influence on the separation performances.

In this test, the effect of the air-gap between the center electrode and its insulated capillary tube is investigated. Two different thicknesses (0.2mm and 0.65mm) of the copper wire are used with the same capillary tube that has an inner diameter of 1.15mm and an outer diameter of 1.65mm. It results in the air-gap of 0.475mm and 0.25mm respectively. The separator on the left has a thinner central electrode (0.2 mm) which leads the extended air-gap, while the separator on right has a thicker central electrode (0.6 mm). The applied voltage is 5kV or 10kV with 5 kHz of frequency, and the operating temperature is 90°C or 100°C.

The simulation implies that the reduced air-gap can enhance the electric field strength as shown in Fig. 5-1 (a). This increased electrical strength can expedite the separation speed of the water-in-oil emulsion. The separations of water and oil phases are indicated in Fig. 5-6. From the results of this test, it is experimentally verified that the reduced air-gap between the center electrode and the capillary tube can expedite the separation speed.

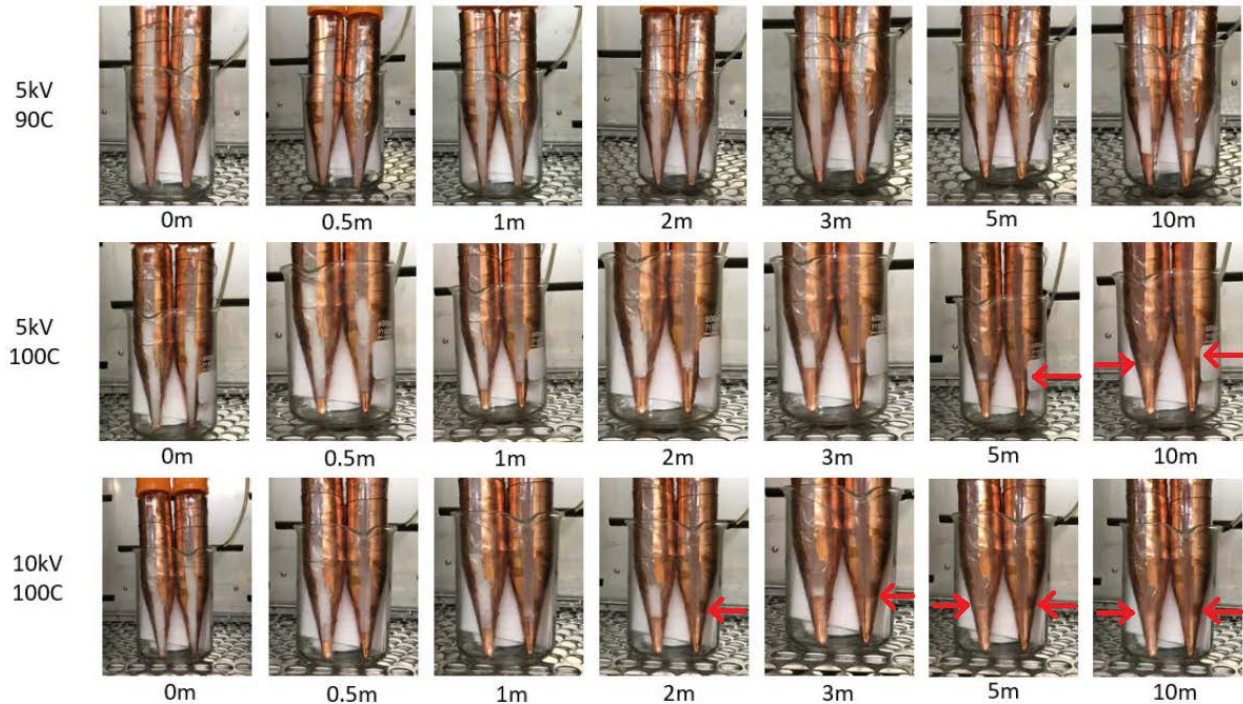


**Figure 5-6: Comparison of water/oil separation with the effect of air-gap between the center electrode and its capillary tube**

### 5.3.5 Diameter of the Separation Tube

The diameter of the separation tube can influence the strength and gradient of the electric field which determine the separation time of the emulsion. Theoretically, the dipole-dipole forces and DEP forces rapidly decrease as the radius increases, and this phenomenon is verified by performing computational simulations. In this experiment, two different dimensions of cylindrical separators are used for the water/oil separations. The inner and outer diameters of the larger separation tube are 30mm and 34mm, while the smaller one has 13mm and 17mm respectively. The applied voltage is 1kV with 50Hz, and the operating temperature is 90°C. The dimensions of the center electrode and its capillary tube are identical for both separators.

The difference of the separation depending upon the diameter of the separator is shown in Fig. 5-7. The upper pictures represent the separations by the larger separation tube, while the lower pictures show the smaller tube separation. As indicated in Fig. 5-7, the reduced diameter of the separator can exceedingly expedite the separation speed of the emulsion by over 2 times. Therefore, the computational simulation accurately predicts the enhancement of the separation by reducing the diameter of the separator.

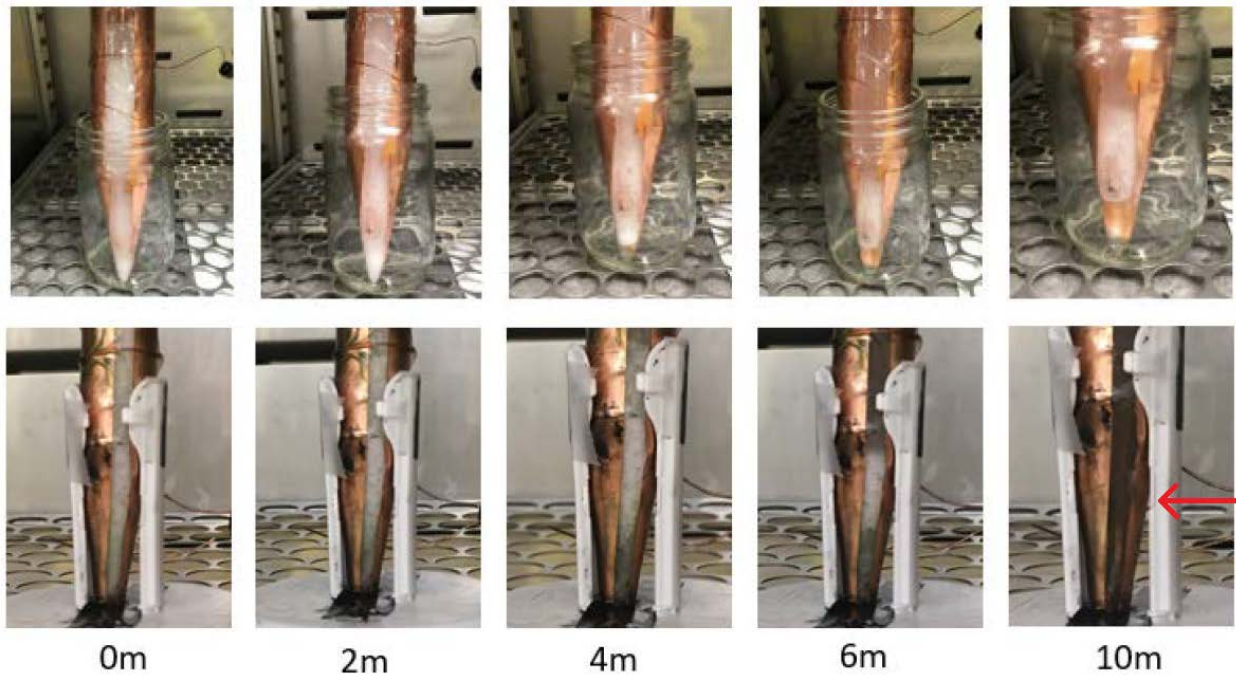


**Figure 5-7: Comparison of water/oil separations with two different lengths of the center electrodes at different temperatures and voltages**

## 5.4 Conclusions

In summary, the design of the water/oil separator is investigated theoretically and experimentally. The separator with cylindrical design shows a higher separation speed compared to the separator using flat-plate electrodes because of the generation of non-uniform electric fields inside. Non-uniform electric fields are generally considered more efficient than uniform electric fields because it introduces both dipole-dipole forces and DEP forces on water droplets, while only dipole-dipole forces can be created in uniform electric fields.

In addition, the effects of the thickness and length of the center electrode, air-gap between the center electrode and insulated capillary tube, and the diameter of the separator are investigated theoretically and experimentally. Both the simulation and experiments show that the electric field strength and gradient in emulsions would be enhanced by narrowing the air-gap, extending the center electrode, and reducing the diameter of the separation tube, which enhance the separation speed.

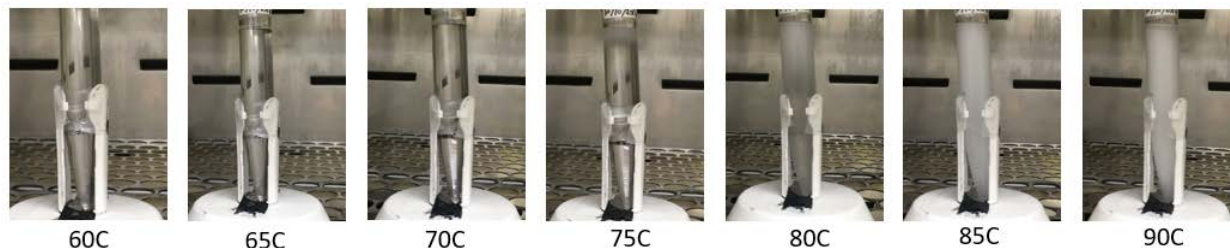
## **Chapter 6. Water /Oil Separation Results**

### **6.1 Introduction**

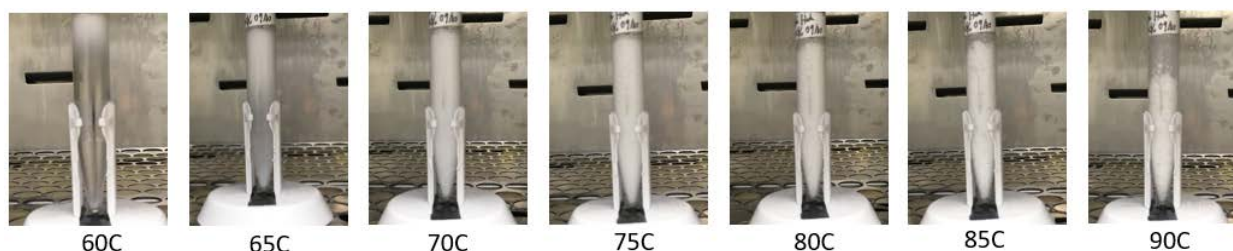
In chapter 4, all of the experimental equipment was introduced for static and dynamic water/oil separation tests. This chapter will present the experimental results for water/oil separations in micro- and macroemulsions. First, the static separation tests for water-in-oil micro- and macroemulsion were performed with different temperatures, voltages, and frequencies. The separation time was observed, and the quality of the separated oil was determined by measuring the residual water concentration after the test. The influence of the temperature, voltage, and frequency on the water/oil separation was investigated, and the experimental results were compared with the calculations of the theoretical consideration. The square wave of Pulsed DC voltage was used for all tests because it is generally considered the most effective wave shape. In addition, the separation results using the combined methods (heating + electric field) were compared to the results of the single method alone. After that, the continuous water/oil separation system was developed and used for the dynamic separation tests. This experimental work can determine whether the combined method is applicable at an industrial scale. Additionally, the influences of the operating temperature and flow rate were determined in this test.

## 6.2 Phase Change of Microemulsions with Heat Treatment

A heat treatment may influence the state of the micro- or macro-emulsion. As the temperature of the emulsion increases, the movement of droplets also increases. This action can expedite the droplet coalescence. Therefore, the collided droplets of microemulsion can be transformed to macroemulsion at certain temperatures. When this phase change occurs, the color of the emulsion is usually changed to opaque because the bulk of the droplet becomes larger than the wavelength of light. The phase changes with increase of temperature on the 5% and 10% water-in-oil microemulsions are shown in Fig. 6-1. This figure indicates the phase (color) change depending on the emulsion temperatures. Temperature of the emulsion can be measured by the immersed thermocouple. The temperature at which phase transition occurs is known as a cloud point and is often characterized by a dramatic color change. A cloud point is different from the type of oil and the water concentrations in the emulsion. The cloud point of 5% water-in-oil microemulsion is around 80 - 85°C, while the cloud point of the 10% water-in-oil microemulsion is between 65 - 70°C as indicated in Fig. 6-1(a) and (b). A cloud point usually decreases as the water concentration increases because the distance between droplets becomes narrow as water concentration increases. This reduced distance can accelerate the coalescence speed of the droplets. Most of the droplets in the microemulsion state (*i.e.* less than 100nm) can be transformed to the macroemulsion state (*i.e.* over 100nm) over the cloud points. White (or opaque) deposits are observed when the temperature reaches a cloud point, and this color becomes transparent when water phase is completely separated at the bottom of the tube.



(a) 5% water-in-oil microemulsion: the cloud point is 80-85°C



(b) 10% water-in-oil microemulsion: the cloud point is 65-70°C

**Figure 6-1: Phase change of 5% and 10% water-in-oil microemulsions by increasing temperature**

In contrary to the microemulsion, macroemulsion does not have a cloud point because it is initially opaque at room temperature. Water-in-sunflower oil was used for the macroemulsion separation tests. The color of the macroemulsion does not change when the temperature reaches a high temperature such as 90°C as shown in Fig. 6-2 because the size of the droplets is already larger than the wavelength of light. Even though the color does not change, the water droplets keep coalesced at the elevated temperature, and finally water phase of this macroemulsion becomes transparent when the emulsion is completely separated into two phases.

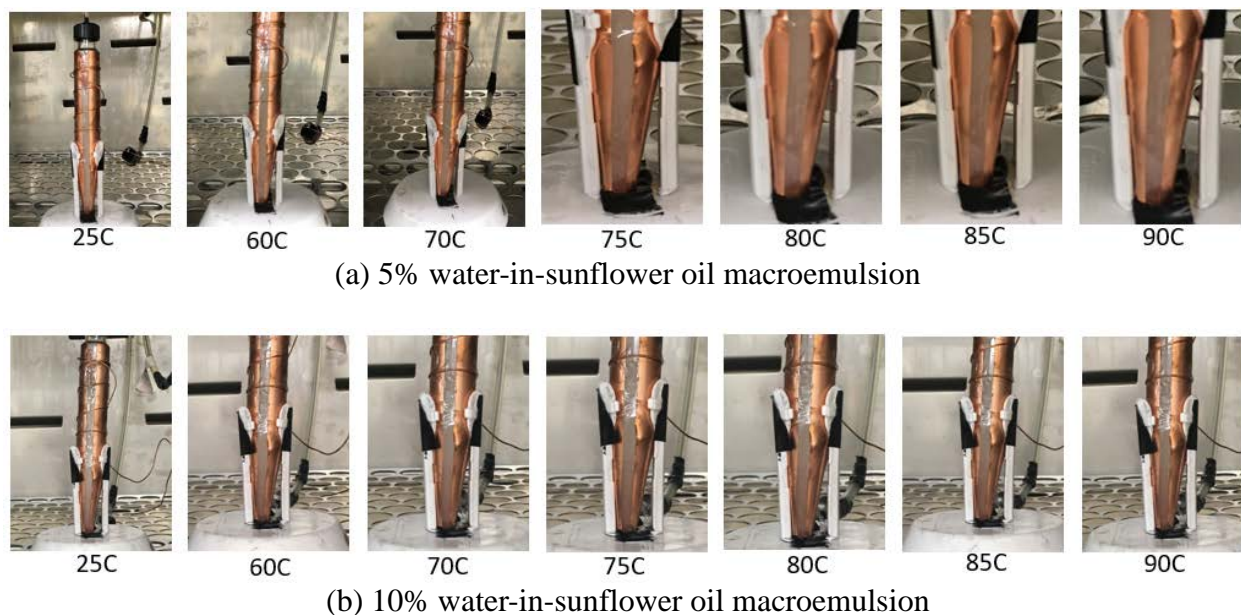


**Figure 6-2: Water-in-sunflower oil macroemulsions by increasing temperature**

## **6.3 Static Separations of Microemulsions by the Combined Method**

### **6.3.1 Water/Oil Separations by Heating or Electrostatic Method Alone**

Water-in-oil macroemulsion can be separated by either heating or electric field method alone. To determine the possibility of the microemulsion separation by a single method such as heating or electrostatic method, two different types of tests with 5% and 10% water-in-oil microemulsions were performed. In contrary to macroemulsion, water-in-oil microemulsion cannot be simply separated by a single method due to its tiny droplet sizes. Hence, multiple (or combined) methods are necessary for adequate separation of the microemulsions. In this study, heating or electric field was applied to the emulsion for 60 minutes.

First, heat treatment was used for the water/oil microemulsion separation. 5% and 10% water-in-oil microemulsions were heated to 90°C in the heating oven, and once the temperature of the emulsion reaches to 90°C, the emulsion remains in the oven at the constant temperature

for 60 minutes. Water/oil separations were observed during the tests as shown in Fig. 6-3. Due to increased water content, 10% water-in-oil emulsion takes more time to be separated when compared to 5% water-in-oil emulsion. Therefore, water-in-oil microemulsion can be separated by a single method of heat treatment if it is exposed to the high temperature for a certain amount of time. In this test, the separations of the emulsion were observed around 20-30 minutes after the temperature reaches to 90°C.

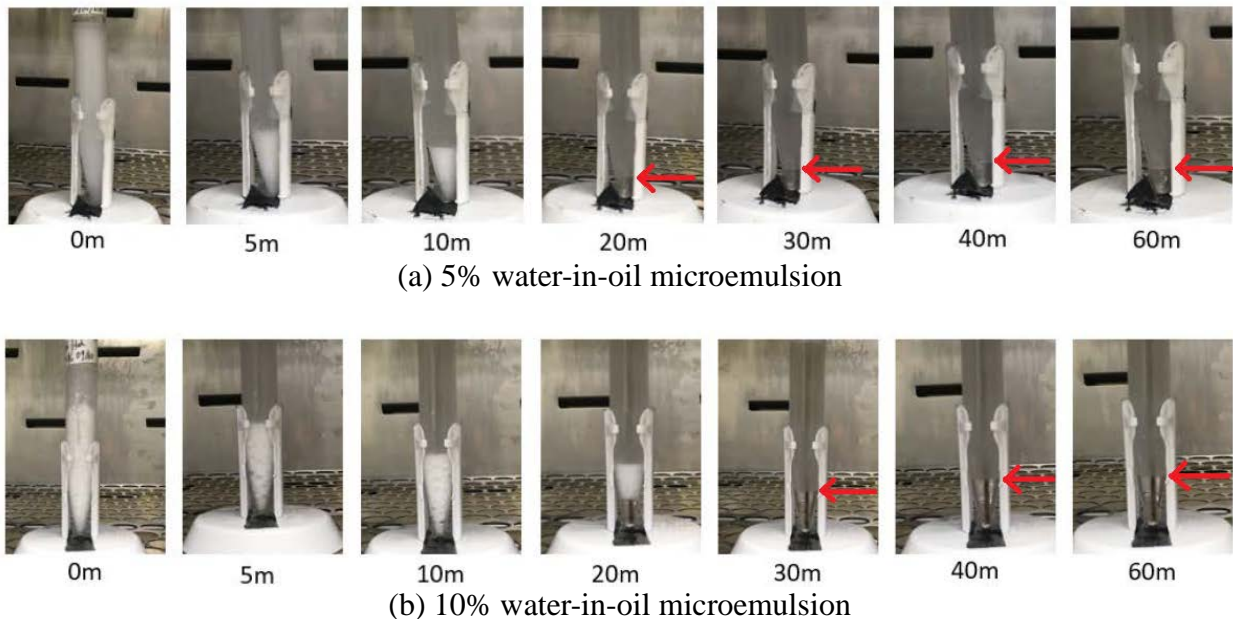


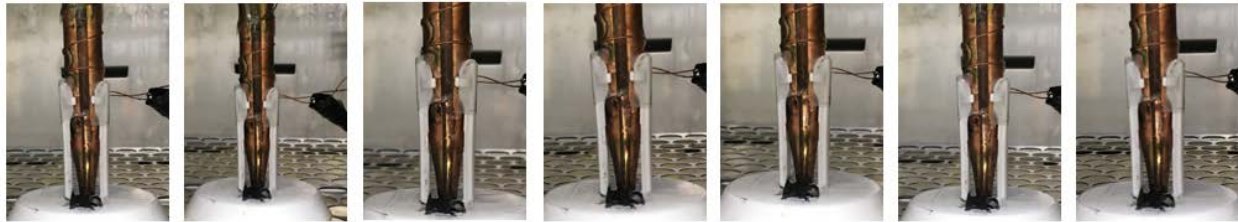
**Figure 6-3: Separations of water/oil microemulsions by heat treatment**

Next, water-in-oil microemulsions may be separated by a single method of an electrostatic field. In this test, electric fields were applied to 5% and 10% water-in-oil microemulsions for 60 minutes at the room temperature (25°C). The voltage and frequency were 1kV and 50Hz with a square wave. No separations were observed for both 5% and 10%

emulsions as indicated in Fig. 6-4. To successfully separate the water-in-oil emulsion, water droplets should be coalesced by electric field and the coalesced droplets can be deposited by the gravitational force. However, the droplet sizes of microemulsion are too small to create sufficient attracting force between droplets and gravitational force for the droplet precipitation. As indicated in Eq. (3-1) and (3-4), both of the gravitational and electrical forces are strongly affected by the droplet sizes ( $\alpha$ ). Therefore, based on this experimental results, water/oil microemulsions cannot be separated by an electrostatic force alone. The calculations of the theoretical consideration in chapter 3 also support this experimental result.

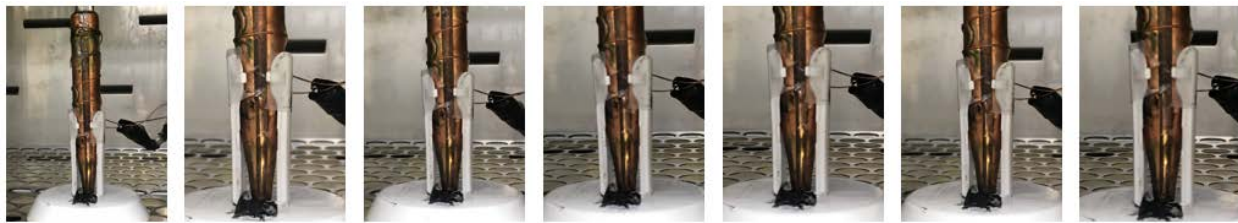
$$F_g = \frac{4}{3}\pi\alpha^3(\rho_w - \rho_o)g \quad (3-1)$$

$$F_{el} = \frac{24\pi\epsilon E_0^2\alpha^6}{t^4} = \frac{24\pi\epsilon E_0^2\alpha^3}{(t/\alpha)^4} \quad (3-4)$$



0m      5m      10m      20m      30m      40m      60m

(a) 5% water-in-oil microemulsion



0m      5m      10m      20m      30m      40m      60m

(b) 10% water-in-oil microemulsion

**Figure 6-4: Separations of water/oil microemulsions by applying electric fields**

In this section, single methods (heating or electric field) were used for the separation of a water-in-oil microemulsion. A microemulsion cannot be separated by electrostatic force alone, while it can be separated by heating method. The separation of water/oil phases was observed around 20-30 minutes after the temperature reaches to 90°C. The separation efficiency of the water-in-oil microemulsions can be significantly improved by using the combination method of heating and electric field. The results of the water/oil separation by this combined method will be introduced in the next several sections. In sections 6.3.2 – 6.3.5, we will discuss the effects of the temperature, voltage, and frequency to enhance the efficiency of the water/oil separations.

### **6.3.2 Temperature Dependence on the Separation of Water-in-Oil Microemulsions**

Temperature dependence on the water/oil microemulsion separation was studied by performing several experiments at seven different temperatures: 25, 40, 50, 60, 70, 80, 90°C. The applied voltage and frequency were kept constant at 1kV and 50Hz with a square wave for all of the tests. First, the water-in-oil microemulsion was heated to the target temperature, then the electric field was applied to the emulsion for 10 minutes. For 5% water-in-oil microemulsions, no separations were observed from 25°C to 70°C of temperature as seen in Fig. 6-5. However, the water/oil separation was partially observed at 80°C test, and this water/oil separation was significantly accelerated at the increased temperature (90°C). The water-in-oil microemulsion was fully separated in less than 1 minute at this temperature as shown in Fig. 6-5.



**Figure 6-5: Temperature effect on the separations of 5% water-in-oil microemulsions**

In addition, for the 10% water-in-oil microemulsion tests, no separations were observed until 60°C. The separated water phase is partially observed at 70°C test, and the amount of separated water increases as the operating temperature increases up to 90°C as shown in Fig. 6-6. Finally, the emulsion is fully separated in less than 1 minute at 90°C. Based on the results shown in Figs. 6-5 and 6-6, water-in-oil microemulsions cannot be separated until they reach the cloud points, which are around 80°C for 5% emulsion and 70°C for 10% emulsion. Therefore, it is

important to firstly increase the temperature of the microemulsions over the cloud point before applying a high voltage to advance the separation efficiency.



**Figure 6-6: Temperature effect on the separations of 10% water-in-oil microemulsions**

The water concentrations of the separated oil phase were measured to determine the quality of the separated oil. Table 6-1 and Fig. 6-7 indicate the residual water concentrations in the separated oils with an initial water concentration of 5% and 10% in emulsions. The water

concentration decreases rapidly when the temperature reaches the cloud point for both 5% and 10% emulsions. Finally, the water concentrations reach around or less than 4% at 90°C. Therefore, the quality of the separated oil can be much improved with the increase of temperature. However, the water concentrations of the separated oil phase from the microemulsion are much higher than the values of the macroemulsion due to its smaller droplet sizes. For example, around 60% of the water is separated at the highest temperature (*i.e.* 90°C) with the 10% initial water concentration. This separation quality may be improved if we extend the experimental time.

**Table 6-1: Water concentration measurements for different temperatures**

Temperature	Voltage	Frequency	Water concentrations (%)	
			5% W-O emulsions	10% W-O emulsions
25 °C	1 kV	50 Hz	5.41	11.22
40 °C			5.34	11.09
50 °C			5.52	10.44
60 °C			5.62	10.22
70 °C			5.58	8.11
80 °C			4.58	5.67
90 °C			3.80	4.05

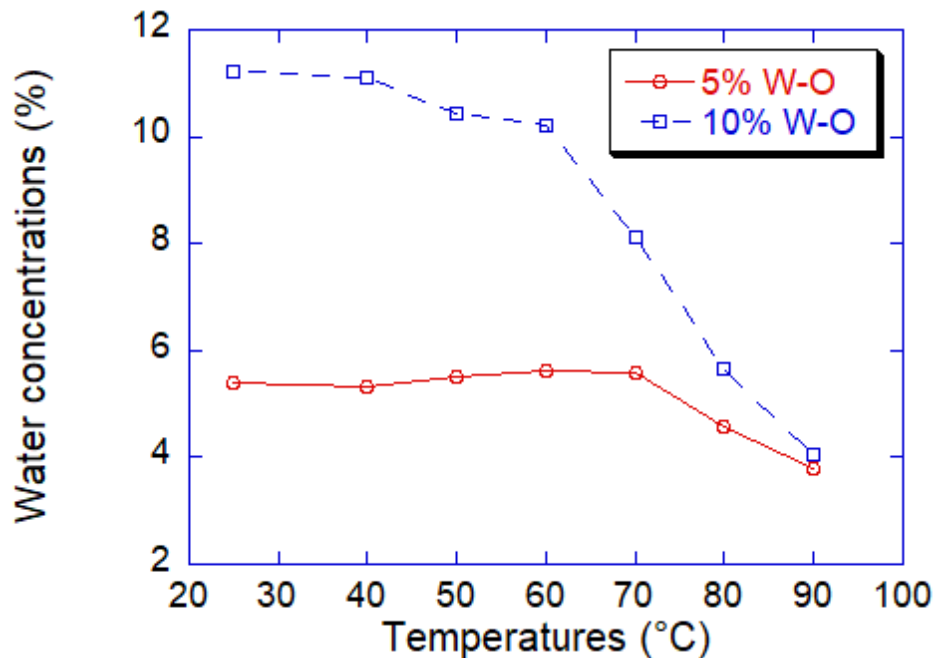


**Figure 6-7: Decrease of the residual water concentrations in oil phase with increasing temperature**

### 6.3.3 Voltage Dependence on the Separation of Water-in-Oil Microemulsions

The dependence of voltage was also investigated for the separation of water-in-oil microemulsion. Five different voltages (0, 0.1, 0.3, 0.5, 1kV) were used for the separation tests while all other conditions remain the same. The operating temperature and the frequency were 90°C and 50Hz respectively. The separations of the 10% water-in-oil microemulsion with the increase of voltages are indicated in Fig. 6.8. Water-in-oil emulsions are not fully separated at the lower voltages such as 0 - 0.1kV, while the water/oil separations are observed when the voltage increases to 0.3kV. The speed of the water/oil separation increases as the applied voltage increases up to 1kV as shown in Fig. 6-8.

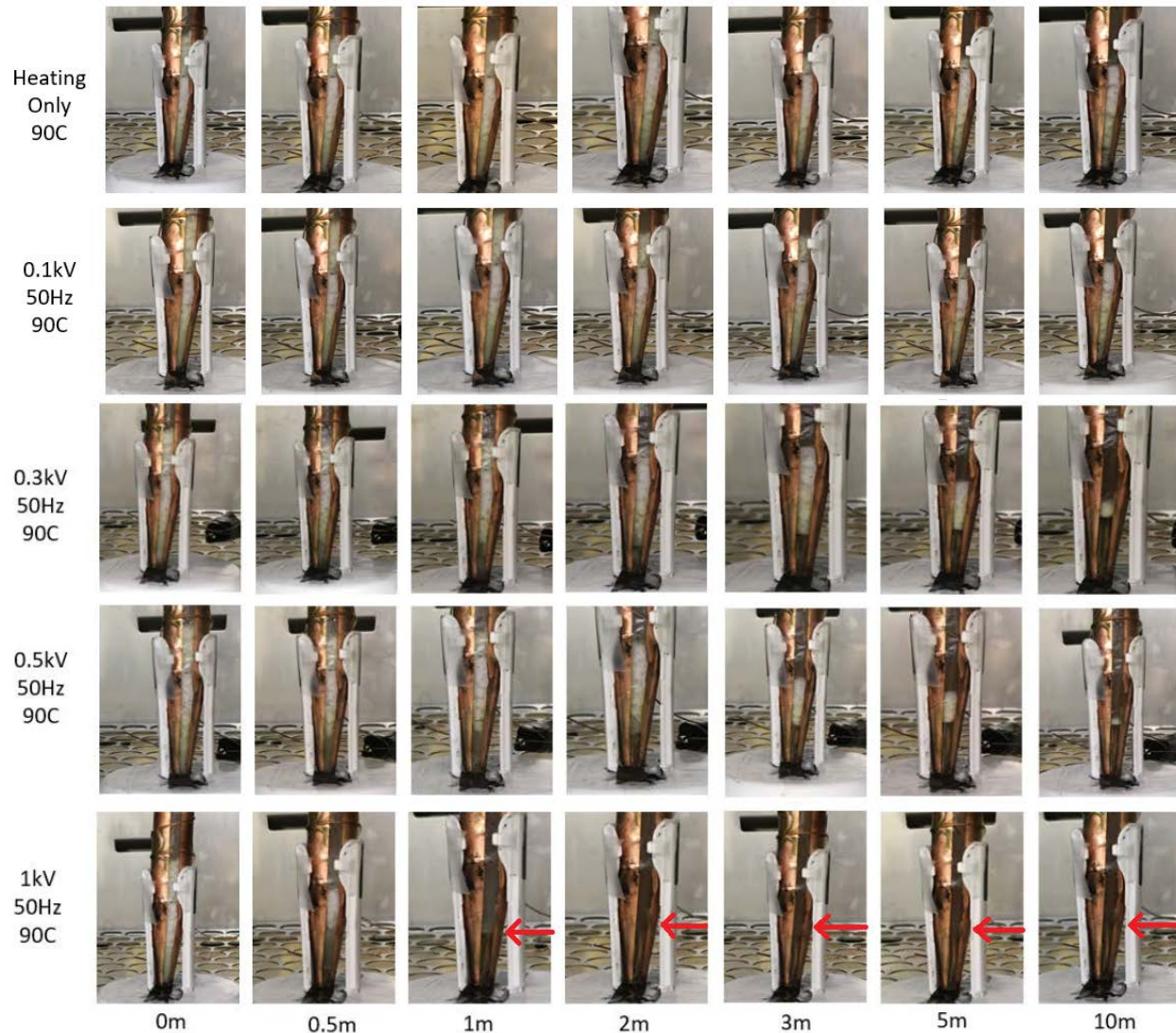


**Figure 6-8: Voltage effect on the separations of 10% water-in-oil microemulsions**

The residual water concentrations in the separated oil phase after the 10-minute tests are indicated in Table 6-2 and Fig. 6-9. The water concentrations are nearly constant as the applied voltage increases. This result indicates that the increase of voltage can expedite the separation speed of water-in-oil emulsion, while the quality of the separated oil is not considerably improved for the 10 minutes of test time. Fig. 6-10 shows the decrease of the residual water concentrations in the oil phase with test time. In this test, 1kV of voltage was applied to the 10%

water-in-oil microemulsion with 50Hz was applied at 90°C. As shown in Fig. 6-10, the water concentration of the oil phase is reduced to 4.6% when the temperature of the emulsion reaches to 90°C. The residual water concentration decreases rapidly at the beginning of the test until 3 minutes, after that it becomes nearly constant until 10 minutes because it already reaches the maximum solubility of water at this temperature. Therefore, the influence of the voltage on the separation speed is significant, while it is relatively small on the quality of the separated oil phase at a certain amount of time. In this test condition, 3 minutes is the optimum test time. The optimum test time can be increased or decreased as the applied voltage reduces or increases.

**Table 6-2: Water concentration measurements for different voltages**

Temperature	Voltage	Frequency	Water concentrations (%)	
			5% W-O emulsions	10% W-O emulsions
90 °C	0	50 Hz	3.53	4.18
	0.1 kV		3.63	3.74
	0.3 kV		3.77	4.04
	0.5 kV		3.74	4.17
	1 kV		3.80	4.05

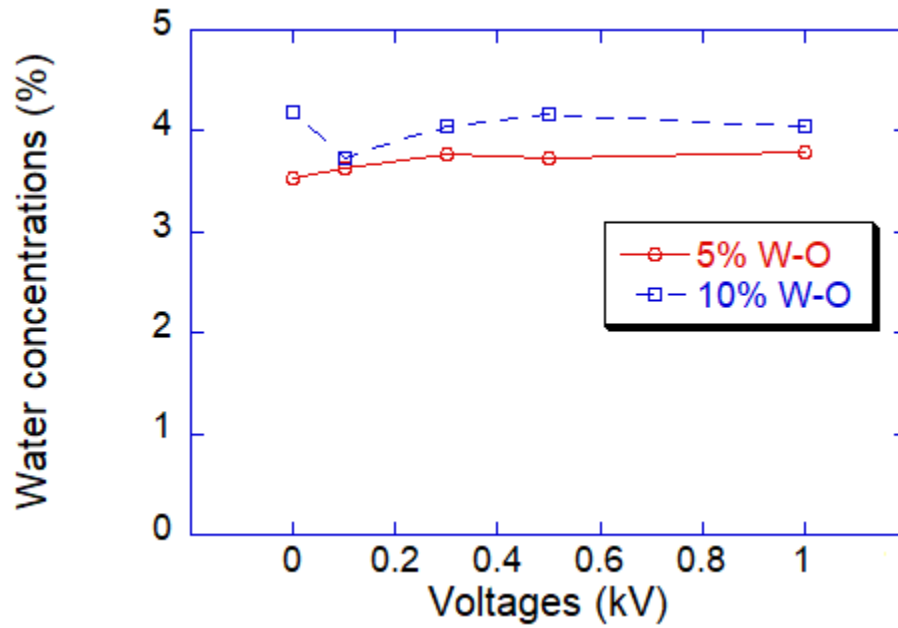


Figure 6-9: Change of water concentrations with increasing voltages

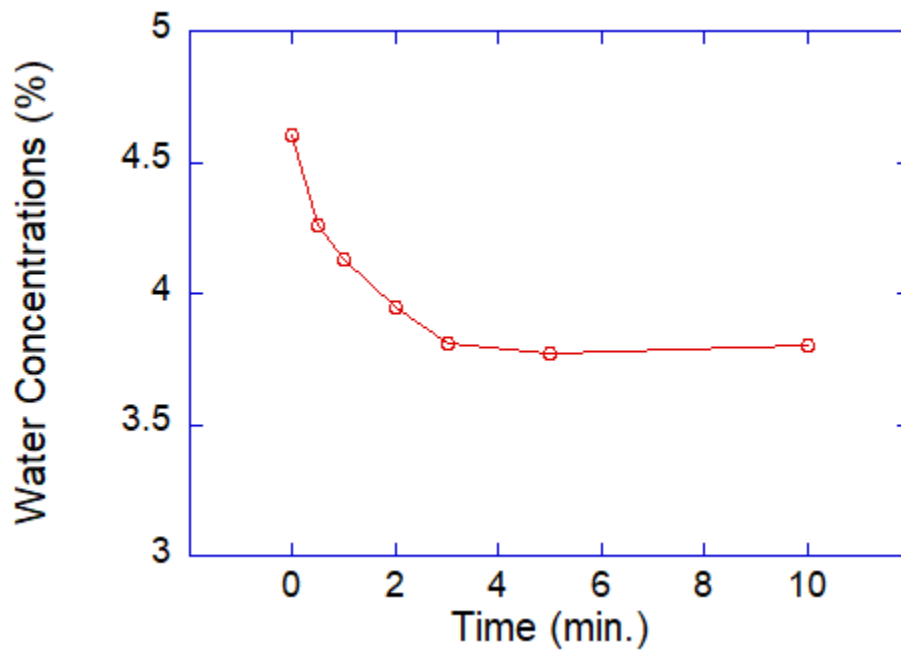
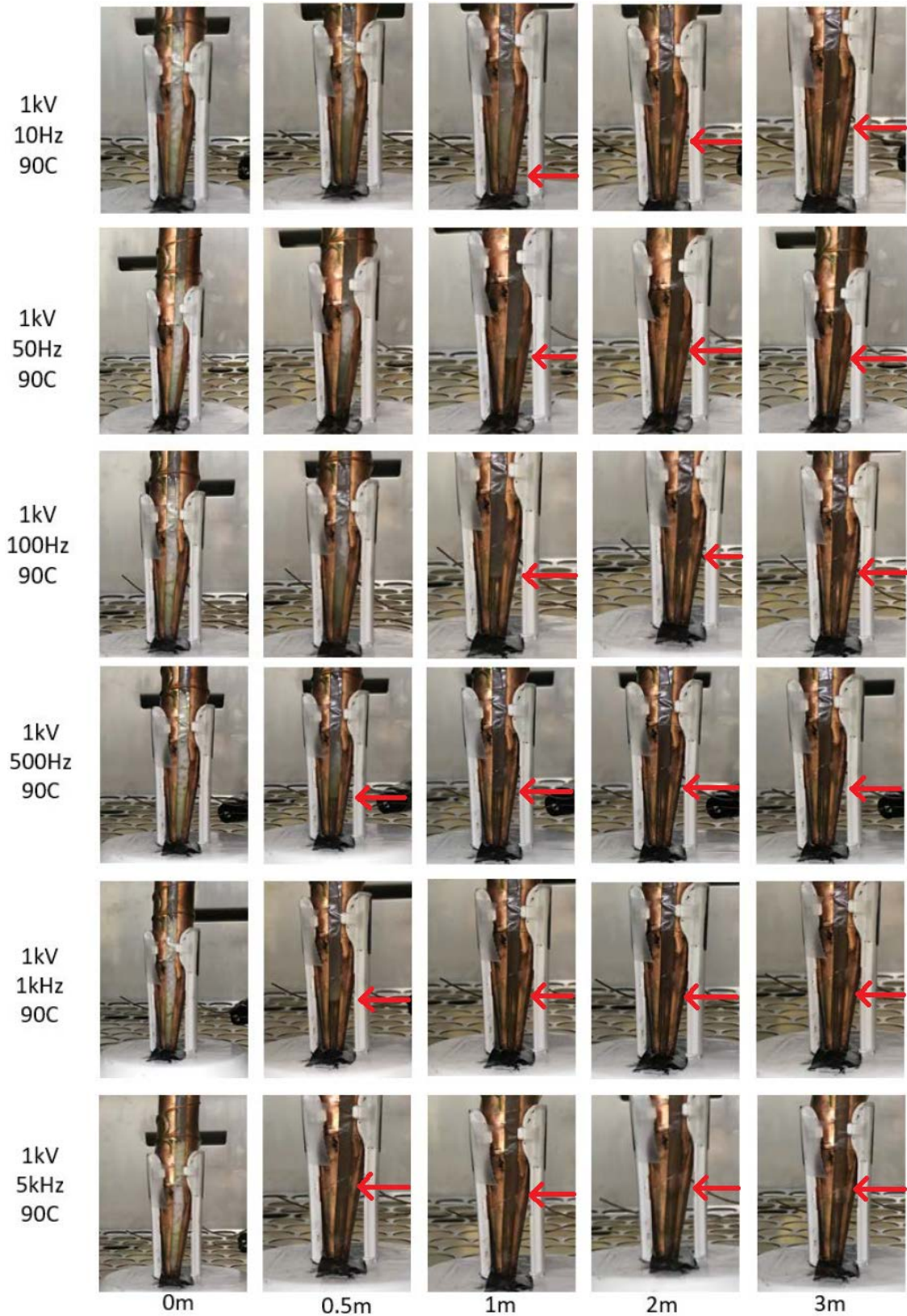


Figure 6-10: Decreases of water concentration of the separated oil phase with test times (10% water-in-oil microemulsion, 90°C, 1kV, 50Hz)

#### **6.3.4 Frequency Dependence on the Separation of Water/Oil Microemulsions**

The water/oil separation tests of microemulsion were executed to determine the frequency effect with six different frequencies: 10, 50, 100, 500, 1000, 5000 Hz. Temperature and voltage are kept at constant at 90°C and 1kV. As indicated in Fig. 6-11, the separation speed can be accelerated as the applied frequency increases. However, the effect of frequency is comparatively smaller than other factors such as temperature and voltage. Water-in-oil microemulsions are fully separated within a few minutes even in a lower frequency such as 10 Hz.

The residual water concentrations in the separated oil phase are indicated in Table 6-3 and Fig. 6-12. As shown in the figure, increasing frequency has a modest effect on the water concentrations of the separated oil phase. Therefore, it is not necessary to use high frequency such as 100 – 5000 Hz for the microemulsion separation test because excessively high frequency leads to unnecessary energy consumption.



**Figure 6-11: Frequency effect on the separations of 10% water-in-oil microemulsions**

**Table 6-3: Water concentration measurements for different frequencies**

Temperature	Voltage	Frequency	Water concentrations (%)	
			5% W-O emulsions	10% W-O emulsions
90 °C	1 kV	10 Hz	3.63	4.34
		50 Hz	3.80	4.05
		100 Hz	3.85	4.16
		500 Hz	3.78	4.01
		1 kHz	3.58	3.99
		5 kHz	3.33	3.99

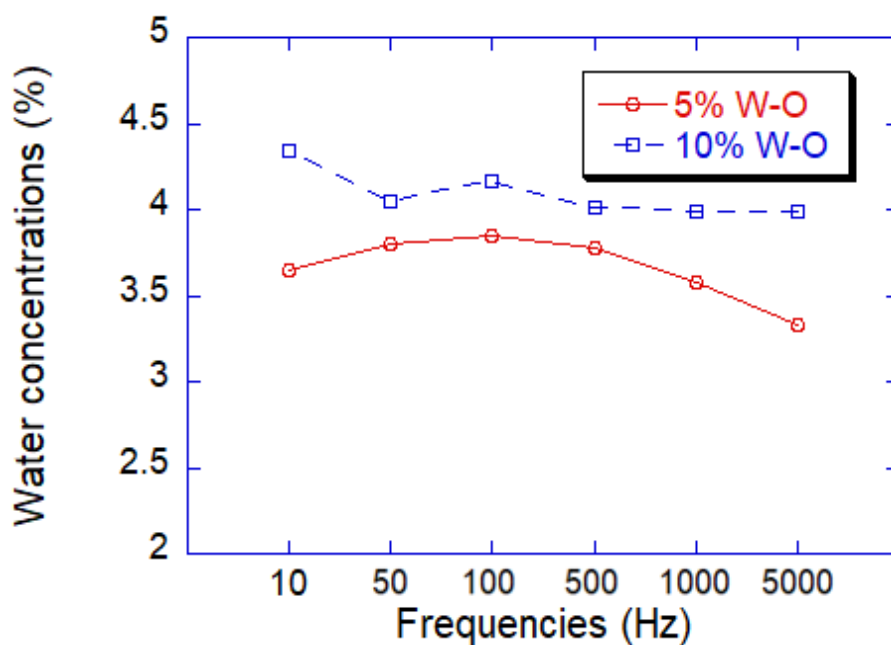


**Figure 6-12: Change of water concentrations with increasing frequencies**

### 6.3.5 Effect of Duty Cycle on the Separation of Water/Oil Microemulsions

Lastly, the duty cycle may also affect the separation of water-in-oil microemulsions. In this test, 10% water-in-oil emulsions were used with 0.5 kV and 50 Hz of square wave at 90°C. Three different duty cycles of the square wave were used: 20, 50, and 80%. The influence of the duty cycle on the water/oil separation speed is shown in Fig. 6-13. It is clearly shown that increased duty cycle from 20 to 80% can expedite the water/oil separations. However, a duty cycle is not a significant factor to determine the separation speed compared to other factors such as temperature and voltage.

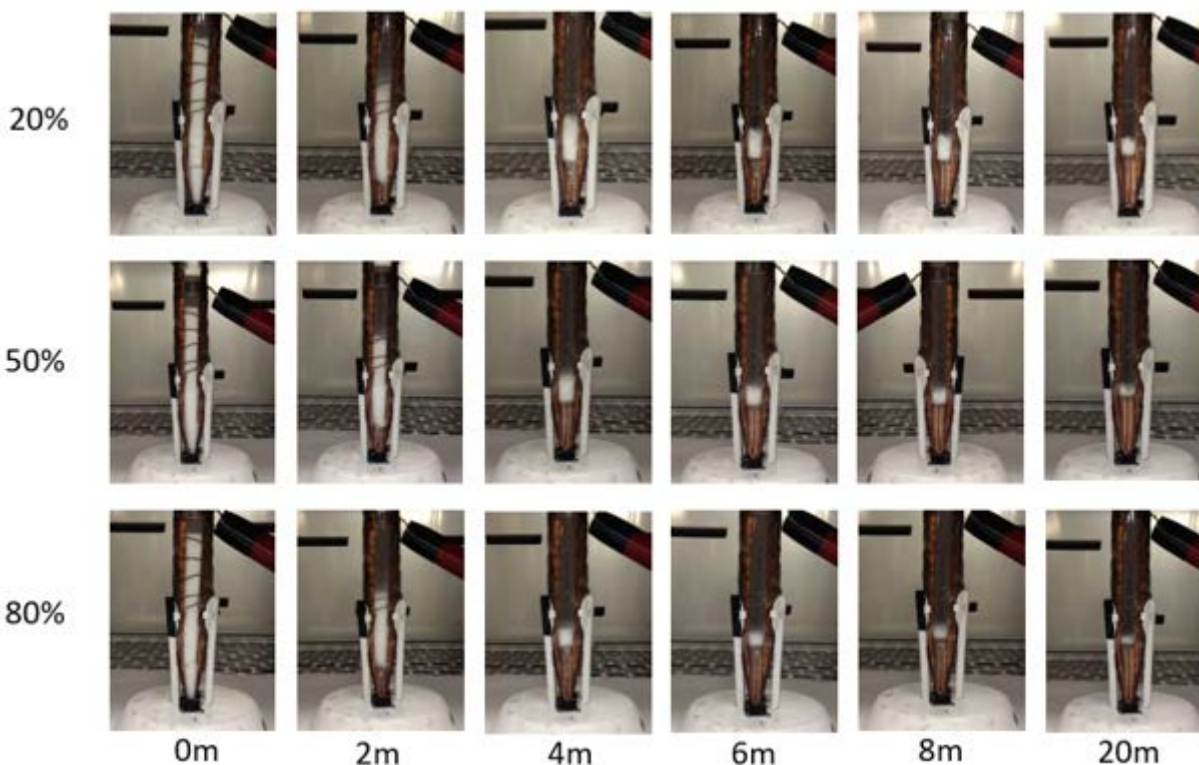


**Figure 6-13: Effect of duty cycle for 10% water-in-oil microemulsion**

## **6.4 Static Separations of Macroemulsion by the Combined Method**

### **6.4.1 Introduction**

The separation speed and quality of the water-in-oil macroemulsion by electrostatic field at elevated temperature can be affected by several factors: temperature, voltage, and frequency. In this test, the range of the operating temperature was 25 - 90°C, and voltage and frequency is 0 - 1kV and 10 - 5,000Hz respectively. Increasing applied voltage and frequency may reduce separation time and lead to higher quality of the separated oil. Sunflower oil was used as a replacement of medium crude oil due to its similar properties (30\_Eow 2003). Sodium Dodecyl Sulfate (SDS) is used as a surfactant to make water-in-sunflower oil emulsion (33\_Hosseini 2012, 30\_Eow 2003). Water-in-sunflower oil emulsions with wt. (H<sub>2</sub>O) = 5% and 10% were investigated in this paper. The water concentrations (%) in the separated oil phase were measured to compare the qualities of separated oils.

### **6.4.2 Comparisons of Heating, Electrostatic, and Combined Method Tests**

Water-in-oil macroemulsions may be separated by either heating or electrostatic method alone. Three different tests with 10% water-in-sunflower oil emulsion were executed to compare the results of the heat treatment, electrostatic field, and the combined method of these two. The water/oil separations with these three conditions are observed in Fig. 6-14, and the residual water concentrations (%) in the separated oil phase after 10-minute tests are listed in Table 6-4. In all of the figures in section 6.4, red arrow indicates the interfaces between the separated water and oil phases. For both heating and electrostatic method tests, the residual water concentrations (%) in the separated oil phase were measured around 5%. This indicates that only about 50% of the

water was separated out of the emulsion by the heating or electrostatic method alone. However, when the combined method was used, the amount of separated water significantly increases. Around 90% of the water was separated from the emulsion as shown in Table 6-4. Therefore, the combination of heating and electrostatic method can be employed to significantly improve the quality of water separation.

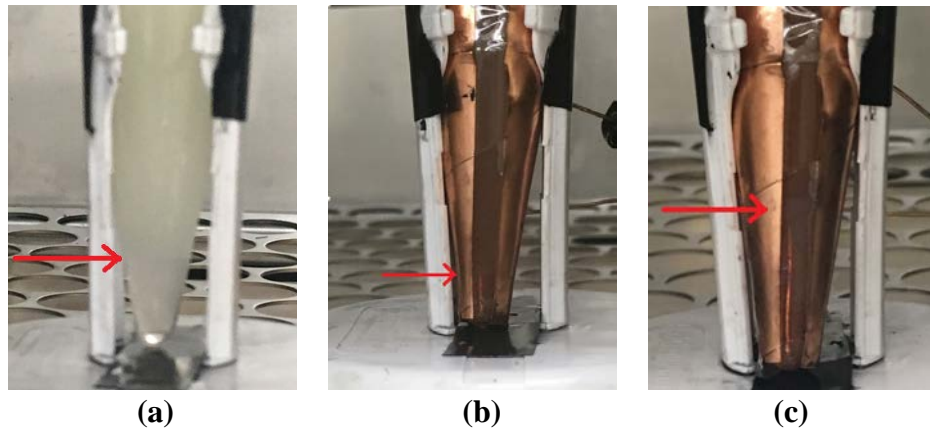


**Figure 6-14: 10% water-in-sunflower oil separations: (a) heating only, (b) electrostatic force only, (c) heating + electrostatic force**

**Table 6-4: Water concentration measurements for heating, electrostatic, and combined methods**

Water-in-sunflower oil separation tests (10 minutes)	Water concentrations (%)	
	5% W-O emulsions	10% W-O emulsions
Heating Only (90°C)	3.30	4.49
Electrostatic Only (25°C, 1kV, 50Hz)	2.98	5.36
Heating + Electrostatic (90°C, 1kV, 50Hz)	0.87	0.94

### 6.4.3 Temperature Dependence

The speed and quality of the water-in-oil macroemulsion separation by the combined method of heating and electric field may be affected by several factors: temperature, voltage, and frequency. Temperature dependence of the water/oil separation was investigated by executing separation tests at seven different temperatures: 25, 40, 50, 60, 70, 80, and 90°C. Other conditions remain constant during the tests. The applied voltage and frequency were 1kV and 50Hz with a square wave. Fig. 6-15 indicates the separations of the emulsion during the test at four different operating temperatures: 25, 50, 70, 90°C. At the room temperature, 25°C, no obvious separation was observed until 5 minutes after applying voltage. However, at 90°C, the water-oil separation was observed in less than 1 minute. The volume of separated water increases during the test. Based on the results, the water/oil separation time is reduced by 5-10 times at 90°C compared to the process under the same electric field at the room temperature (25°C). This reduced separation time by elevating temperature 25 to 90°C was accurately predicted by the theoretical calculations in chapter 3.

The water concentrations of the separated oil phase were measured after 10-minutes test. The results of residual water concentration in the separated oils, with an initial water concentration of 5% and 10%, are indicated in Fig. 6-16. At 25°C, 40-50% of the water was separated out from the emulsion for both 5% and 10% emulsions. The amount of separated water also increases as the operating temperature increases. At the temperature of 90°C, over 90% of the water was separated from the emulsion, and the residual water concentration was measured around 0.8 - 0.9% in the separated oil phase. This result indicates that increasing the operating temperature from 25 to 90°C can reduce the residual water concentration up to 5-6 times. Therefore, the quality of the separated oil can be significantly enhanced with elevated

temperature. Especially, this high-temperature treatment coupled with the electrostatic method can efficiently separate the emulsified oil (*e.g.* crude oil).

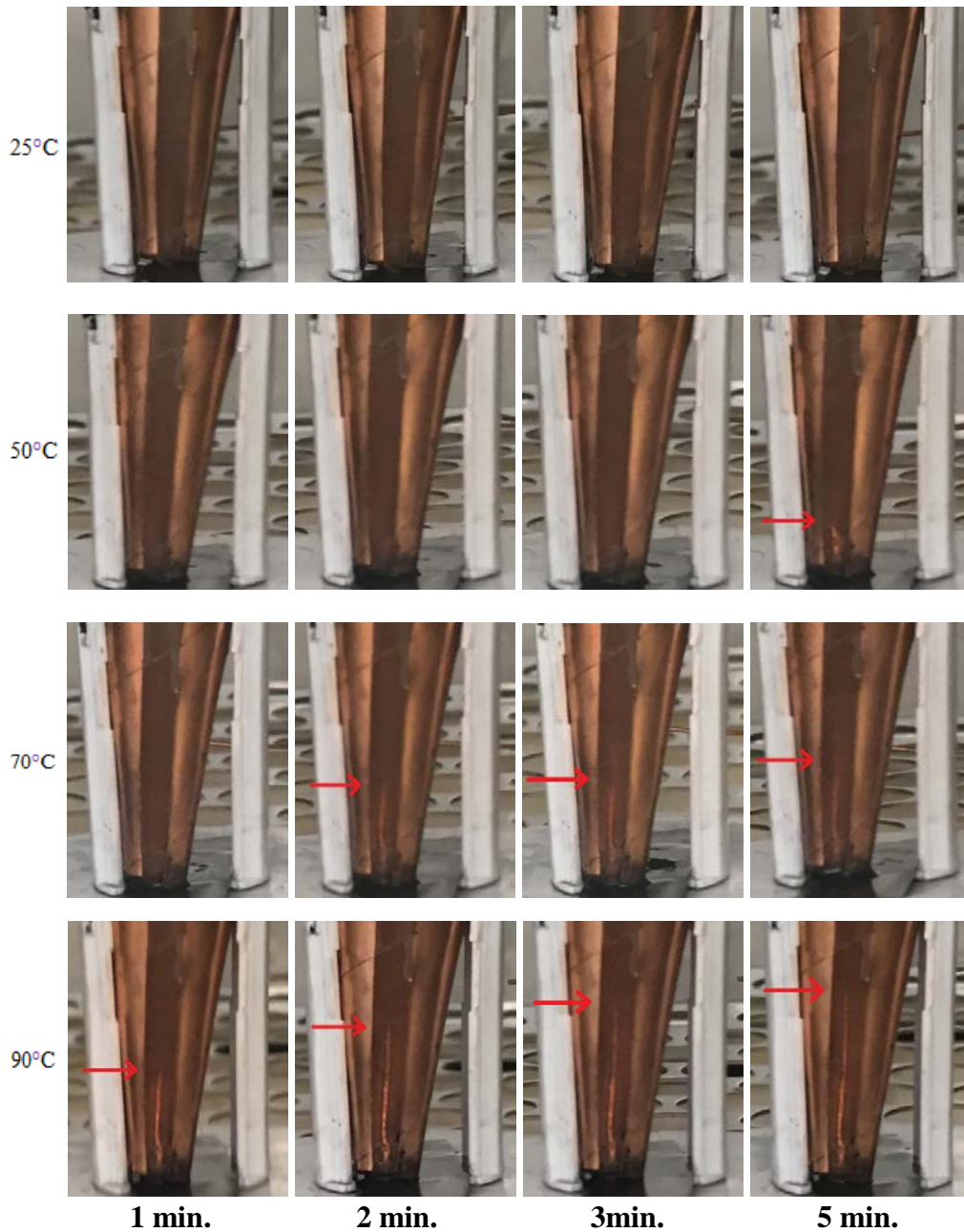


**Figure 6-15: 10% water-in-sunflower oil emulsion separations for different temperatures**

**Table 6-5: Water concentration measurements for different temperatures**

Temperature	Voltage	Frequency	Water concentrations (%)	
			5% W-O emulsions	10% W-O emulsions
25 °C	1 kV	50 Hz	2.98	5.36
40 °C			2.71	4.18
50 °C			1.65	2.99
60 °C			1.25	1.63
70 °C			1.07	1.35
80 °C			0.93	1.13
90 °C			0.87	0.94

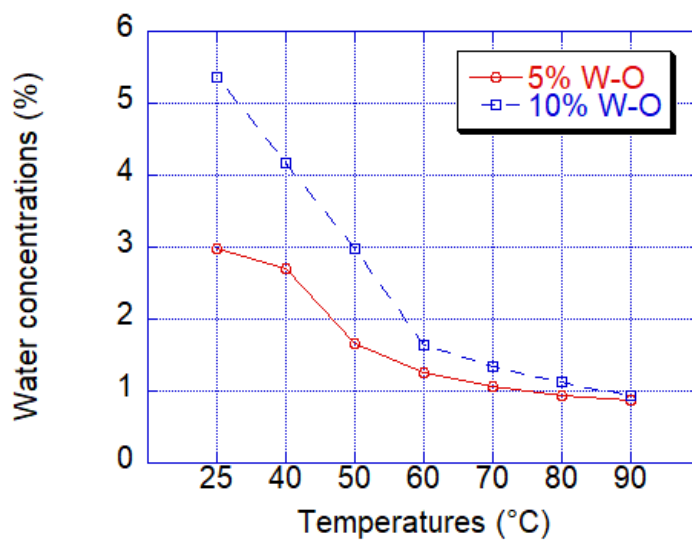


**Figure 6-16: Decrease of water concentrations with increasing temperature**

#### 6.4.4 Voltage Dependence

The dependence of voltage was also investigated for the electrostatic separation. Five different voltages (*i.e.* 0, 0.1, 0.3, 0.5, 1kV) were applied to the water-in-sunflower oil emulsions while all other conditions remain the same. The operating temperature was 90°C, and the frequency of the electric field was 50Hz. The observed water-oil separations are shown in Fig. 6-17. The separation of water and oil phase was not observed with zero voltage (*i.e.* heating only) test in five minutes, and the separations were observed when a voltage was applied to the system. As the applied voltage is increased from 0.1 to 1kV, the separation of the water phase is also expedited. Table 6-6 and Fig. 6-18 present the residual water concentrations in the separated oil phase after the 10-minute test. The increased voltage can deliver a higher quality of the separated oil phase with residual water concentration less than 1%. Therefore, voltage can be considered as a significant factor of the water/oil separation speed and quality. For example, the application of 1kV voltage reduces the separation time by 5-10 times and decreases the residual water concentration by 4-5 times when compared to the test without applying voltage. However, when the voltage reaches a certain point (*i.e.* 0.5kV), the effect of increasing voltage becomes very small. Therefore, it is important to find the optimal voltage for the tests because the increase of voltage may induce higher energy consumption.

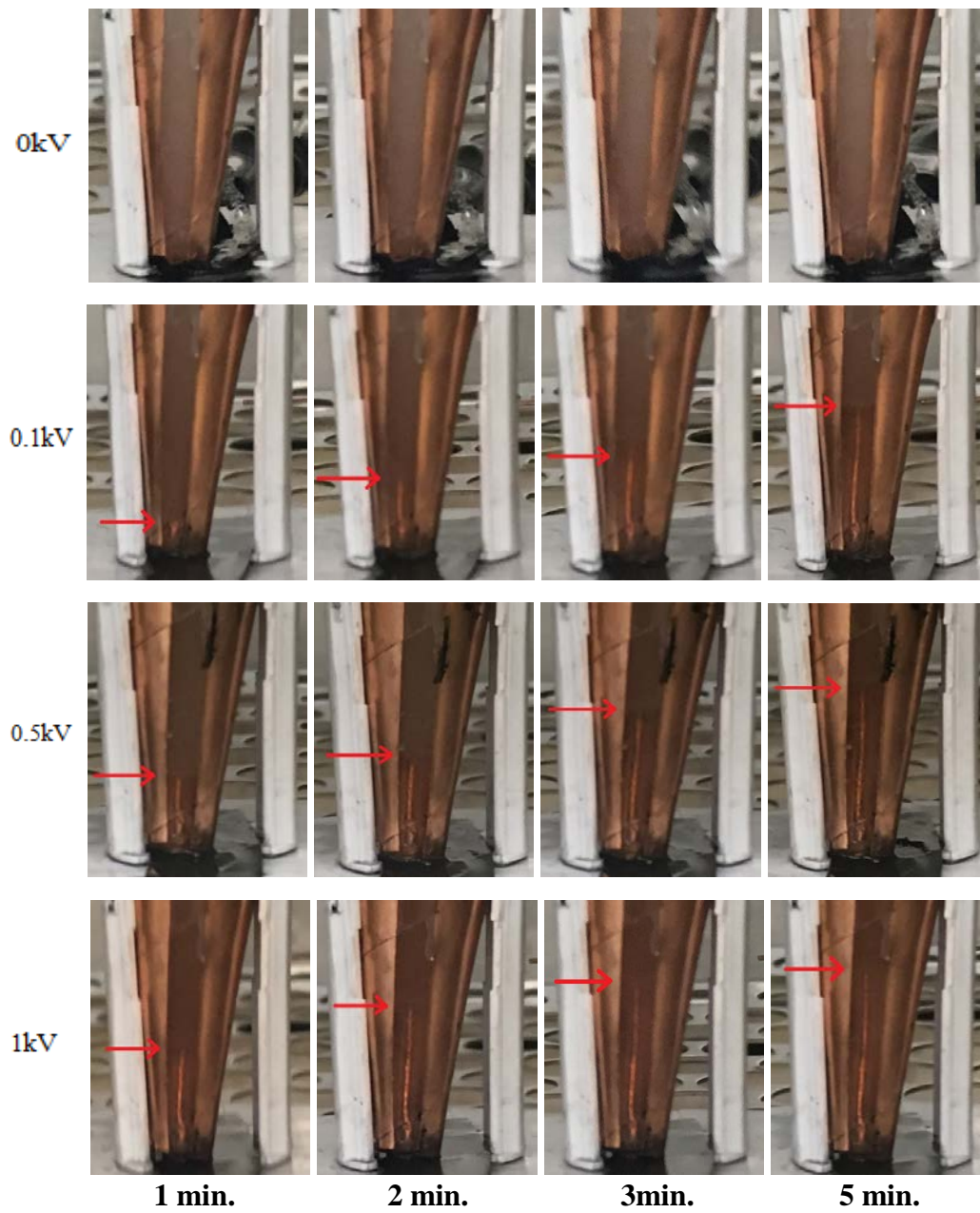


**Figure 6-17: 10% water-in-sunflower oil emulsion separations for different voltages**

**Table 6-6: Water concentration measurements for different voltages**

Temperature	Voltage	Frequency	Water concentrations (%)	
			5% W-O emulsions	10% W-O emulsions
90 °C	0	50 Hz	3.30	4.49
	0.1 kV		1.44	2.23
	0.3 kV		0.86	1.31
	0.5 kV		0.91	1.04
	1 kV		0.87	0.94

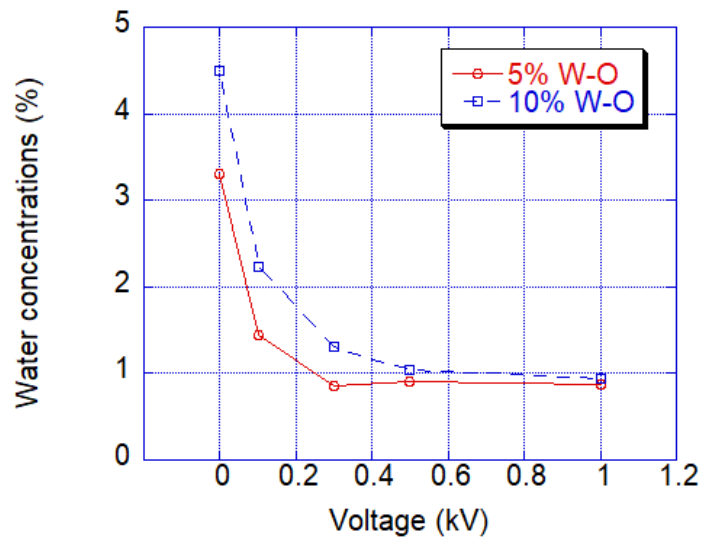


**Figure 6-18: Change of water concentrations with increasing voltage**

### 6.4.5 Frequency Dependence

The separation tests to determine the frequency dependence were executed with six different frequencies: 10, 50, 100, 500, 1000, and 5000 Hz. Applied voltage and temperature were constant at 1kV and 90°C. The increase of frequency expedites the separation speed of

water-in-oil emulsion as shown in Fig. 6-19. However, the effect of the frequency on the separation speed is relatively small compared to the influences of temperature and voltage. Table 6-7 and Fig. 6-20 indicate the residual water concentrations in the separated oil phase. As can be seen in Fig. 6-20, the effect of increasing frequency becomes negligible when the frequency reaches a certain point (*i.e.* 50Hz). Water concentrations were also measured to be less than 1% when the applied frequency was over 50 Hz.

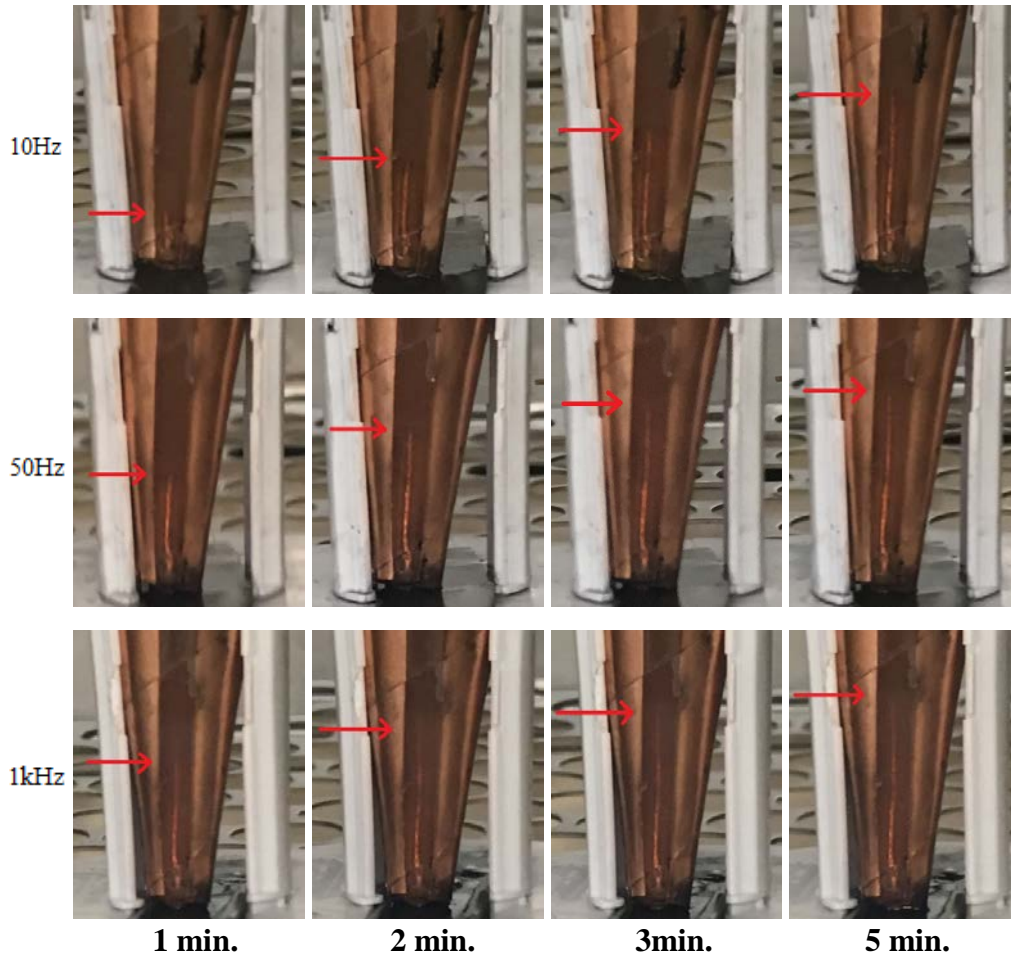


**Figure 6-19: 10% water-in-sunflower oil emulsion separations for different frequencies**

**Table 6-7: Water concentration measurements for different frequencies**

Temperature	Voltage	Frequency	Water concentrations (%)	
			5% W-O emulsions	10% W-O emulsions
90 °C	1 kV	10 Hz	1.01	1.17
		50 Hz	0.87	0.94
		100 Hz	0.84	0.93
		500 Hz	0.83	0.87
		1 kHz	0.90	0.86
		5 kHz	0.84	0.92

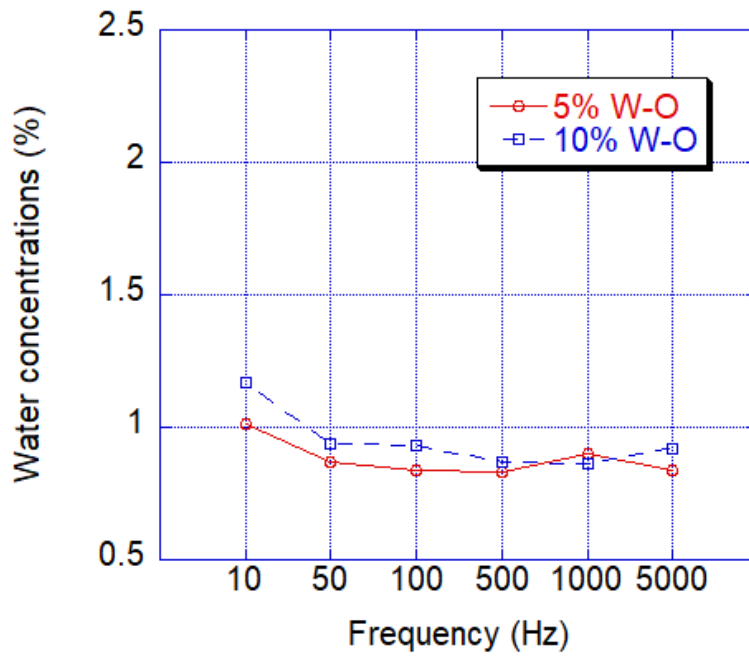


**Figure 6-20: Change of water concentrations with increasing frequencies**

#### 6.4.6 Extended Test Time

The extension of separation time may bring a higher quality to the separated oil. To illustrate that, separation tests of 10% water-in-sunflower oil emulsions for the extended time (1 hour) were conducted with heat treatment, electric field, and the combined method. The residual water concentrations (%) in the separated oil after 1-hour tests are shown in Table 6-8. As can be seen in the table, the extension of separation time can reduce the water concentrations in separated oil. The electrostatic method brings much less water concentration (0.89%) compared to the heating only method (2.75%). However, the water concentration (0.89%) of the one-hour test with electrostatic method is almost the same as the value (0.94%) of the 10 minutes test with the combined method. Therefore, the combined method can reduce the separation time substantially with similar oil quality. This reduced separation time can also decrease energy consumption. Finally, when the test time (time of exposure to the electric field with heating) is increased to 1 hour for the combined methods, the water concentration decreases around 0.5%. Therefore, the combined method can achieve not only a higher quality of separated oil but also a reduction of the separation time.

**Table 6-8: Water concentration measurements for extended measurement time**

<b>10% Water-in-sunflower oil separations</b>	<b>Water concentrations (%)</b>	
	<b>10 minutes</b>	<b>60 minutes</b>
Heating Only (90°C)	4.49	2.75
Electric Field Only (25°C, 1kV, 50Hz)	5.36	0.89
Heating + Electric Field (90°C, 1kV, 50Hz)	0.94	0.48

## 6.5 Energy Consumptions

Reduction of the energy consumption is one of the major motivations to develop this combined W/O separation method using heating and electric field. For example, there are several methods that can remove the water particles in the oil phase, such as distillation or electric field. However, compared to these single methods, our combined separation method can decrease the separation time by 5-10 times, and this reduced separation time would result in a significant reduction in the energy consumptions. The power consumption rapidly increases as the voltage and/or frequency increases as shown in Figs. 6-21 and 22. Therefore, we may also reduce the energy consumption by using this combined method at the optimized operating conditions.

Increased voltage and frequency can enhance the separation time and quality. However, when the voltage or frequency reaches a certain point, the effect of increasing voltage or frequency becomes minimal. This increased voltage or frequency may induce higher energy consumption. Therefore, it is important to find the optimal values of voltage and frequency to minimize unnecessary power consumption. The power consumptions increase as voltage and/or frequency increases as indicated in Figs. 6-21 and 6-22. In addition, 10% water-in-oil emulsion consumes slightly more energy than 5% emulsion because the resistance of the emulsion decreases with the increase of water concentration. The optimum voltage and frequency can be changed for different separation systems because it is also affected by the configuration and dimensions of the system.

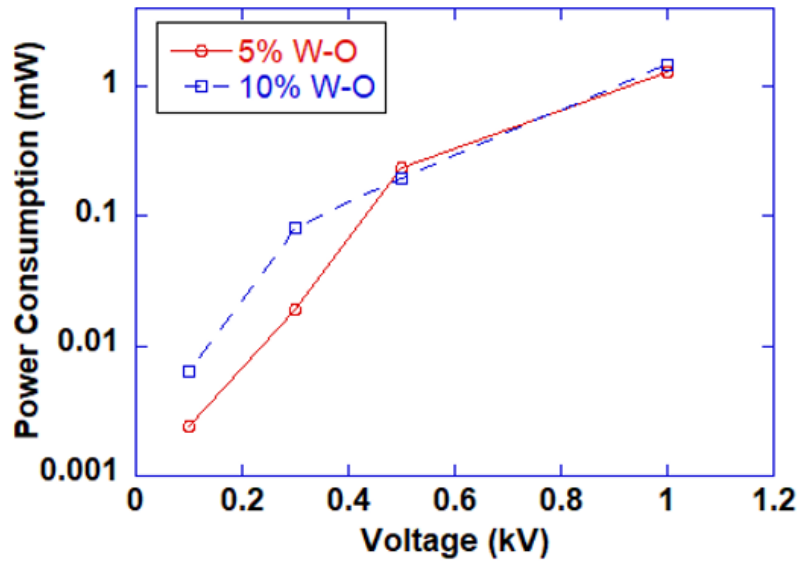


Figure 6-21: Power Consumptions of the system with different voltages

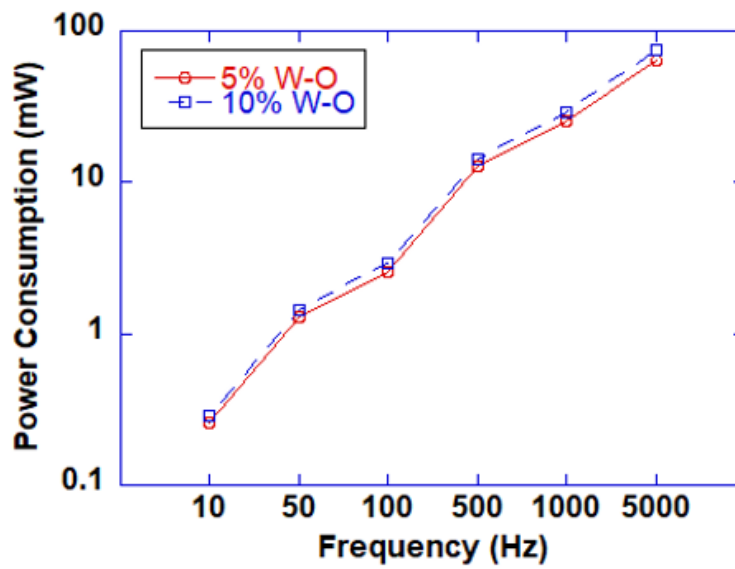


Figure 6-22: Power Consumptions of the system with different frequencies

## 6.6 Comparisons of Micro- and Macro-emulsions for Static Separations

### 6.6.1 Introduction

The size of the water droplet is a significant factor in determining the movement of the droplet. The forces of gravity and electric field on the droplets in the oil phase are described in Eq. (3-1) and (3-4). The sedimentation and collision times of the droplets are expressed in Eq. (3-10) and (3-15), and the expected values from the numerical calculations are indicated in Figs. 6-23 and 6-24. The sedimentation and collision times can be rapidly reduced as the droplet size increases. Therefore, water-in-oil macroemulsion is expected to have a reduced separation time when compared to the microemulsion. Previously, water/oil separation tests for both micro- and macro-emulsions were executed, and the results will be compared in this section.

$$F_g = \frac{4}{3}\pi\alpha^3(\rho_w - \rho_o)g \quad (3-1)$$

$$F_{el} = \frac{24\pi\epsilon E_0^2\alpha^6}{l^4} = \frac{24\pi\epsilon E_0^2\alpha^2}{(l/\alpha)^4} \quad (3-4)$$

$$t_V = \frac{4.5\mu_o h}{\alpha^2(\rho_w - \rho_o)g} \quad (3-10)$$

$$t_c = \frac{\mu_o l^5}{40\epsilon E_0^2\alpha^5} = \frac{\mu_o}{40\epsilon E_0^2} \cdot \left(\frac{l}{\alpha}\right)^5 \quad (3-15)$$

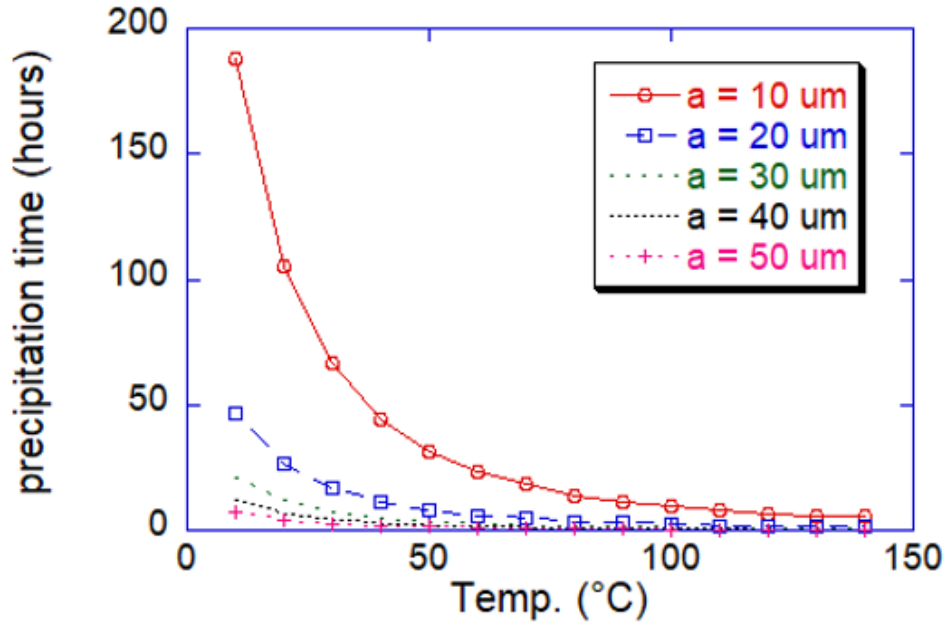


Figure 6-23: Precipitation time of the water droplets with various droplet sizes

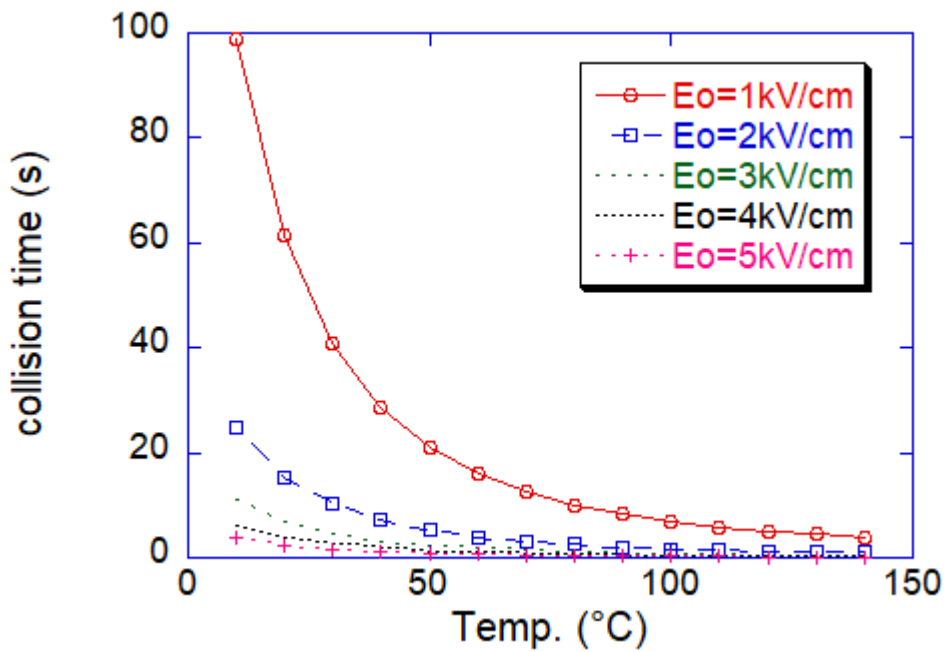


Figure 6-24: Collision time of the water droplets with various electric strengths

### 6.6.2 Temperature Dependence

The water concentrations of separated oil phase from the micro- and macro-emulsion separation tests are compared. The initial water contents were 5% and 10%. The emulsion was heated until it reached the target temperature, and a voltage was applied to the emulsion for 10 minutes. The applied voltage and frequency were 1kV and 50Hz with a square wave. After the test, water concentration from the separated oil phase was measured. Fig. 6-25 indicates the difference of the water concentrations between micro- and macro-emulsions. The water concentrations of the separated oil from macroemulsion are much less than the values from microemulsions as shown in Fig. 6-25. The water concentration from macroemulsion is reduced to below 1% at 90°C, while the result from microemulsion only decreases to around 4% at 90°C. In addition, the water concentration from the separated oil in macroemulsion is constantly decreasing from 25°C to 90°C. The water concentration is rapidly reducing until 60°C, and it keeps slightly decreasing up to 90°C. This result indicates that the theoretical calculation accurately predicts the reduction of precipitation and collision times with increasing temperature as shown in Fig. 6-25.

However, the separation of microemulsion does not match with the results of theoretical calculation. As shown in Fig. 6-25, the water concentration from the separated oil in microemulsion slightly decreases under the cloud points, and the water content starts rapidly reducing when it reaches the cloud point. The water concentration keeps decreasing until 90°C from the cloud point. This result shows that the separation of the microemulsion is expedited when the phase change occurs. The microemulsion is transformed to macroemulsion state around

the cloud point. At this point, the separation speed is increased and water content is rapidly reduced.

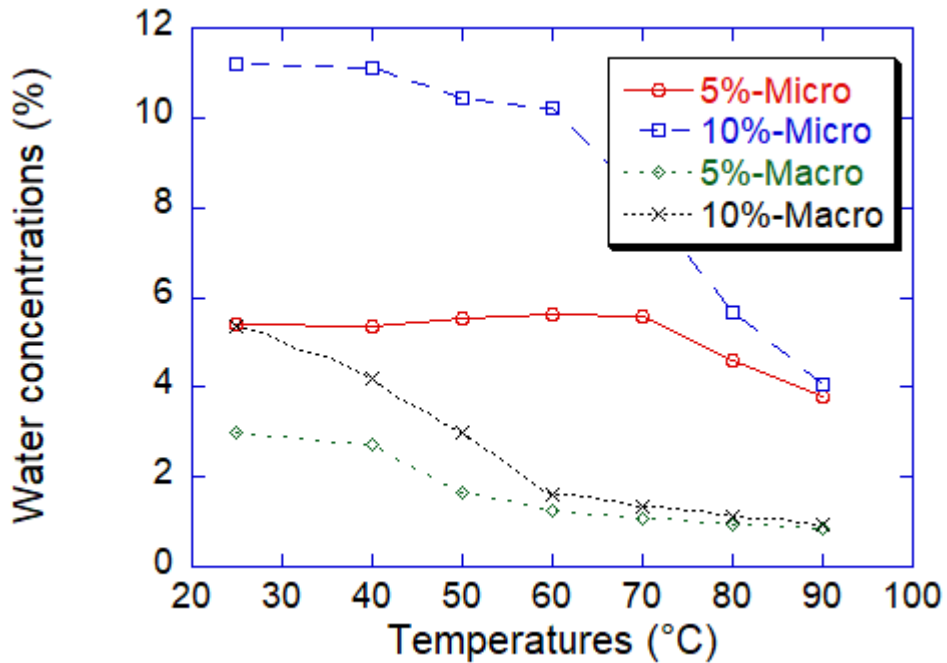


**Figure 6-25: Comparison of the residual water concentrations between micro- and macroemulsions**

### 6.6.3 Voltage Dependence

The effect of voltage on the water concentrations of separated oil phase from the micro- and macroemulsion was investigated. The separation tests of 5% and 10% water-in-oil emulsions were performed with various voltages at a fixed temperature and frequency for 10 minutes. The influence of the droplet size on the quality of the separated oil with increasing electric strength is shown in Fig. 6-26. The residual water concentrations of the separated oil between micro- and macro-emulsions are similar when no electric field is applied at 90°C. However, the water

concentration of the separated macroemulsion rapidly decreases as a voltage is applied to the emulsion, while the water content of the separated microemulsion does not decrease much. To see why the water content does not change in the microemulsion, it is necessary to consider the entire process of microemulsion separation. A water-in-oil microemulsion can start separating when it is transformed to the macroemulsion state over the cloud point, and applying voltage can accelerate the speed of the separation. However, after some amount of the water phase is separated, the residual water droplets still remain in oil phase. The distance between water droplets is extended because the emulsion becomes more dilute after the separation. The remaining droplets in the oil phase become more difficult to separate due to the extended distance. The precipitation and collision times rapidly increase due to the extended distance. Therefore, the water concentration of the oil phase in microemulsion does not decrease much even though it is exposed to the electric field for an extended time. Fig. 6-10 shows the decrease of the water concentration of the separated oil phase in the microemulsion. It decreases for 3 minutes after applying voltage, and after that the water concentration is almost constant for 10 minutes. However, the water content of the residual oil phase in macroemulsion keeps decreasing when the voltage is applied for extended periods of time due to its comparably larger droplet size.

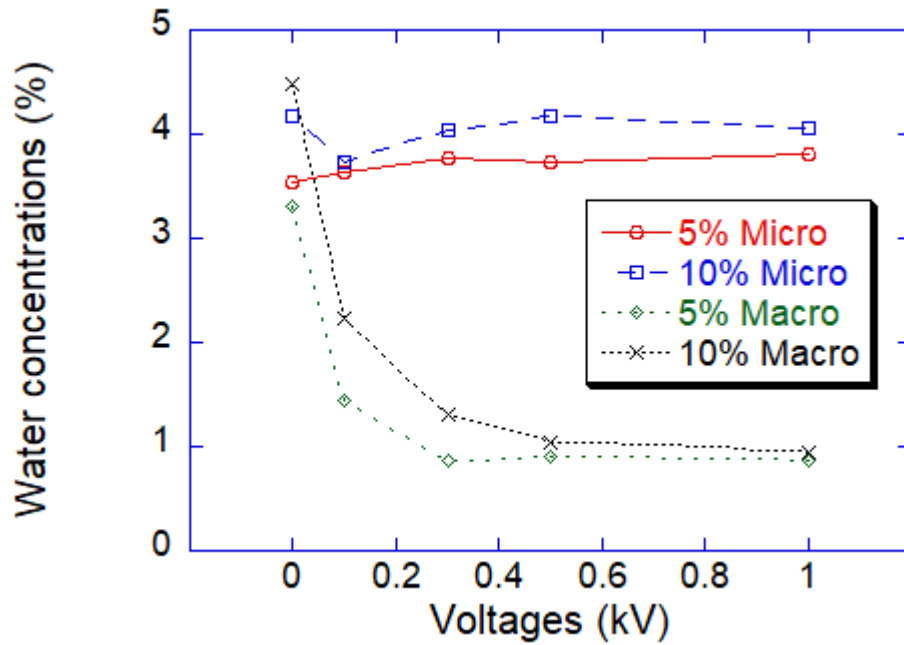


Figure 6-26: Comparison of the residual water concentrations between micro- and macroemulsions with various applying voltages

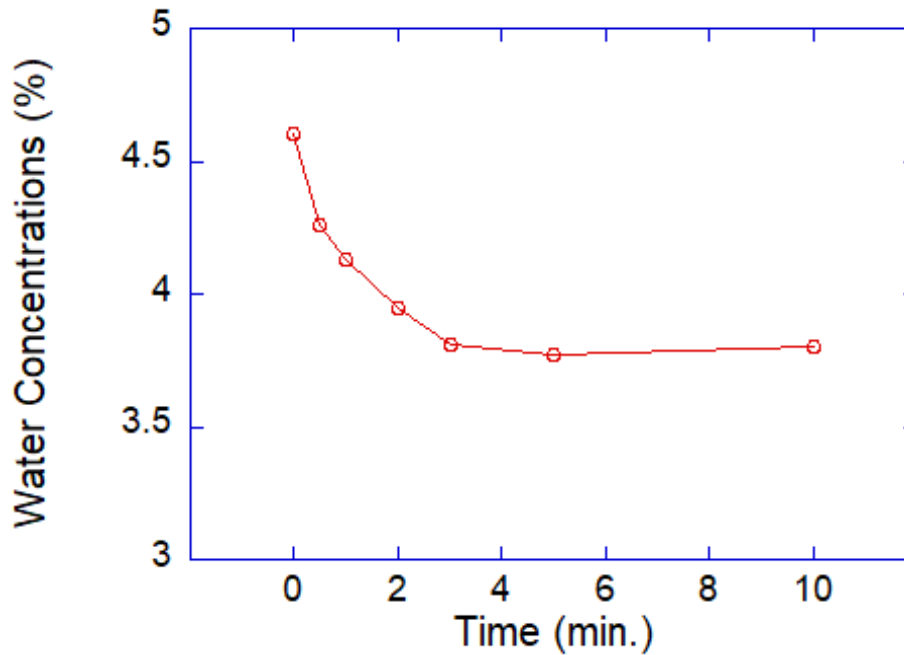
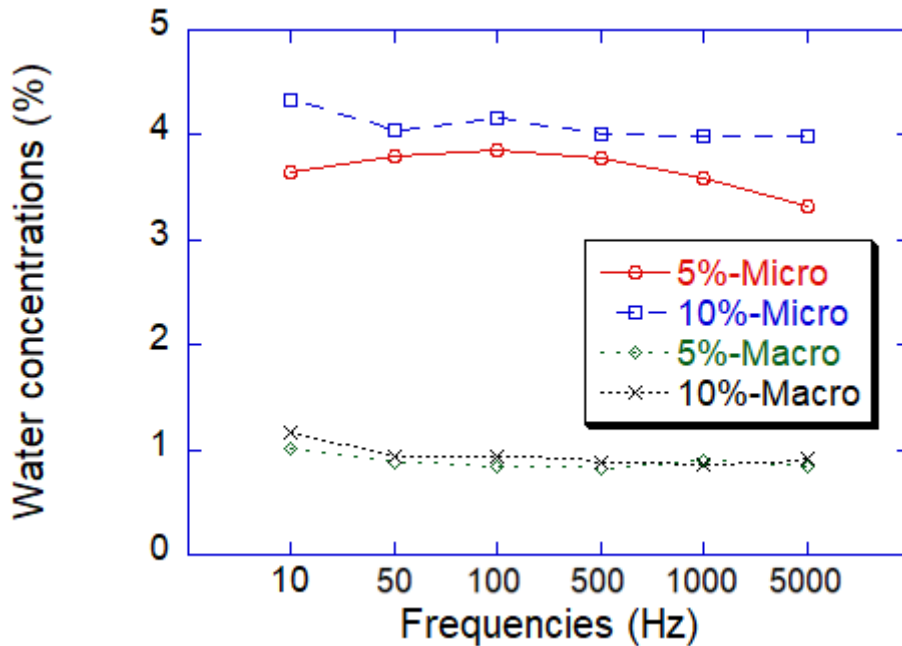


Figure 6-10: Decreases of water concentration of the separated oil phase with increased test times (10% water-in-oil microemulsion, 90°C, 1kV, 50Hz)

### 6.6.4 Frequency Dependence

The effect of frequency is comparably smaller than the effect of the temperature or voltage on the water/oil separation. Fig. 6-27 shows the water concentrations of the residual oil phase between micro- and macroemulsions. The water concentration of the residual oil phase does not decrease much for both micro- and macroemulsion separations. The water contents in macroemulsion is around 4 times smaller than the values of the microemulsion as shown in Fig. 6-27. Therefore, the size of water droplets in the oil phase is also an important factor to determine the coalescence of the droplets, and the quality of the separated oil phase is improved as the droplet size is enlarged.



**Figure 6-27: Comparison of the residual water concentrations between micro- and macroemulsions with different frequencies**

## **6.7 Static Separations of Water-in-Oil Microemulsion by Combined Method over the Boiling Point**

Previously, the temperature effect on the water/oil separation was investigated only up to 90°C because the cone-shaped tube cannot completely prevent the water evaporation over the boiling point (100°C). A special pressurized tube was designed to study the effect of the temperature over the boiling point. Water/oil separation tests with extremely high temperatures such as 120°C were executed with this new pressure tube. Two different temperatures, 90 and 120°C, were used, and the water concentrations of each temperature are obtained and compared. The applied voltage and frequency maintain constant at 1kV and 10 kHz with 1.5 hours of operation time. The water/oil separation by this pressure tube is shown in Fig. 6-28 (a). The microemulsion is completely separated 5-7 minutes after applying voltage, and the speed of separation is much slower than the results with the cone-shaped tube, which takes less than one minute as indicated in Fig. 6-28 (b).

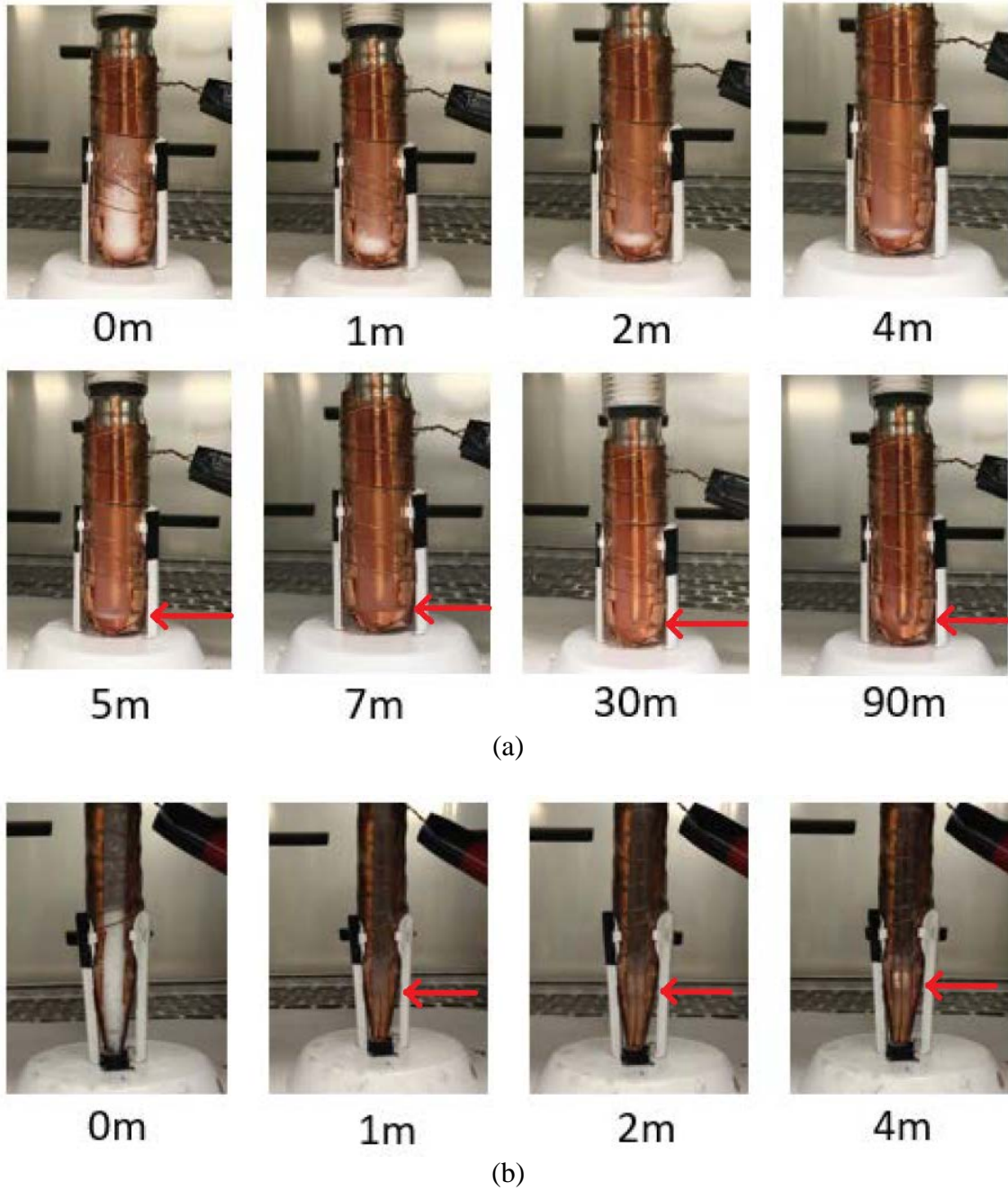


**Figure 6-28: Comparison of water/oil separation between high pressure and cone-shaped tubes**

The effect of increased temperature over the boiling point on the separation of the water-in-oil microemulsion is displayed in Table 6-9. The water concentrations of the separated oil are

remarkably decreased at the temperature above the boiling point of water (*e.g.* 120°C) compared to results of the temperature of 90°C. This result shows that the effect of increasing temperature is still significant on the water/oil separations at extremely high temperatures.

**Table 6-9: Residual water concentrations at 90 and 120°C with high pressure tube**

<b>Temperatures</b>	<b>5%</b>	<b>10%</b>
90°C	2.73	3.34
120°C	1.45	1.80

## **6.8 Dynamic Separations of Water-in-Oil Microemulsion by Combined Methods**

### **6.8.1 Introduction**

The dynamic water/oil separation system with electric fields at high temperature was designed. A water-in-oil emulsion can be continuously separated with this system because this system has an inlet for emulsion and outlets for separated oil and water phases. First, the dynamic separation system for lower flow rate was fabricated. This system can produce high quality of separated oil phase, while the separation speed is low. Therefore, another continuous separation system was necessary to be designed for higher flow rate separations. For the higher flow rate tests, the dimensions of the separation tubes are enlarged. This enlarged tube may reduce the separation efficiency of the emulsion. Therefore, the optimum dimensions of separation tube and electrodes were determined by executing many different tests with various dimensions of the tube and electrodes.

Dynamic water-in-oil microemulsion separation tests were executed to produce a large amount of separated oil, and the water concentrations of the separated oil phase were measured to determine the feasibility of the looping system. Two different water/oil separation systems were used in this study based on the flow speed: lower and higher flow rate.

### **6.8.2 Dynamic Water/Oil Separation at Lower Flow Rate**

The first generation of the continuous water/oil separation system was built for the lower flow rate tests. Three vertical separation vessels are connected to each other and located in the heating oven. The range of the flow rates for this system is 0 - 10 mL/min. For the tests, 10% of the water-in-oil emulsion was separated with the flow rate of 0.044 g/sec (~3 mL/min). The applied voltage was 5 kV of a square wave with 5 kHz of frequency. The various operating temperatures were used: 90, 100, 110, and 120°C. The water concentrations were measured after the tests, and the results are displayed in the Table 6-10. As indicated in Table 6-10, the best separation efficiency (2.44%) is shown at 100°C. The water concentration increases as the temperature increases over the boiling point due to the effect of the water evaporation.

This result of the dynamic separation system is different from the result of the static tests. For the stagnant separation test, the tube was perfectly sealed, and this sealed tube completely prevents water evaporation effect. Previously, the static separation tests showed that the quality of the separated oil is improved as the operating temperature increases up to 120°C. However, the looping separation system cannot be completely sealed due to the open inlet and outlets. Therefore, at the high temperature over the boiling point (100 °C), water vapor may not stay in the separation tube. This water vapor can move into the sequential separation tube through the oil outlet, and this process induces the separated oil phase contains more water concentrations.

Therefore, for the continuous water/oil separation system, the operating temperature must be maintained below the boiling point (100°C).

**Table 6-10: Water concentrations from the separated oil with different operating temperatures**

<b>Temperature (°C)</b>	<b>Water concentrations (%)</b>
90	3.51
100	2.44
110	4.78
120	6.38

### **6.8.3 Dynamic Water/Oil Separation at Higher Flow Rate**

Previous dynamic water/oil separation system showed good quality of the separated oil phase. However, it is not suitable for higher flow rate tests due to its small dimension of the separation tubes. Therefore, the second generation of the continuous water/oil separation system was designed for the higher flow rate tests.

Several water-in-oil separation tests with higher flow rates were executed with this separation system. 10% W/O emulsions were continuously separated with the 10 kV of voltage and 5 kHz of frequency. Various flow rates were applied: 17 - 500mL/min (0.27 – 8.0 g/sec). The operating temperature was maintained around 90 – 95°C because water evaporating and vapor expansion issues may arise if the temperature reaches close to 100°C. For example, evaporated vapor may move to the oil outlet, and this can decrease the quality of the separated oil. Also, the

increased pressure in the system by expanding vapor may create serious problems such as leaking of the emulsion or cracking of the tube fittings.

Water concentrations of the separated oil phase were measured with different flow rates (mL/min) as shown in Table 6-11. Water-in-oil microemulsion initially contains 10% of water in the oil phase. When heating (90 - 95°C) is applied to the system with high flow rate (500 mL/min), the water concentration of separated oil phase is still high (9.60%). When 5kV of voltage is applied to the system, the water content is reduced to 7.30%. As the flow rates decrease from 500 to 17 mL/min, the water concentration of the separated oil phase also reduces down to 3.84% as indicated in Table 6-11 and Fig. 6-29. The increased residence time by reducing its flow rate can improve the quality of the separated oil phase. In Table 6-11, the residence time can be roughly calculated using the total volume of the separation tubes and the flow rate (volume/flow rate).

**Table 6-11: Water concentrations from the separated oil with different flow rates**

<b>Flow Rate (mL/min)</b>	<b>Residence time (min.)</b>	<b>Water Concentrations (%)</b>
17	24	3.84
33	12	4.39
50	8	5.95
100	4	6.03
200	2	6.81
500	0.8	7.30
500 (Heating Only)	0.8	9.60

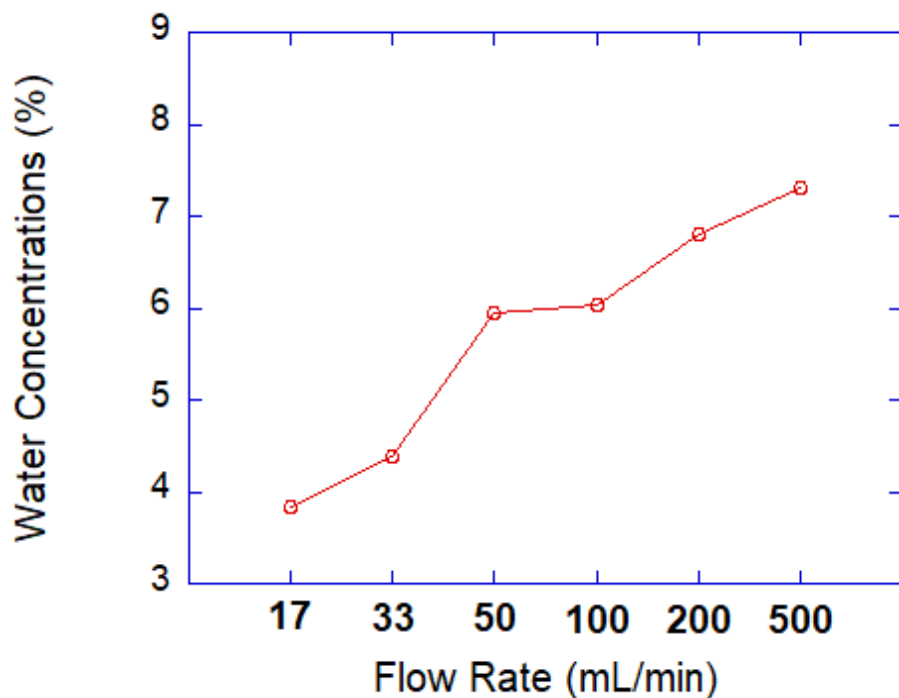


**Figure 6-29: Water concentrations of the separated oil with different flow rates**

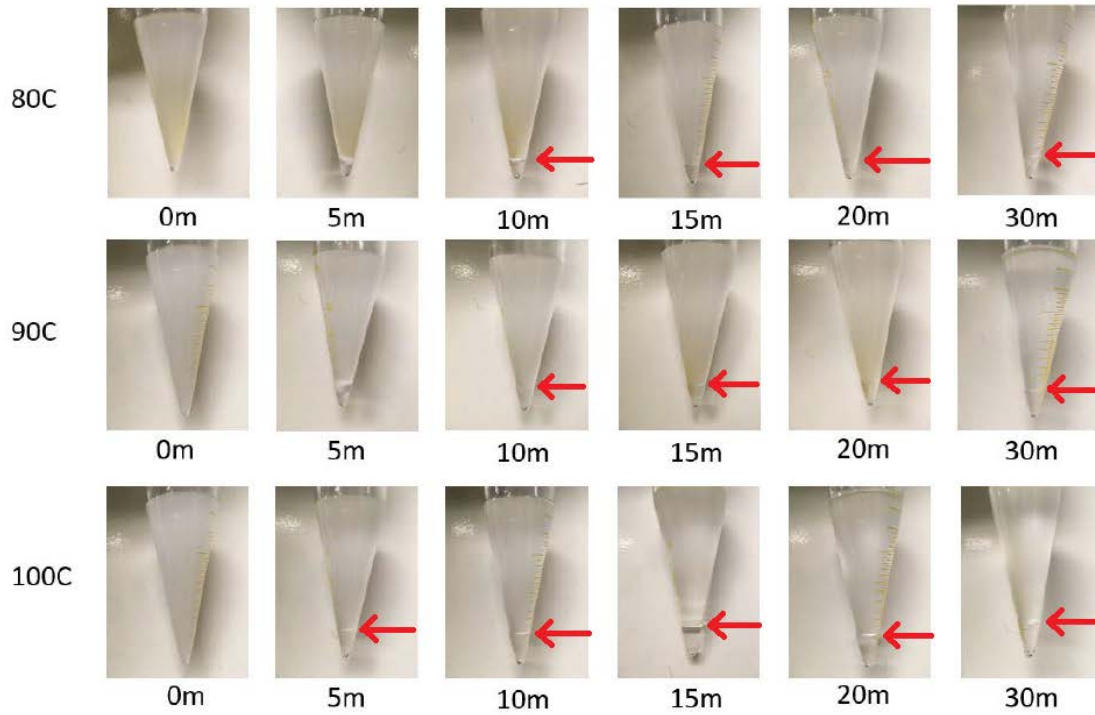
## **6.9 Static Separations by Centrifugal Force at the Elevated Temperatures**

### **6.9.1 Introduction**

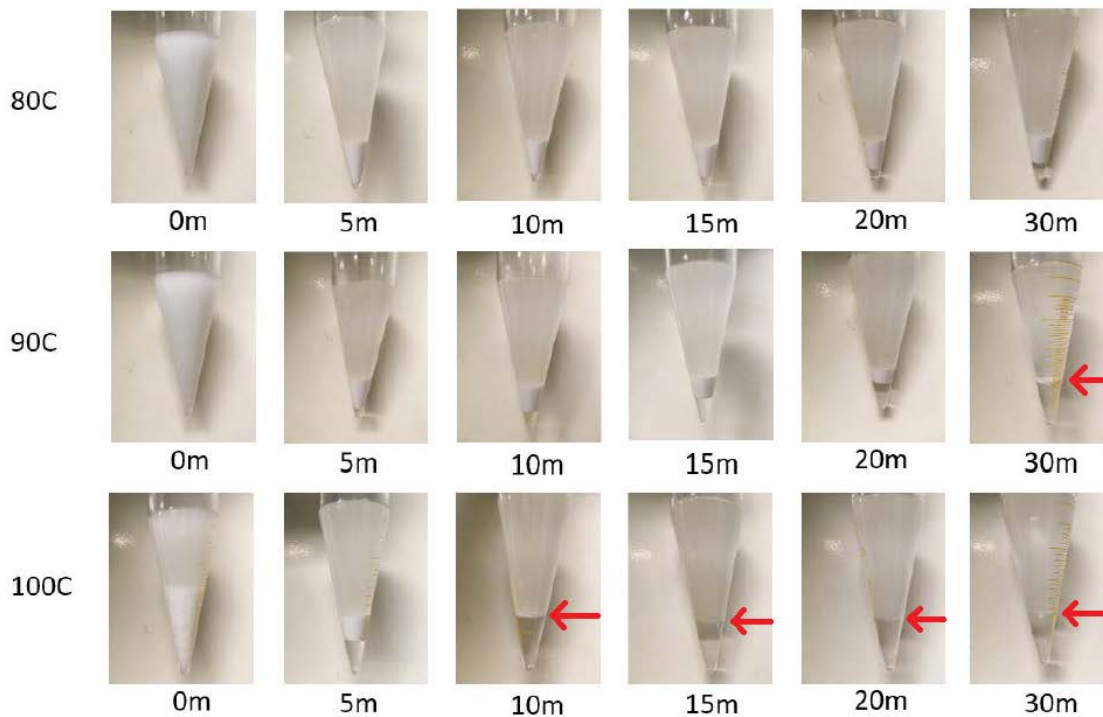
The separation of water-in-oil emulsions can be influenced by a combination method of heating and centrifugal force. In this study, temperature and revolution speed (RPM) are considered as main factors. Separation tests of the 5% and 10% water-in-oil microemulsions were executed by a centrifugal force at elevated temperatures. The separation results of this centrifuge test will be also compared with the values of water/oil separations by an electric field with increased temperature.

### **6.9.2 Experimental Results**

Water-in-oil microemulsion separation tests with the heating centrifuge were executed with two independent variables: temperature and rotation speed (RPM). First, the effect of the operating temperature was examined. In this test, three different temperatures (80, 90, 100°C) were used, and the rotation speed was fixed at 1500 RPM. The temperature effect on the separation of the 5% and 10% water-in-oil microemulsions by centrifugal force is shown in Fig. 6-30. Increased temperature expedites the water/oil separation in the centrifuge. As the operating temperature increases, the viscosity of the oil phase is decreased. This reduced viscosity can expedite the separation speed of the emulsion.



(a) 5% W/O microemulsion



(b) 10% W/O microemulsion

**Figure 6-30: Temperature effect on the W/O separation at 1500 RPM: (a) 5% W/O microemulsion, (b) 10% W/O microemulsion**

Revolution speed is also an important factor to determine the water/oil separation by centrifugal force at high temperature. In this test, three different revolution speeds (500, 1000, 1500 RPM) were applied to the system at the elevated temperature (90°C). The effect of increased revolution speed is indicated in Fig. 6-31. The water/oil separation can be accelerated as the rotation speed increases. For example, in Fig. 6-31 (b), the water/oil separation is observed in 30 minutes at 1500 RPM, the color of the separated water phase is clear on the bottom of the tube. However, the separation is not completely for 500 RPM test at the same time (30 minutes). The color of the water phase is still opaque, this color represents that the water/oil separation is still in transit. This separation method, which is combined high temperature and centrifugal force, shows a reliable performance of water-oil separation. However, this method is not as effective as the previous combination method of heating and electric field. For instance, water-in-oil microemulsion can be separated within a minute when 1kV of voltage is applied at 90°C, while it takes more than 10 minutes to separate emulsions if centrifugal force is applied at the same temperature. Therefore, we decided to use the previous combined method using heating and electric field for further investigation of the water/oil separation.

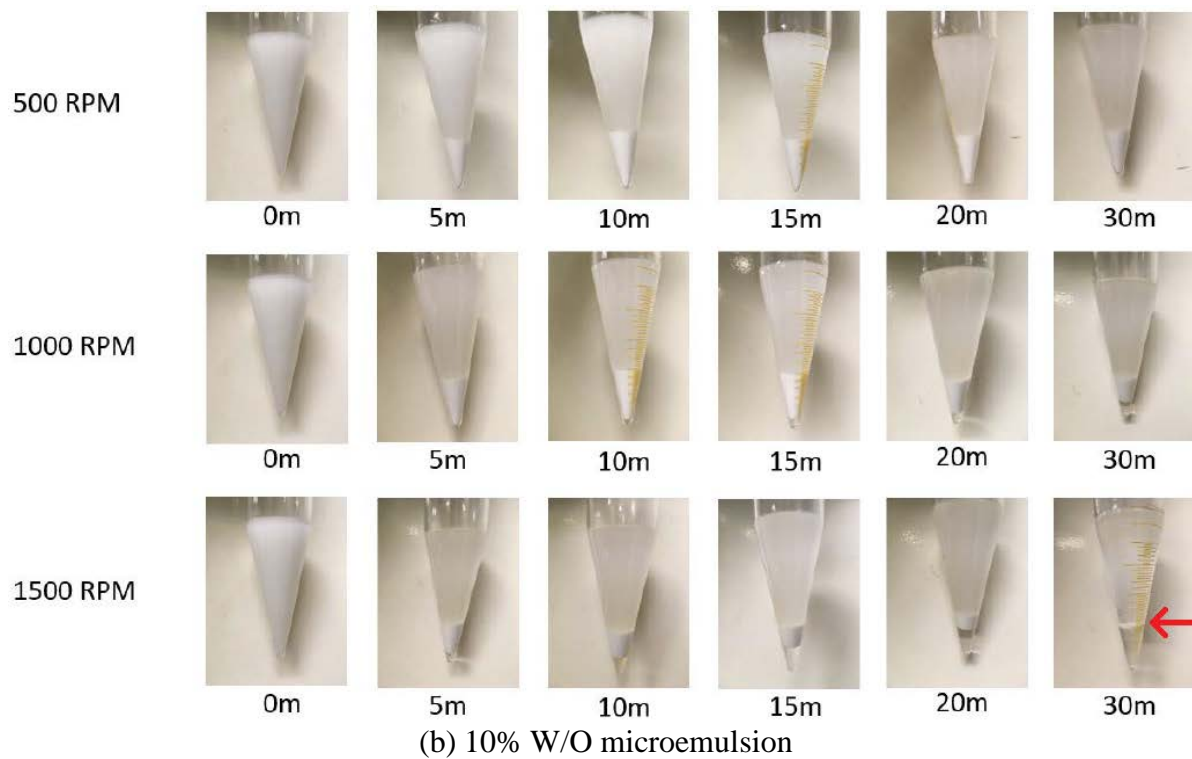
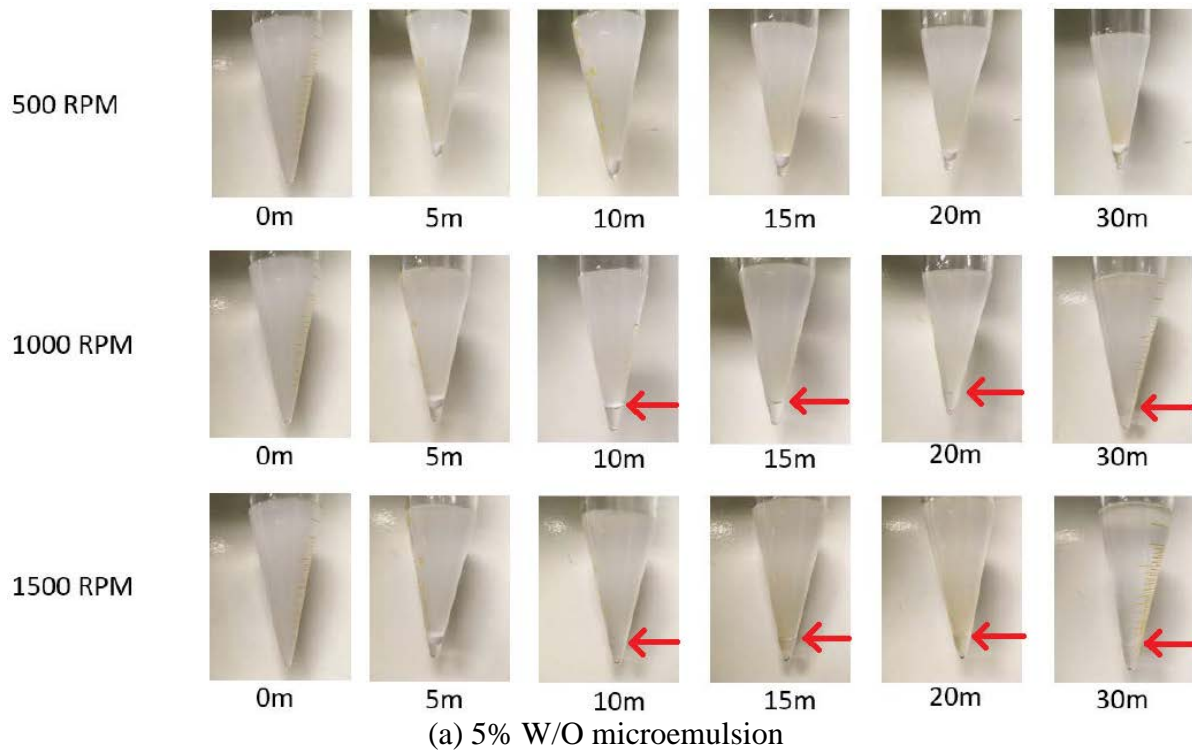


**Figure 6-31: The effect of revolution speed on the W/O separation at 90°C: (a) 5% W/O microemulsion, (b) 10% W/O microemulsion**

## 6.10 Measurement Uncertainty

The measurement uncertainty has significant influences on the assessment of the results. The measurement device, Karl Fischer Titrator, shows less than 0.5% of standard deviation with the range of 1-10% of water concentrations. Therefore, the uncertainty of measurement devices is negligible. However, a human experimental error may affect the measurement error. Even though the tests are performed in same conditions, the values of the separation speed and the water concentrations can be measured differently. Based on the results of several repeated tests, the experimental test error can be considered to be less than  $\pm 10\%$ .

## 6.11 Conclusions

The experimental tests of the water/oil separations in micro- and macroemulsion were performed by using combined separation methods of heating and electric field. First, static tests were executed for the separations of water-in-oil micro- and macroemulsions. It is verified that the combination of heating and electric field methods can enhance the separation speed of the emulsion and quality of the separated oil phase.

The microemulsion cannot be separated by an electrostatic separation method alone due to its tiny droplet size. Therefore, the microemulsion must be heated to transform its phase to the macroemulsion state over the cloud point, and the electric field can accelerate the separation speed of the emulsion in this state. The increase of the temperature, voltage, and frequency can enhance the speed of the water/oil separation.

The separation tests of the water-in-oil macroemulsion were also executed. The separation speed and quality of the macroemulsion are also enhanced by the increase of the

temperature, voltage, and frequency. Specifically, temperature and voltage are considered as significant factors, while the effect of frequency is relatively small. For example, increasing the operating temperature to 90°C can reduce the separation time by 5-10 times and decrease the residual water concentration by 5-6 times when compared to the results under the same electric field at 25°C. This influence of the temperature shows an exact match with the calculations of the theoretical consideration. In addition, the application of the 1kV voltage can reduce the separation speed by 5-10 times and decrease the residual water concentration by 4-5 times when compared to the test with heating method alone. This reduced separation time with improved quality can also provide the reduction of energy consumption in industries.

The dynamic water/oil separation tests with electric fields at elevated temperature were also executed. Two different types of continuous separation systems were fabricated based on the flow rate of the emulsions. Several water/oil separation tests were performed with various operating temperatures: 90, 100, 110, and 120°C. The water concentrations from the separated oil phase were measured to determine the quality of the separation. The best result was obtained at the temperature of 100°C. If the operating temperature exceeds the boiling temperature (100°C), water evaporations can occur. This evaporated vapor can decrease the quality of the separated oil phase. This continuous separation system for lower flow rate can produce a high quality of separated oil due to its extended residence time. However, the water/oil separation speed with this system is very low due to its limited flow rate (up to 10 mL/min).

To enhance the separation speed of the water-in-oil emulsion, the 2nd generation of the continuous separation system was fabricated. The flow rate can be increased up to 1000 mL/min in this system. Several separation tests for water-in-oil microemulsion were performed with various flow rates (17 – 500 mL/min), and water concentrations of the separated oil phase were

measured. The water concentrations of the separated oil are reduced by decreasing the flow speed due to the extended residence time.

The static water/oil separation tests by centrifugal force at the high temperature were executed. This system also shows reliable results of the water/oil separation. However, the performance of this system was not effective compared to the performance with the results of the combined methods of electric field and heating.

## Chapter 7. Summary and Conclusions

### 7.1 Summary of Important Findings

#### 7.1.1 Theoretical Considerations for the Movement of Droplets in Oil Phase

An electric field assisted coalescence is one of the most efficient methods for water/oil separation. The water droplets in oil phase can be moved by the influence of gravity and electric forces. Dipole-dipole and dielectrophoresis (DEP) forces are two major electric forces that affect droplet movement in the oil phase. Therefore, it is important to investigate the forces acting on the droplets to anticipate their movement in electric fields.

The balance of the forces and the movement of water droplets under the electric fields were theoretically investigated. The movement of droplets can be influenced by gravity, dipole-dipole, and DEP forces when exposed to electric fields. In addition, the sedimentation and collision times of water droplets are significantly affected by the temperature, droplet size, and electric strength. For example, the theoretical calculations show that increasing the temperature to 90°C can reduce the precipitation and collision times of water particles by 5-10 times when compared to the results under the same conditions at 25°C. This result indicates that the elevated temperature can expedite the coalescence of the droplets by electric fields. This reduced coalescence time can accelerate the separation speed of the water-in-oil emulsion. Therefore, the experimental tests of water/oil separation will be performed with different temperature and electric field (*i.e.* voltage and frequency) as the purpose about seeing if theoretical values hold true.

### **7.1.2 Shape of Separation Tube and Electrodes**

A cylindrical cone-shaped separator equipped with coaxial cylindrical electrodes was fabricated for the static water/oil separation tests. This separation tube can create non-uniform electric fields that cover most of the space in the separation tube. Non-uniform electric fields can enhance the water-oil separation compared to the uniform field. By this design, the distance between the center and surrounding electrodes can be reduced. This reduced gap delivers a higher strength of electric fields and promotes the separation. Also, the separated water phase can be clearly observed due to the reduced area of the cone-shaped tube.

### **7.1.3 Simulations and Experiments for the Design of the Separators**

The effect of the water/oil separator's design was studied computationally and experimentally. The cylindrical separator showed a higher separation efficiency compared to the separator using flat-plate electrodes because non-uniform electric fields can be created inside the separation tube. Non-uniform electric fields are more efficient than uniform electric fields because they introduce both dipole-dipole forces and DEP forces on water droplets, while the uniform electric field can only generate the dipole-dipole forces.

The influence of the thickness and length of the center electrode, air-gap between the center electrode and insulated capillary tube, and the diameter of the separator were investigated computationally. The simulations showed that the electric field strength and gradient in emulsions can be enhanced by narrowing the air-gap, extending the center electrode, and reducing the diameter of the separation tube. Moreover, the strength of electric fields in emulsion increases as the length of the center electrode extends. These simulation results were validated by

executing several experiments. The experimental tests showed very consistent results with the simulations.

#### **7.1.4 Static Separation Tests of Water-in-Oil Microemulsions**

A water-in-oil microemulsion is difficult to be separated by an electric force due to its tiny droplet size. The combined methods of heating and electric field was used for the separation of water-in-oil microemulsions. The separation process by this combined methods is that the microemulsion is first heated to the target temperature (*i.e.* 90°C), in this process the phase of the microemulsion can be transformed to the macroemulsion state around the cloud point. The color of the microemulsion, which is initially clear at room temperature, is usually changed to opaque (or white) when the temperature reaches over the cloud point. Then, an electric field is applied to the emulsion to accelerate the separation while holding the operating temperature constant. The water/oil separation time can be reduced as the applied voltage or frequency increases.

For further investigation of the effects of key factors, the separation tests of water-in-oil microemulsion were executed with various temperatures (*i.e.* 25 – 90 °C), voltages (*i.e.* 0 – 1kV), and frequencies (*i.e.* 10 – 5,000Hz). The increase of the temperature, voltage, and frequency can enhance the speed of the water/oil separation. However, when the voltage or frequency reaches a certain point, the improvement of water-in-oil emulsion separation becomes negligible. Therefore, establishing the optimum voltage and frequency are important to balance the power consumptions and separation efficiency. Water concentrations of the separated oil phase were measured to determine the quality of the separated oil. After 10-minute tests, the water concentrations of the separated oil were about 3.5 – 4.0%. This water content is roughly higher than the result of the macroemulsion by 4 times due to its tiny droplet size.

### **7.1.5 Static Separation Tests of Water-in-Oil Macroemulsions**

The separation tests of water-in-oil macroemulsion were performed to investigate the feasibility of the crude-oil separations by this combined method as a practical application. Sunflower oil is used as a substitute for the medium crude-oil due to its similar properties (*i.e.* viscosity, density, and dielectric constant). The combination of heating and electrostatic methods is more efficient than either method alone for the separation of water-in-oil macroemulsions.

Previously, theoretical calculations showed that the precipitation and collision times of water droplets can be reduced by increasing temperature or electric strength. For instance, the water/oil separation speed is reduced by 5-10 times at high temperature (90°C) when compared to the same process at room temperature (25°C). These results are experimentally validated in macroemulsion by executing water/oil separation tests with different temperatures and voltages. Increasing the operating temperature to 90°C can reduce the separation time by 5-10 times and decrease the residual water concentration by 5-6 times when compared to the results under the same electric field at 25°C. In addition, the application of the 1kV voltage can decrease the separation time by 5-10 times and reduce the residual water concentration by 4-5 times when compared to the test without electric field, but with the same heating condition. This reduced separation time with improved quality can also provide the reduction of energy consumption in industries.

In this separation study, the separated oil phase contains normally less than 1% of water after only a 10-minute separation using the combined methods (*i.e.* heat treatment + electrostatic). Temperature and voltage are significant factors that influence the speed and quality of separation,

while frequency shows less effect. By increasing the temperature, voltage, and frequency, we may improve the quality of separated oil with reduced separation time.

Once the voltage and frequency reach certain points, the improvement of water-in-oil emulsion separation becomes negligible. Therefore, establishing the optimum voltage and frequency is important to balance the energy consumptions and separation efficiency. By estimating the power consumption, the optimum condition of our system is found to be 0.5kV and 50Hz with 90°C of heating. In this condition, the water-oil separation is observed around 30 seconds after applying the voltage, and the amount of separated water continues to increase during the experiment. After a 10-minute test, the water concentration of the separated oil is about 0.8%. The result can be further increased to around 0.5% with an extended separation time of 1 hour.

#### **7.1.6 Dynamic Separation Tests of Water-in-Oil Microemulsions**

The dynamic water/oil separation tests with the combined method of heating and electric field were performed. Two different types of continuous separation systems were used for this study based on the flow rates. First, water/oil separation tests were performed using a lower flow rate system with various operating temperatures: 90, 100, 110, and 120°C. The flow rate of these tests was 3 mL/min, and the 5kV of voltage was applied with 1 kHz of frequency. The water concentrations of the separated oil phases were measured, and the optimum temperature for separation was determined to be 100°C. The quality of the separated oil phase is reduced if the operating temperature exceeds the boiling temperature (100°C) because water evaporation occurs. At this operating temperature (100°C), this system can achieve high quality separation of oil. However, the separation speed of the emulsion is slow due to its limited flow rate (10 mL/min).

To overcome this limited separation speed, the 2<sup>nd</sup> generation of the separation system was built with enhanced flow rates up to 1000 mL/min. The influence of the flow rate on the quality of the separated oil phase was determined by executing several tests with different flow rates (17 – 500 mL). The operating temperature was around 90 - 95°C and the voltage was 10kV with 1 kHz frequency. The water concentration of the separated oil increases as the flow speed increases due to reduced residence time. From the results of the dynamic water/oil separation tests, this dynamic system can also achieve high quality separation of oils. The operating temperature should be maintained slightly below the boiling point to achieve the high efficiency with avoiding water evaporation effect. The quality of the separated oil phase from this dynamic separation system was reliable compared to the values of the static tests. The experimental tests with this continuous separation system show the feasibility of the water/oil separation in the industry by using the newly developed combined separation methods with heating and electric fields.

## **7.2 Contributions of this Work**

### **7.2.1 Academic Contributions**

The movement of water droplets in the oil phase under the electric field is theoretically investigated using the balance of the forces acting on the water droplets. Specifically, there are several major factors that affect the water droplet movement such as droplet size, temperature, voltage strength, *etc.* The separation time of the emulsions can be reduced by enhancing these factors. In addition, water-in-oil microemulsions, which are very difficult to be separated due to the stability, are successfully separated using the combined separating method of heating and electric field. These academic concepts and predictions are verified by experimental tests.

### **7.2.2 Practical Contributions in Industries**

The newly developed water/oil separation system for the purpose of the water-in-oil microemulsion separation can also be applied to the practical macro-emulsion separations. Especially, the separation/dehydration efficiency of crude-oils can be considered significant in industries. This combined (heating + electric field) method can reduce the separation time by 5-10 times when compared to the single method using distillation or electric field. This reduced separation time can reduce the energy consumption of the water/oil separation system. This water-in-oil microemulsion separation system can be also used to develop an absorption chiller in industries. Especially, if microemulsions are used as absorbents, the performance of the absorption chiller may be improved compared to the conventional absorbents.

### **7.3 Concluding Remark**

In this study, the movement of the droplets in the oil phase was theoretically investigated from the effects of temperature, electric fields, and droplet size. The sedimentation and collision times of the droplets can be reduced as the operating temperature or/and electric field increases. These results of numerical calculations were validated by performing experimental tests. The combined water/oil separation system was developed, and this newly designed system can enhance the performance of water/oil separations. Furthermore, this combined method can separate water-in-oil microemulsions, which cannot be separated by a single method of an electric field due to its tiny droplet size. The applied heat can transform the phase of the microemulsion to the macroemulsion state, and the separation speed of the emulsion can be expedited by incorporating electric fields. The influence of temperature, voltage, and frequency

were also studied for the static separation of micro- and macroemulsions. Increasing the applied electric voltage and/or temperature can significantly reduce the separation time and the residual water concentration in the emulsion. Next, dynamic water/oil separation systems were designed, and water-in-oil emulsion can be continuously separated with this system. The influence of the operating temperatures and flow rates on the quality of the separated oil phase were determined by measuring the residual water concentration in separated oil. The results of this dynamic separation design might allow this water/oil separation study for easier, more well-controlled, and well-understood scale up for the industry.

#### **7.4 Recommendations for Future Work**

The current work presented in this dissertation provided the theoretical study of the water droplet movement in the oil phase in electric fields with different temperatures. This theoretical study was verified by executing several experimental tests using the combined method (heating + electric field) for water/oil separation. However, additional experimental tests can be recommended to achieve further insight into this study. The details of the recommended future work are demonstrated below.

Static water/oil separation tests of the macroemulsion were conducted as a practical application such as crude-oil separation. In this paper, sunflower oil was used as a replacement for medium crude-oil. Further insight can be achieved by applying this combined method to the separation of the light and/or heavy crude-oil. Silicone oil and castor oil can be used as substitutes for light and heavy crude-oils respectively. There are some difficulties to execute water/oil separation tests with these oils. For example, it is difficult to produce water-in-silicone oil emulsion due to the light density of the silicone oil. Also, water-in-castor oil is difficult to be

separated due to the small density difference between water and castor oil. However, many types of researches already have been performed with the oils, and the combined method (heating + electric field) must provide higher efficiency of the water/oil separation compared to the single method.

Dynamic water/oil separation system was built and showed great performance for the water-in-oil microemulsion separation. This dynamic separation system can be also utilized to the separation of macroemulsion such as crude-oil. For instance, water-in-sunflower oil emulsion can be also separated from this dynamic separation system and the results such as water concentration from the separated oil phase can be compared with the results of the static test.

The performance of the dynamic water/oil separation system can be enhanced with the following methods. First, the quality of the separated oil phase can be improved by adding more separation tubes in the heating oven. Three separators were used in the current dynamic separation system in this paper and the maximum quantity of the separator in the current system is six. The quality of the separated oil phase increases as the number of the separation tube increases due to the extended residence time. Therefore, we can simply improve the separation efficiency by adding more separation tubes in the heating oven. With this process, we may obtain the optimum numbers of the separators in the oven. Another method to improve the separation quality is attaching water filtration system on the outlet of the separation tube. The separation system may become more complicated if we add another separation method. However, this new method may deliver the higher quality of the separated oil.

The quality of the separated oil phase can be improved by increasing the operating temperature. In this paper, the maximum temperature used for most of the tests is 90°C due to the water evaporation effect. However, the water/oil separation test with the pressurized tube

showed that increased operating temperature such as 120°C can significantly enhance the quality of the separated oil phase. It is necessary to build a pressurized separation tube to enhance the operating temperature over the boiling point (100°C). However, it is not difficult to fabricate this high-pressure separation tube and already manufactured. Even though the increased temperature over the boiling point is very difficult to be applied to the dynamic system, this increased temperature can significantly enhance the quality of the separated oil in the static separation system.

As the initial water concentration increase (*e.g.* 5% to 10%), the separation time and water concentration of the separated oil phase are reduced in the water-in-oil emulsion. However, these two variables are not enough to predict the trend change with different water concentrations. Therefore, it is necessary to execute more tests with different water concentrations such as 7.5%, 15%, or 20% of water-in-oil emulsions.

The effect of the water droplet size on the droplet movement was theoretically investigated and verified by experimental tests. The further insight can be obtained if the actual droplet size is measured for both micro- and macroemulsions. For example, the separation speed of the W/O emulsion may reduce as the droplet sizes increase. In addition, the difference of the droplet size between 5% and 10% of water-in-oil emulsions can be determined.

In summary, the potential future works are as follows:

1. To conduct water/oil separation tests with silicone and/or castor oil as a replacement for light and/or heavy crude-oil
2. To perform dynamic separation tests for the water-in-oil macroemulsion as a practical application of the crude-oil dehydration

3. To enhance the quality of the separated oil phase in the dynamic separation system by adding more separators in the heating oven or installing a filtration system on the outlet of the oil phase
4. To improve the efficiency of the water/oil separation in the static test by increasing the operating temperature over the boiling point
5. To perform more W/O separation tests with different initial water concentrations to obtain the trend change influenced by initial water concentrations
6. To measure the droplet size for macro- and microemulsions to verify the effect for the W/O separation

## Bibliography

- [1] Boxall, J. A. & Koh, C. A., Measurement and Calibration of Droplet Size Distributions in Water-in-Oil Emulsions by Particle Video Microscope and a Focused Beam Reflectance Method, American Chemical Society, Ind. Eng. Chem. Res., 49, 1412–1418 (2010).
- [2] Eow, J. S. & Ghadiri, M., Electrostatic enhancement of coalescence of water droplets in oil: a review of the technology, Chemical Engineering Journal 85 357–368 (2002).
- [3] Zhang, L., Zhong, Y., Cha, D. & Wang, P. A self-cleaning underwater superoleophobic mesh for oil-water separation. Scientific Reports 3, (2013).
- [4] Wang, C., Huang, H. & Chen, L. Protonated Melamine Sponge for Effective Oil/Water Separation. Scientific Reports 5, (2015).
- [5] Moroi, Y, Surfactant Aggregation: Relationship between solubility and micellization of surfactants: The temperature range of micellization, Progr Colloid & Polymer Sci 77:55-61 (1988)
- [6] Tadros 2013 Tharwat F. Tadros, Emulsion Formation, Stability, and Rheology, Emulsion Formation and Stability, First Edition, Wiley, (2013)
- [7] McClements, David Julian, Nanoemulsions versus microemulsions: terminology, differences, and similarities, The Royal Society of Chemistry (2012)
- [8] Dixit, P. D., Jain, A., Stock, G., Dill, K. A. Journal of chemical theory and computation, 11, 5464-5472, (2015)
- [9] Butt H.J., Graf K., Kappl M., Physics and Chemistry of Interfaces, Wiley (2003)
- [10] Shah, Dinesh O., Macro- and microemulsions : theory and applications : based on a symposium sponsored by the Division of Industrial and Engineering Chemistry at the 186th Meeting of the American Chemical Society, Washington, D.C., August 28-September 2, (1983)
- [11] Stokes, Robert, *Fundamentals of Interfacial Engineering*. VCH. pp. 245–247. ISBN 0471-18647-3 (1997).
- [12] Milner, S. T., Safran, S. A. Phys. Rev. A (1987), 36, 4371 (1988)
- [13] Talmon. Y., Prager. S. Statistical thermodynamics of phase equilibria in microemulsions, The journal of Chemical Physics 69, 2984 (1978)

- [14] Talmon. Y., Prager. S. The statistical thermodynamics of microemulsions. II. The interfacial region, *The journal of chemical physics* 76, 1535 (1982)
- [15] Schulman, J.H., Stoekenius, W., Prince, L.M., Mechanism of formation and structure of microemulsions by electron microscopy. *J. Phys. Chem.* 63, 1677–1680, (1959)
- [16] Ohshima Hiroyuki, *Encyclopedia of Biocolloid and Biointerface Science*, 2 Volume Set, Wiley (2016)
- [17] Mehta S.K. and Kaur G., *Microemulsions: Thermodynamic and Dynamic Properties*, Department of Chemistry and Centre of Advanced Studies in Chemistry Panjab University, Chandigarh India, (2011)
- [18] Rosen M.J. & Kunjappu J.T. *Surfactants and Interfacial Phenomena* (4th ed.). Hoboken, New Jersey: John Wiley & Sons. p. 1. ISBN 1-118-22902-9. Archived from the original on 8 January (2017)
- [19] Mishra M. et al., Basics and Potential Applications of Surfactants – A Review, *International Journal of PharmTech Research*, Dec (2009)
- [20] Dukhin, A. S., Goetz, P. J. How non-ionic “electrically neutral” surfactants enhance electrical conductivity and ion stability in non-polar liquids. *Journal of Electroanalytical Chemistry* 588, 44-50 (2006)
- [21] Williams J., *Handbook for Cleaning/Decontamination of Surfaces*, (2007)
- [22] Bjorkegren S., A study of the heavy metal extraction process using emulsion liquid membranes, CHALMERS UNIVERSITY OF TECHNOLOGY, Sweden (2011-2012)
- [23] Souza W. J., Santos K. M., EFFECT OF WATER CONTENT, TEMPERATURE AND AVERAGE DROPLET SIZE ON THE SETTLING VELOCITY OF WATER-IN-OIL EMULSIONS, *Brazilian Journal of Chemical Engineering*, Vol. 32, No. 02, pp. 455 - 464, April - June, (2015)
- [24] Anton Paar, Viscosity of Crude-Oil, <https://wiki.anton-paar.com/en/crude-oil>
- [25] Prestridge, F.L., "Electric system for coalescing water", U.S. Patent No. 3,772,180. (1973)
- [26] Abbott. S., *Surfactant Science: Principles in Practice*, (2016)
- [27] Sellman E., et al., Use of Advanced Electrostatic Fields for Improved Dehydration and Desalting of Heavy Crude Oil and DilBit, World heavy oil congress, (2012)

- [28] Atta A.M., Electric Desalting and Dewatering of Crude Oil Emulsion Based on Schiff Base Polymers As Demulsifier, *Int. J. Electrochem. Sci.*, 8 9474 - 9498 (2013)
- [29] Hajivand P. and Vaziri A., OPTIMIZATION OF DEMULSIFIER FORMULATION FOR SEPARATION OF WATER FROM CRUDE OIL EMULSIONS, *Brazilian Journal of Chemical Engineering*, Vol. 32, No. 01, pp. 107 - 118, January - March, (2015)
- [30] Eow, J. S. & Ghadiri, M., Drop drop coalescence in an electric field: the effects of applied electric field and electrode geometry, *Colloids and Surfaces A: Physicochem. Eng. Aspects* 219, 253\_/279 (2003).
- [31] Sjoblom, J., Urdahl, O., Stabilization and destabilization of water-in-crude oil emulsions from the Norwegian continental shelf, *Advances in Colloid and Interface Science* 41, 241–271 (1992).
- [32] Spiecker, M.P., Kilpatrick, P.K., Interfacial rheology of petroleum asphaltene at the oil–water interface. *Langmuir* 20, 4022– 4032 (2004).
- [33] Hosseini, M. & Shahavi, M.H., Electrostatic Enhancement of Coalescence of Oil Droplets (in Nanometer Scale) in Water Emulsion, *SEPARATION SCIENCE AND ENGINEERING*, *Chinese Journal of Chemical Engineering*, 20(4) 654—658 (2012).
- [34] Bresciani A.E., Coalescence of Water Droplets in Crude Oil Emulsions: Analytical Solution, *Chem. Eng. Technol.*, 33, No. 2, 237–243 (2010)
- [35] Giljarhus N., Numerical investigation of electrostatically enhanced coalescence of two drops in a flow field, *IEEE International Conference on Dielectric Liquids* (2011)
- [36] Bailes, P.J. & Larkai, S.K., Electrostatic separation of liquid dispersions, UK Patent 2171031A (1986).
- [37] Neelamegam P., Estimation of liquid viscosities of oils using associative neural networks, *Indian Journal of Chemical Technology* (2011)
- [38] Lesaint, C. & Glomm, W.R, Dehydration efficiency of AC electrical fields on water-in-model-oil emulsions, *Colloids Surf. A: Physicochem. Eng. Aspects*, 352: 63–69 (2009).
- [39] Zhang X. et al., Electric-field control of the ferro-paraelectric phase transition in Cu:KTN crystals, Vol. 25, No. 23, *OPTICS EXPRESS* 28779 (2017)
- [40] Lundgaard L.E., Berg G., Ingebrigtsen S., and Atten P., "Electrocoalescence for oil-water separation: Fundamental aspects," in *Emulsions and emulsion stability*, J. Sjöblom, Ed., *Surfactant science series*, vol. 132, Taylor & Francis, pp. 549-592, (2006)

- [41] Esteban B. *et al*, Temperature dependence of density and viscosity of vegetable oils, *Biomass and Bioenergy* (2012)
- [42] Semancik P., DIELECTRIC ANALYSIS OF NATURAL OILS, *Acta Electrotechnica et Informatica* No. 3, Vol. 7 (2007)
- [43] Wu, P. & Qiao, R. Physical origins of apparently enhanced viscosity of interfacial fluids in electrokinetic transport. *Physics of Fluids* 23, 072005 (2011).
- [44] Waterman, L.C., Electrical coalescers, *Chem. Eng. Progr.* 61 (10), 51-57 (1965)
- [45] Galvin, C.P., Design principles for electrical coalescers, *ICHEME Symp. Series 88* 101-113 (1984)
- [46] Cottrell, F.G. & Speed, J.B., Separating and collecting particles of one liquid suspended in another liquid, *US Patent 987115* (1911)
- [47] Fjeldly, T.A. & Hansen, E.B., Nilsen, P.J., Novel coalescer technology in first-stage separator enables single-stage separation and heavy-oil separation. *SPE Projects Facil. Constr.* 3 (2), (2008)
- [48] Taylor, S.E., Theory and practice of electrically-enhanced phase separation of water-in-oil emulsion, *Trans. IChemE A* 74 526-540 (1996)
- [49] Pellemounter, D. & Carter, D., The Pulsed-DC Advantage: Improve Film Quality and Reduce Downtime in Reactive Sputtering Applications, 55<sup>th</sup> Annual Technical Conference Proceedings, Santa Clara, CA, (2012)
- [50] Hsu Wan-Thai, Clark John R., and Clark T.-C. Nguyen, A SUB-MICRON CAPACITIVE GAP PROCESS FOR MULTIPLE-METAL-ELECTRODE LATERAL MICROMECHANICAL RESONATORS, , *IEEE Int. Micro Electro Mechanical Systems Conf.*, Interlaken, Switzerland, (2001)
- [51] Kim Byoung-Yun *et al*, Demulsification of water-in-crude oil emulsions by a continuous electrostatic dehydrator, *SEapration Science and Technology* Volume 37, Issue 6 (2002)
- [52] Pesce Giuseppe *et al.*, Simultaneous measurements of electrophoretic and dielectrophoretic forces using optical tweezers, *OPTICS EXPRESS* 9363, (2015)
- [53] Mhatre S. and Thaokar R., Electrostatic phase separation: A review, *chemical engineering research and design*, 96, 28-38. (2015)
- [54] Molla S. H., Masliyah J. H., and S. Bhattacharjee, *J. Colloid Interface Sci.*, 287(1), 338–350. (2005)

- [55] Alinezhad K., Hosseini M., Movagarnejad K., and M. Salehi, *Korean J. Chem. Eng.*, 27(1), 198–205. (2010)
- [56] Luo, S., Schiffbauer, J. & Luo, T., Effect of electric field non-uniformity on droplets coalescence, *Physical Chemistry Chemical Physics* 18, 29786-29796 (2016)
- [57] Tharwat F. Tadros, *Emulsion Science and Technology: A General Introduction*, (2009)
- [58] Fingas, M., Stability and resurfacing of dispersed oil. Final Report prepared for the Prince William Sound Regional Citizens' Advisory Council, Anchorage, Alaska 99051. Prepared by Environmental Technology Center, Environment Canada. 102 pp November (2005)
- [59] Mortadi A., Melouky E., STUDIES OF THE CLAUSIUS–MOSSOTTI FACTOR, *JOURNAL OF PHYSICAL STUDIES*, v. 20, No. 4, 4001(4 p.) (2016)
- [60] Azimi, P., & Golnabi, H., Precise formulation of electrical capacitance for a cylindrical capacitive sensor. *Journal of Applied Science*, 9, 1556-1561. (2009)
- [61] Väkeväinen, K., The effect of material properties to electric field distribution in medium voltage underground cable accessories, (2010)
- [62] Griffiths D.J., *Introduction to Electrodynamics* (3rd Edition), Pearson Education, Dorling Kindersley, ISBN 81-7758-293-3 (2007)
- [63] Winslow Jr, J.D., Electrical treater with a.c.–d.c. electrical field, US Patent 4049535 (1977)
- [64] Egawa, S., & Higuchi, T., Multi-layered electrostatic film actuator. In *Micro Electro Mechanical Systems, Proceedings, An Investigation of Micro Structures, Sensors, Actuators, Machines and Robots. IEEE* (pp. 166-171). IEEE. (1990)
- [65] Sun, P., Zhao, M., Jiang, J., Zheng, Y., Han, Y., & Song, L. The Differential Method for Force Measurement Based on Electrostatic Force. *Journal of Sensors*, (2017)
- [66] Miyoshi, K., Onoue, Y., & Miyoshi, Y., The use of the energy balance principle for the derivation of current due to a moving flat charge in a one-dimensional system. *Journal of Physics D: Applied Physics*, 26(6), 913. (1993)
- [67] Raison, J, Atten, P, and Rebund, J. Field induced coalescence of two free water drops in a viscous dielectric fluid
- [68] Martin Perry et al., *Emulsifier Technology*, Emollient & Emulsifiers, Cosmetic Science Technology (2012)

- [69] Pichot. R., *Stability and Characterisation of Emulsions in the presence of Colloidal Particles and Surfactants*, PhD thesis of The University of Birmingham, (2010)
- [70] Ghosh. P, *Emulsions, Microemulsions and Foams (Part III)*, Joint Initiative of IITs and IISc
- [71] Ohashi. T. et al., Control of aqueous droplets using magnetic and electrostatic forces, *analytica chimica acta* 612 218–225 (2008)
- [72] Carlos Javier Morales Henriquez, *W/O Emulsions:Formulation, Characterization and Destabilization*, (2009)
- [73] Warren, K., G. Sams, T. Nakayama. *Electrostatic Fields: Essential Tools for Desating*, *AlChE Spring Meeting*, (1998)
- [74] Sung J. M., *Dielectrophoresis and Optoelectronic Tweezers for Nanomanipulation* Stanford University, (2007)
- [75] Xu. Jun, et al, Design of ARM-Based Inverter Electrostatic Dehydrator for Crude Oil Emulsions, Fifth IEEE International Symposium on Embedded Computing, (2008)
- [76] Jamshidi. A., Study of the dipole-dipole interaction between metallic nanowires trapped using optoelectronic tweezers (OET), (2008)
- [77] Hsu, E.C. & Li, N.N., Electrodes for electrical coalescence of liquid emulsions, US Patent 4415426 (1983)
- [78] Borges. B., *Natural Surfactants from Venezuelan Extra Heavy Crude Oil - Study of Interfacial and Structural Properties*, Mar (2012)
- [79] Lee. Hak Seung, Zheng. Chaolun, Yang. Bao, Separation of Water-in-Oil Emulsions by Electrostatic Field at the Elevated Temperature, *Journal of Applied Mechanical Engineering*, 7:4, (2018)
- [80] Akay. G., et al, Process Intensification in Water-in-Crude Oil Emulsion Separation by Simultaneous Application of Electric Field and Novel Demulsifier Adsorbers Based on Polyhipe Polymers, American Chemical Society (2005)
- [81] Ghosh A., *Mechanics Over Micro and Nano Scales*, Chapter 2, DOI 10.1007/978-1-4419-9601-5\_2, Springer Science+Business Media, LLC (2011)
- [82] Hsu et al, ELECTRODES FOR ELECTRICAL COALESCENCE OF LIQUID EMULSIONS, US Patent 4415426, (1981)
- [83] Luma Husain Mahmood, *Demulsifiers for Simulated Basrah Crude Oil*, thesis, (2009)

- [84] Raisin. J., et al, Electrocoalescence of Two Water Drops in Oil: Experiment and Modeling, Grenoble Electrical Engineering laboratory, CNRS, France, (2009)
- [85] Mousavi. S. H., et al, Effect of Pulsatile Electric Fields on Electrocoalescence of Water Drops in Oils, Chemical Engineering Science, 2014
- [86] Vera. Antonio J.Eow, Study of the parameters to generate different sizes of micro-droplets, Master thesis, 2013
- [87] Ahmed A.Mohammed et al., SEPARATION OF OIL FROM O/W EMULSION BY ELECTROFLOTATION TECHNIQUE, Number 3 Volume 16 Sep 2010 Journal of Engineering
- [88] Mehdi Mohammadi et al, Electrocoalescence of binary water droplets falling in oil: Experimental study, chemical engineering research and design (2014)
- [89] Bruvik. E. M., et al, Monitoring oil–water mixture separation by time domain reflectometry, Meas. Sci. Technol. 23 125303 (12pp) (2012)
- [90] Akuma Oji et al, Electrocoalescence of Field Crude Oil using High voltage Direct Current, International Journal of Engineering Science and Technology (IJEST), May (2012)
- [91] Kerry L. Sublette et al, METHOD AND APPARATUS FOR SEPARATING OILFIELD EMULSIONS, USPATENT, (1986)
- [92] Harpur. I. G., et al, Destabilisation of water-in-oil emulsions under the influence of an A.C. electric field: Experimental assessment of performance, Journal of Electrostatics 40&41 135-140 (1997)
- [93] Brown. A. H., et al, Effect of Oscillating Electric Fields on Coalescence in Liquid+ Liquid Systems, Dept. of Chemical Engineering, Bradford Institute of Technology, Bradford 7 Received 8th December, (1964)
- [94] Jasem M. Al-Besharah, Omar A. Salman, and Saed A. Akashah, Viscosity of Crude Oil Blends, *Ind. Eng. Chem. Res.*,26, 2445-2449 (1987)
- [95] Anisa. A.N. Iliia, and Abdurahman H.Nour, Affect of Viscosity and Droplet Diameter on water-in-oil (w/o) Emulsions: An Experimental Study, World Academy of Science, Engineering and Technology, Vol:4, No:2, (2010)
- [96] Chegenizadeh Negin, Saeedi Ali, Quan Xie, Most common surfactants employed in chemical enhanced oil recovery, Petroleum 3 197e211 (2017)

- [97] Kingsley Urum, Turgay Pekdemir, Mehmet Çopur, Surfactants treatment of crude oil contaminated soils, *Journal of Colloid and Interface Science* 276 456–464 (2004)
- [98] Fasina. O. and Z. Colley, VISCOSITY AND SPECIFIC HEAT OF VEGETABLE OILS AS A FUNCTION OF TEMPERATURE: 35°C TO 180°C, *International Journal of Food Properties*, 11: 738–746, (2008)
- [99] Parekh. P, et al, Cloud point and thermodynamic parameters of a non-ionic surfactant heptaoxyethylene dodecyl ether (C12E7) in presence of various organic and inorganic additives
- [100] Lee. N. M., Lee. B. H., Effects of temperature and surfactant structure on the solubilisation of 4-chlorobenzoic acid by various surfactants, *J. Chem. Thermodynamics* 101 1–6 (2016)
- [101] Pruneda E. F., et al, Optimum Temperature in the Electrostatic Desalting of Maya Crude Oil, *Sociedad Química de México* (2005)
- [102] Lee. Hak Seung, Zheng. Chaolun, Yang. Bao, Modeling and Experimental Study on the Design of Separators for Water/Oil Separations using Electric Fields, *Journal of Applied Mechanical Engineering*, 7:4, (2018)
- [103] Mandal, B. & Sirkar, A., Effects of Geometry of Electrodes and Pulsating DC Input on Water Splitting for Production of Hydrogen, *INTERNATIONAL JOURNAL of RENEWABLE ENERGY RESEARCH*, Biswajit Mandal et al., Vol.2, No.1, (2012).
- [104] Pellemounter. D. and Carter. D., The Pulsed-DC Advantage: Improve Film Quality and Reduce Downtime in Reactive Sputtering Applications, 55<sup>th</sup> Annual Technical Conference Proceedings, Santa Clara, CA, (2012)
- [105] Daaou. M. and Bendedouch. D. Water pH and surfactant addition effects on the stability of an Algerian crude oil emulsion, *Journal of Saudi Society* 16, 333-337 (2012)